Contextual Biases and Information Processing in Visual Perception

Yannan Su

Graduate School of
Systemic Neurosciences
LMU Munich

Dissertation
der Graduate School of Systemic Neurosciences
der Ludwig-Maximilians-Universität München

Munich, 5th December, 2023

Supervisor:

Prof. Dr. Thomas Wachtler-Kulla

Faculty of Biology

Ludwig-Maximilians-Universität München

First Reviewer: Prof. Dr. Thomas Wachtler-Kulla

Second Reviewer: Dr. Virginia Flanagin

External Reviewer: Prof. Dr. Wolfgang Einhäuser-Treyer

Date of Submission: 05.12.2023

Date of Defense: 21.03.2024

Summary

Human visual perception relies on context, as the brain integrates visual sensory evidence with contextual information to form a visual percept. When physical visual features are perceived differently from what they actually are, visual biases can occur. Extensive research has been conducted to investigate contextual information processing for different types of contextual biases and distinct visual features. The current thesis aimed to investigate biases resulting from natural and instructive contexts, with a particular focus on two visual features: color and orientation. Two specific questions are addressed in this thesis: (1) whether perceptual bias reflects information from natural context in color vision, and (2) how a reference acts as a context that biases the perception of orientation or color features.

The thesis consists of three studies presented as three manuscripts, each addressing a different aspect of contextual biases in visual perception. The first study tackles the first question by measuring perceptual biases in discriminating between noisy hue ensembles. The results show systematic biases with zero-crossings near a non-cardinal, blue-yellow color space axis. A Bayesian observer model further reveals a prior for natural daylights underlying these perceptual biases. The second and third studies focus on the second question by investigating the typical phenomenon of contextual biases: reference repulsion. The second study shows that reference repulsion can occur in a late, decision-related stage of visual processing, where explicit and implicit processes might differ. The third study demonstrates the repulsion effects of hue reference in color vision, along with striking non-uniformities of the effects across colors. Both studies explain the repulsion biases with an encoding-decoding model, suggesting different visual features might share context-dependent reweighting of sensory representations. Overall, this thesis provides new evidence of contextual biases for various visual features and offers insights into the visual processing of contextual information.

Contents

1 Introduction

We do not see things as they are,
we see them as we are.

Anaïs Nin

Visual perception is never an isolated island but grounded on the continent of contextual information. In the face of enormous amounts of visual input, context plays a significant role in selecting sensory information and stabilizing visual percepts. For instance, the context of a coffee shop helps us to recognize the person as a friend who frequents the coffee shop, even at a distance where their facial features are not immediately discernible. On the other hand, context can also lead to biases, which are mismatches between visual percepts and physical features, sparking increased interest in vision science research.

Contextual biases have been widely reported across various visual features, including orientations (Gibson and Radner, 1937, Schwartz et al., 2007, Girshick et al., 2011, Luu and Stocker, 2018), motion (Weiss et al., 2002, Stocker and Simoncelli, 2006, Jazayeri and Movshon, 2007, Zamboni et al., 2016), brightness (Eagleman et al., 2004), colors (Klauke and Wachtler, 2015, Kellner and Wachtler, 2016) and faces (Webster et al., 2004). Studying contextual biases in visual perception is essential for advancing our understanding of visual processing underlying perception, as well as for uncovering common mechanisms of information processing across different visual features.

The definition of context in visual perception is broad and refers to a wide variety of influences from the environment, experiences, and other factors on how individuals perceive and interpret information, leading to various types of contextual biases. Contextual biases can occur in the spatial or temporal dimension. For example, spatial context can tilt the visual percept of orientations, which is known as the tilt illusion (Gibson and Radner, 1937, O'Toole and Wenderoth, 1977, Smith et al., 2001, Schwartz et al., 2007, Clifford, 2014): the perceived orientation of an object is susceptible to the orientations of its surroundings and appears to be tilted to the opposite direction (Fig. 1.1a). Similarly, a preceding orientation can function as a temporal context that biases the perceived orientation of an object, showing a tilt after-effect (Gibson and Radner, 1937, O'Toole

and Wenderoth, 1977, Schwartz et al., 2007, Webster, 2015).

Alternatively, context can result from a particular behavioral task and even influence the following decisions and actions. When appreciating the woodcut print "Sky and Water I" by Maurits Cornelis Escher (Fig. 1.1b), visual perception goes through a dynamic and continuous separation of ground and object, known as figure-ground reversal (Hochberg, 1950). If we are required to identify the birds and ignore the fishes, we are likely to constantly consider the birds as objects and the fishes as background, and vice versa. The context in this case is a task instruction that can often be manipulated under laboratory circumstances.

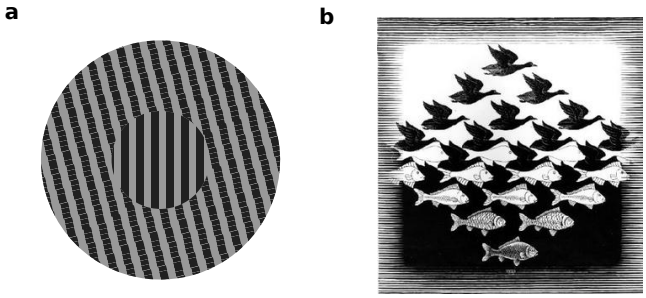

Figure 1.1: Examples of contextual biases. (a) The tilt illusion. The vertical grating in the center appears repelled in orientation away from the 15° surrounding grating. Figure adapted from Clifford (2014). (b) Sky and Water I by Maurits Cornelis Escher (1938). Birds and fishes are alternatively foreground or background, depending on what objects are the targets for recognition.

Investigating various types of contextual biases provides insights into the principles and mechanisms of information processing for different visual features. In this section, I will introduce two examples of contextual biases that are addressed in this thesis. Chapter 1.1 will focus on a particular visual feature, color, by reviewing visual processing and contextual biases in color perception. Chapter 1.3 will introduce reference repulsion, a task-relevant effect from an instructive context. Each example will be followed by a review of corresponding computational models that aim to predict and explain contextual biases (Chapter 1.2 and Chapter 1.4).

1.1 Contextual biases in color vision

Likewise to other visual features, our color percept is susceptible to the context. For example, the color of a banana will remain to appear yellow regardless of whether it is under blue or green lighting. This phenomenon is known as color constancy (Foster, 2011), which means that humans perceive an object's color as constant, even if the lighting conditions or the surrounding colors change. Color constancy effects illustrate that visual perception takes the context into account to obtain a relatively constant estimate of the color of an object, even though the physical colors of the stimuli are changing (see Foster (2011) for a review). In other words, context can modulate our color percept and lead to perceptual illusions. Before diving into the regime of contextual biases in color perception, the next section will provide a brief introduction to the basic color sensory processing and the representation of a color space.

1.1.1 From color sensory processing to cone-opponency

The human visual system begins processing color information in the retina, where cone cells, the photoreceptor cells that are responsible for color vision, detect different wavelengths of light that are reflected off of objects in the environment. There are three types of cones in the human retina, each sensitive to different ranges of wavelengths: short-wavelength sensitive cones (S-cones), medium-wavelength sensitive cones (M-cones), and long-wavelength sensitive cones (L-cones). The information from the cones is transmitted to bipolar cells with lateral inhibition by horizontal cells, showing a center-surround antagonism: signals from a central region in the retina are combined with opposing signals from the surrounding area. Then, retinal ganglion cells, which constitute the output layer of the retina, transmit signals to the lateral geniculate nucleus (LGN) in the thalamus and then to the primary visual cortex and other cortical areas.

Three types of retinal ganglion cells project to different layers of the LGN and result in three parallel visual pathways (see Lee (2011) and Dacey (2000) for reviews). These visual pathways transmit information efficiently, by removing the redundant inputs from different types of cones and conveying only the difference among cone signals. The magnocellular pathway passes through parasol

ganglion cells and projects to the magnocellular (large-cell) layers of the LGN, which transmit signals of achromatic contrast and exclusive to same-sign input from L and M cones. The parvocellular pathway passes through in midget ganglion cells (Derrington et al., 1984), which project to the parvocellular (small-cell) layers of the LGN and receive opposed signals from L and M cones (L-M). The last pathway passes through in the bistratified ganglion cells (Martin et al., 1997), which project to the koniocellular layers of the LGN and receive signals from S cones while opposing combined signals from L and M cones (S-(L+M)).

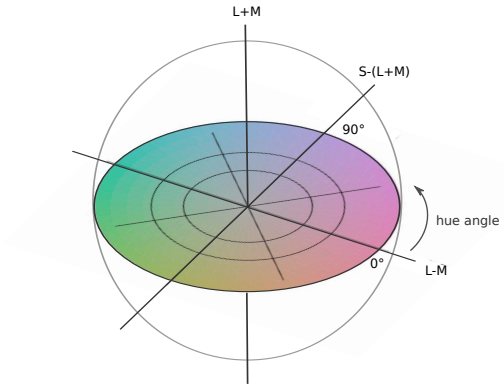

Figure 1.2: Cone-opponent color space. The axes correspond to signals from L+M, L-M, and S-(L+M) cone contrasts, respectively. The value along the L+M axis represents a luminance change, the distance from the origin corresponds to chromatic contrast, and the azimuth angle corresponds to hue. The horizontal plane represents an isoluminant plane.

The evidence of antagonism and parallel signals reveals cone opponency, which, in color vision research, can be represented in a color space — a metric of colors with a set of coordinates. For example, a cone-opponent contrast color space developed by Derrington et al. (1984), which is used in the present thesis, represents colors in terms of the relative activity of different types of opponent mechanisms and, in particular, the contrasts between them. Fig. 1.2 shows an example of this color space. Cone contrasts are defined with respect to a neutral gray at the origin. Each of the three axes represents one of the opponent contrasts. The vertical axis represents the combined signals from L and M cones (L+M), corresponding to changes in luminance. Orthogonal to this axis, there are two axes that correspond to L-M and S-(L+M) cone contrast and thus capture reddish-greenish and bluish-yellowish variation, respectively. In this color

space, colors can be specified by a set of coordinates, where the value along the L+M axis represents a luminance change, the distance from the origin corresponds to chromatic contrast, and the azimuth angle corresponds to hue. Colors sharing the same luminance are referred to as isoluminant and are located on an isoluminant plane that is orthogonal to the L+M axis.

1.1.2 Contextual biases in hue perception

As introduced at the beginning of this chapter, the color appearance of an object depends on its context. Even if under the same lighting, a neutral gray color will appear reddish when presented on a green surround, and vice versa, demonstrating contextual effects explicitly in the dimension of hue. Fig. 1.3 shows how colored surrounds influence color appearance. The colors of the patches in the bottom rows appear similar on both neutral gray (left) and chromatic (right) surrounds. Yet, in fact, the colors of the bottom patches on the neutral gray surround have the same RGB values as that of the upper patches on the chromatic surrounds (marked by the asterisk signs).

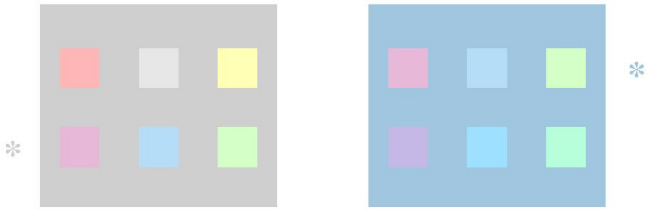

Figure 1.3: An example of contextual modulations in color perception. The patches in the bottom row on the gray background have the same colors (i.e. the same RGB values) as the colors of the patches in the upper row on the chromatic background, marked with star signs. Figure adapted with permission from Wachtler et al. (2003).

This phenomenon demonstrates that colored surrounds induce hue shifts in the perceived color of the stimulus. Klauke and Wachtler (2015) have systematically measured such hue shifts induced by isoluminant chromatic surrounds in various hues. This study employed an adjustment experiment, where participants were presented with a display comprising a neutral gray and a chromatic

surround. Participants had to adjust the hue of a colored stimulus in the neutral surround to match it to the hue of a colored test stimulus in the chromatic surround. The hue shift was computed as the difference between the adjusted hue and the test stimulus, and it showed a systematic pattern as a function of the hue difference between the stimulus and the surround. As the hue difference between the stimulus and its surround increased, the induced hue shift also increased, reaching a peak value before gradually decreasing. This induction effect resembles the tilt effect in orientation perception (Gibson and Radner, 1937), suggesting similar mechanisms of processing contextual information for color and orientation.

The findings of Klauke and Wachtler (2015) not only provide evidence of the contextual modulations in hue perception but also suggest a striking non-uniformity of color perceptual quantities. Among the distinct colored surrounds, the induction effect was qualitatively similar but differed in strength. The strongest induction effect was along an oblique axis that connects blue and yellow in the color space. Perceptual quantities exhibit non-uniformity not only in contextual biases but also in color sensitivity. Boynton et al. (1986) found an ellipse pattern of color discrimination thresholds in the CIELAB color space, a color space that is supposed to be perceptually uniform. Subsequently, other findings using various color spaces agreed that color discrimination is nonuniform among colors, showing lower thresholds at blue and yellow compared to other colors (Danilova and Mollon, 2010). A similar bimodal pattern of color discrimination thresholds has also been found in the DKL color space (Witzel and Gegenfurtner, 2013).

Notably, the non-uniformity of color perception does not correspond to the cardinal axes in the cone-opponent color space but matches an oblique axis that connects unique blue and yellow hues (Webster et al., 2000, Valberg, 2001, Wuerger et al., 2005). Furthermore, this blue-yellow axis is closely related to the characteristics of colors in natural environments. The color distributions in natural scenes are not uniform, revealing a strong bias of chromatic contrasts along a bluish to yellowish axis that is midway between the $S - (L + M)$ and $L - M$ axes (Webster and Mollon, 1997). Moreover, natural daylight varies along this blue-yellow axis. By rotating a white plaque to switch its source of illumination between sunlight and skylight, Mollon (2006) measured the corresponding chromaticities of light reflected from the plaque, which moved along

a color space axis that connects unique blue and unique yellow. As Shepard (1992) pointed out, color perception depends not only on the contrast of retinal signals but also on adaptation to color statistics in the surrounding environment. Grounded in this theory, color perceptual nonuniformities may result from adapting and exploiting color information in natural environments.

1.2 Modeling contextual biases and Bayesian perception

From the perspective of information processing, the brain is an information processor that never rests. Every second of the day, it receives sensory information, transforms the information into neural codes, and cracks the codes to generate percepts that can be used to make sense of the world and guide behaviors. The process, known as sensory encoding, involves mapping sensory input from the physical world to a neural representation. These encoded representations should correspond to neural activities and can be used by downstream neurons. Conversely, a decoder interprets the representations and maps them back to the stimuli.

The encoding and decoding processes are, however, not deterministic due to the noise resulting from the ambiguity of physical features and limitations of the nervous system (Faisal et al., 2008). Therefore, it is necessary to represent the outputs of the encoder and decoder in probabilities. Given a sensory input s, the encoded representation will be a conditional probability $p(m|s)$, where m represents sensory measurements. Then, the observer will select an estimate $\hat{s}$ (often corresponding to a peak) from the decoded conditional probability $p(s|m)$. The brain is thus often hypothesized to be an encoder-decoder observer, with the notion that an ideal observer should have probabilistic components that represent the states of the world, observations, following actions, and the losses of actions (Kersten and Mamassian, 2009). The observer is considered ideal in the sense that its performance for a specific task is statistically optimal (Kersten and Mamassian, 2009).

The power of the encoder-decoder observer model lies in its ability to explain how context shapes perception. The model achieves this through various approaches, such as illustrating how context can influence the encoding process, assigning different weights to certain features of the sensory input or represen-

tations, or providing expectations to the observer. From a probabilistic inference perspective, contextual information can combine with sensory measurement distributions to create a joint probability that the decoder uses to generate an estimate. In some cases, the estimate may not match the physical stimulus, leading to a contextual bias that can be measured in behavioral experiments. Therefore, the observer model and the related computational approaches are powerful in providing explanations for contextual biases and revealing how contextual information is processed. I will present two model examples to illustrate this point, respectively in this section and Chapter 1.4.

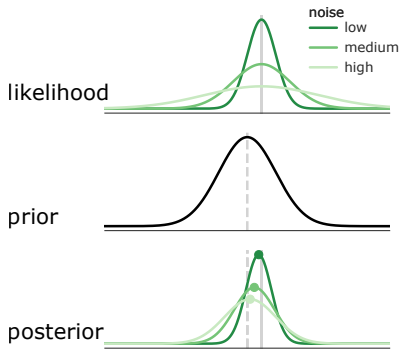

Figure 1.4: Bayesian model of perception: the posterior distributions are the results of combining likelihoods with a prior distribution. The likelihoods are Gaussian functions with three noise levels. The solid gray lines represent the values of the true stimulus. The prior function is a Gaussian function with a center at the dashed gray line. The green dots in the bottom figures indicate the point of the estimate of the posterior.

Since Thomas Bayes (1701-1761) formulated his most famous rule of probability, the Bayes' theorem, this simple and elegant formula has been applied to various fields of research for centuries. Not surprisingly, inspired by Hermann von Helmholtz's notes, "previous experiences act in conjunction with present sensations to produce a perceptual image" (von Helmholtz, 1867), researchers have ushered in an era of understanding perception and action with the Bayes theory since the late 20th century.

The theory of the Bayesian brain proposes that our brain continuously forms prior beliefs about the environment and updates the beliefs with new sensory

evidence. In other words, the neural system relies on prior knowledge to obtain reliable measurements from the noisy sensory information about the physical world. The process of combining the two sources of probabilistic information is called Bayesian inference, which can be described mathematically:

$$p(s|m) \propto p(s)p(m|s)$$

In the framework of Bayesian perception, the likelihood $p(m|s)$ represents the probability of measurements given the stimulus, and the prior probability $p(s)$ represents the prior knowledge about the stimulus. The inference results in a posterior probability $p(m|s)$, which represents the density function of the stimulus given the measurements (Fig. 1.4). An optimal Bayesian observer selects an estimate corresponding to the peak (maximum a posteriori probability, MAP) or the mean of the posterior, depending on the context of the inference problem.

Over the decades, Bayesian theories have been successfully applied to numerous problems, including sensory cue integration (Ernst and Banks, 2002, Battaglia et al., 2003), sensorimotor learning (Körding and Wolpert, 2004, 2006), time perception (Jazayeri and Shadlen, 2010, Shi et al., 2013), visual perception of depth (Knill, 2007), object perception (Kersten et al., 2004), illumination perception (Brainard et al., 2006), motion speed perception (Weiss et al., 2002, Stocker and Simoncelli, 2006), and orientation perception (Girshick et al., 2011). While Bayesian models have shown success in these research areas, concerns about priors have emerged, leading to the exploration of reasonable choices of priors.

There are different ways to classify priors in perception, based on whether they are induced by short-term context or based on long-term knowledge (Sotiropoulos and Seriès, 2015). The former, so-called "contextual expectations", can be manipulated in experiments by explicit cues or implicit learning and show immediate effects. For example, when participants are explicitly reminded of the range in which the orientation stimulus would occur, their orientation estimates depend on such prior expectations (Luu and Stocker, 2018). In the case of successive visual stimulus presentations, participants can form particular expectations implicitly without explicit cues, such as learning the statistical regularity of the stimulus from the perceptual history (Fritsche et al., 2020).

On the other hand, another type of prior expectation has been considered to have long-term effects, more "structural", and "conceptually more akin to

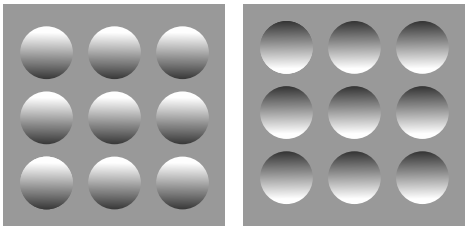

Figure 1.5: Convex/concave illusion. The spheres appearing as convex half-spheres (left) would appear as concave half-spheres if the image is flipped upside down (right).

Bayesian priors" (Sotiropoulos and Seriès, 2015). These expectations originate from our knowledge about the world, often developing over the course of life and reflecting the structure of the environment. One well-known example is that human assumes light comes from above (Sun and Perona, 1998). This expectation, for example, would make the spheres in Fig. 1.5 appear as protruding (convex) half-spheres (left). However, flipping the image upside down would lead to the percept of hollow (concave) half-spheres (Fig. 1.5, right). Indeed, studies have predicted such convex-concave shape judgments of participants using a 'light-from-above' prior (Adams et al., 2004, Thomas et al., 2010).

By its definition, structural prior expectations should match environmental statistics to facilitate the optimal performance of a Bayesian observer. Taking the visual perception of motion speed as an example, it is well-known that the perceived motion speed depends on the contrast of visual stimuli: a moving stimulus appears slower when its contrast decreases (Thompson, 1982). To explain this effect as well as other visual illusions of motion, Weiss et al. (2002) followed the assumption of Wallach (1935) (see review in Wuerger et al. (1996)) that humans prefer slow speed, consistent with the fact that most objects move slowly or remain stationary in the natural world. The authors proposed that this bias corresponds to the visual system's preference for low speed that combines noisy local image measurements. They formulated this assumption using Bayes' rule and derived an optimal Bayesian estimator that could predict the bias.

However, like other Bayesian models in the same era, Weiss et al. (2002)'s model was successful in accounting for psychophysical phenomena but had a prior for-

mulated from theoretical assumptions and could not be validated. The challenge of deriving a precise prior from perceptual measurements remained, until a new methodology was developed by Stocker and Simoncelli (2006). Stocker and Simoncelli (2006) measured subjects' discrimination responses of motion speed and observed that a moving stimulus with lower contrast appeared slower. The authors applied a Bayesian observer model, of which components were recovered from psychophysical experiment measurements of perceptual variability and bias. Specifically, in this observer model, the prior affects the position of the distribution of estimates and thus contributes to the bias. Meanwhile, the width of the likelihood affects both the width and the position of the distribution of estimates, which influences both perceptual variability and bias. The relationship thus constrains the Bayesian components, leading to a recovered prior favoring low stimulus speed.

Using the methodology linking the Bayesian model and psychophysical quantities, Girshick et al. (2011) investigated the discrimination of orientations and revealed a prior that matched environmental statistics. The authors measured the threshold and bias in participants' ability to discriminate the orientations of a pair of noisy stimulus ensembles. The discrimination results showed not only the well-known "oblique effect" in perceptual variability, but also non-negligible discrimination biases towards cardinal orientations. Based on these findings, the authors estimated a prior that peaked at cardinal orientations, which coincides with the observation that cardinals dominate the distribution of orientations in natural scenes. Thus, these results suggested the match between the Bayesian observer's internal prior and the environmental distribution, indicating that the brain may adapt to the natural context and exploit the environmental statistics to infer perceptual estimates.

1.3 Reference as a context: Reference repulsion

On a display of a group of disks, the same center disk appears larger or smaller, depending on whether the surrounding disks are smaller or larger than it (Fig. 1.6). The phenomenon, known as the Ebbinghaus illusion, demonstrates the powerful effect of a context that has similar features to an embedded stimulus. It is the same in real life, where contexts are so rich that any particular item we are interested in is always presented together with other things. To evalu-

ate, estimate, or memorize a stimulus feature, we often compare it with other things explicitly or unconsciously. These "other things" can be categorized as references, as we use them to obtain more information about the stimulus we are interested in. While the reference context may contribute to forming or maintaining a coarse estimate of a stimulus, researchers have been studying other influences of the references with features similar to the stimulus. One particular effect, reference repulsion, has become a focus of visual perception scientists.

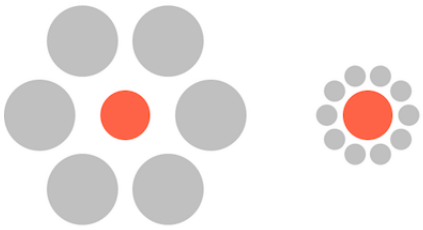

Figure 1.6: Ebbinghaus illusion. The center orange disks are identical in the left and right groups.

The term *reference repulsion* was first used by Rauber and Treue (1998) in the study of the perceived direction of a moving random-dot pattern (RDP). The participants were asked to compare the perceived direction of a moving RDP with a test direction presented either following or simultaneously with the RDP stimulus. The perceived directions showed biases, which were systematically repulsed away from the horizontal and vertical directions, suggesting that participants might use cardinals as internal reference directions and overestimate the difference between the presented direction and the nearest cardinal direction. These findings were not confined to motion perception but were also shown in the judgment of spatial distance, in which the presentation consisted of a stimulus circle followed by a test point, while a vertical reference line was presented throughout the trial. Participants were asked to judge whether the center of a circle was to the left or right of a test point, and their responses clearly showed the overestimation of the distance between the circle and the reference line. Altogether, participants tended to overestimate the difference between a stimulus and a reference, indicating the repulsion of the perceived stimulus from the

reference.

Nearly ten years later, Jazayeri and Movshon (2007) revisited reference repulsion again as a new kind of perceptual illusion. The authors also measured the perceived direction of moving RDP, but different from Rauber and Treue (1998), who only used cardinal reference directions, they examined the phenomenon with a full spectrum of reference directions, Besides, they instructed participants to report the direction estimate after completing a fine discrimination task. In these experiments, a stimulus presentation consisted of a reference boundary and a stimulus of moving RDP. The stimulus disappeared while the reference remained presented throughout the trial, and participants were asked to judge whether the perceived direction of moving RDP was more clockwise (CW) or counterclockwise (CCW) than the orientation of the reference. Following such a discrimination task, participants reported the estimated motion direction of the stimulus by reproducing it with a computer mouse. What Jazayeri and Movshon found was close to Rauber and Treue's conclusion: participants seemed to overestimate the difference between the stimulus and the reference, resulting in direction estimates repulsive away from the reference boundary.

Jazayeri and Movshon also characterized significant features of such reference repulsion biases. One feature is that estimated directions were consistent with preceding discrimination choices. For example, if the subject reported that the stimulus was more clockwise than the reference beforehand, the direction was likely to be estimated clockwise to the reference. Moreover, the magnitudes of the bias depended on the noise of the stimulus and the similarity between the direction of the stimulus and the reference boundary. The biases were larger for stimuli with lower motion coherence and for directions of stimuli closer to the boundary. These findings are characteristic of reference repulsion, which has been evidenced in various studies, as mentioned below.

1.3.1 At which stages does reference repulsion occur?

The findings of Jazayeri and Movshon (2007) on reference repulsion sparked the interest among vision researchers, who were not only interested in the phenomenon itself, but also in understanding when and how it occurs. A trial in Jazayeri and Movshon's experiments consisted of two successive tasks, thus

separating it into several stages corresponding to a series of hypothesized processes. At the time of stimulus presentation, the visual system encodes the stimulus and subsequently decodes the sensory information with high-level visual processing. Then, a decision-making process takes over to form the subject's response required by the tasks. In which of these stages does reference induce repulsion? This question could not be answered by Jazayeri and Movshon's study because the reference was presented throughout each trial.

To investigate when a reference orientation influences the estimated direction of the moving RDP, Zamboni et al. (2016) adapted the dual-task paradigm used in Jazayeri and Movshon (2007)'s study by removing the reference during the estimation task in which participants reproduced the memorized stimulus. They found that with this design, no repulsion effects were observed, indicating that reference repulsion only occurs when the reference is present during the estimation phase. The authors further slightly shifted the reference orientation before the onset of the estimation task, with the hypothesis that such manipulation would not affect estimates if reference repulsion occurs in an early sensory process. Yet, the distribution of estimates shifted with the manipulated reference. For example, when the reference was shifted 6° clockwise from its original orientation, the distribution of estimates also shifted clockwise, and the bias was repulsive away from the shifted reference. The authors thus concluded that an explicit reference cue results in repulsive bias at a late, decision-related stage rather than in early visual processing.

Recent studies (Luu and Stocker, 2018, 2021) also challenge the hypothesis that reference repulsion occurs in early sensory processing. Instead, they suggested that the effect is a post-decision bias resulting from a self-consistency principle in perceptual inference. The hypothesis posits that reference repulsion arises from perceptual inference, where a preceding discrimination choice conditions working memory representations. In other words, the dual tasks in the measurements on reference repulsion are not independent, so that participants rely on a categorical prior formed in preceding categorical judgments to obtain an estimate through a perceptual inference process. The hypothesis explained the observed bias of estimated stimulus orientation being repulsive away from a reference orientation following a categorical judgment. The authors also found that the participant's confidence in their prior knowledge can influence the strength of the bias, further supporting the theory (Luu and Stocker, 2018).

In a follow-up study, Luu and Stocker (2021) investigated if a categorical choice directly modifies working memory representations by measuring the reference repulsion effect when participants were given feedback about their judgment. The results showed that, when participants received feedback indicating incorrect choices, they were able to flexibly update their categorical judgment and utilize correct categorical information for the successive estimation. Taken together, these findings demonstrate that, given sensory presentations remaining unchanged, the manipulation of subjective categorical judgment can lead to changes in reference repulsion bias, which highlights the strong relationship between reference repulsion and perceptual decision-making.

Another recent study (Fritsche and de Lange, 2019) challenges the perceptual nature of reference repulsion. A bias arising in early visual processing would influence the perceptual appearance and result in persistent behavioral biases independent of when the sensory representation is read out. Conversely, a post-perceptual decision-related bias could be interfered with by manipulation after stimulus presentation and would depend on when a decision is made. Based on these assumptions, the authors examined whether a reference orientation cue could affect the perceptual appearance of an orientation stimulus in a following discrimination task. While they observed shifts in the point of subjective equality (PSE) in orientation discrimination, which suggests the perceived orientation was biased away from the reference, the bias indicated by the PSE shift showed a profile distinct from the reference repulsion bias in reproduction responses. This effect seemed to be explained by random trial-by-trial fluctuations in stimulus measurement rather than a perceptual bias. Therefore, the findings of this study suggest that, discrimination judgments involving a reference lead to a post-perceptual bias related to decision-making or working memory, rather than affecting the perceptual appearance of stimuli.

1.3.2 Open issues in studying reference repulsion

As outlined above, categorical judgment plays a critical role in inducing reference repulsion, especially when such repulsion bias can be manipulated through decision-making. However, while several studies have consistently demonstrated the reference repulsion effect, there has been inconsistency in whether explicit discrimination choices were involved in corresponding measurements.

Typical studies investigating reference repulsion used an explicit discrimination task that is prior to the estimation task (Jazayeri and Movshon (2007), Luu and Stocker (2018), Experiment 1 in Zamboni et al. (2016)). Other studies, while not explicitly requesting participants to make categorical judgments (Rauber and Treue (1998), Experiment 2 in Zamboni et al. (2016), Experiment 3 in Fritsche and de Lange (2019), Ye and Liu (2020)), may nonetheless result in participants being exposed to a categorical discrimination task, which could likely influence their subsequent estimation responses. Such inconsistency indicates that, most of these studies simply assumed that explicit choices are not necessary to induce the repulsion effect and lacked rigorous comparison between the effects with and without explicit choices.

In fact, the presence of an explicit commitment can influence whether underlying processes are categorized as explicit or implicit—hinging on whether the task necessitates conscious and deliberate cognitive effort—and this distinction may lead to disparate behavioral responses. For example, a recent study has revealed a dissociation between implicit and explicit encoding of ensemble representations (Hansmann-Roth et al., 2021). In the visual search task of an odd-one-out target, when participants were asked to explicitly report the summary statistics of the ensemble distractor, their responses showed an underestimation of the richness of visual representations compared to their implicit assessment. Therefore, to better understand the mechanisms of reference repulsion, it is necessary to directly compare the reference-induced biases under explicit and implicit instructions.

So far, I have focused on reviewing the studies on reference repulsion in two domains of visual perception: motion directions and orientations. While similar effects have been found in various processes of perception and cognition, such as numerical decision-making (Talluri et al., 2018, 2021) and cognitive judgment (Spicer et al., 2022), it remains unclear whether reference repulsion also occurs for visual features beyond simple spatial features, such as colors. In color vision, repulsion effects have been revealed in the contextual modulation of colored surrounds on hue stimuli (Klauke and Wachtler, 2015, Kellner and Wachtler, 2016). The repulsion not only shows similarities to the tilt effect in orientation perception (Gibson and Radner, 1937, Clifford, 2014), but also suggests the possibility of resembling the reference repulsion effects. The surrounding environment may implicitly act as a reference, potentially causing repulsive biases

without requiring participants to make any discrimination decisions or report them explicitly. It is thus essential to systematically measure the repulsion from an explicit color reference, which may also help determine whether reference repulsion reflects common contextual information processing across different visual features.

1.4 Modeling reference repulsion

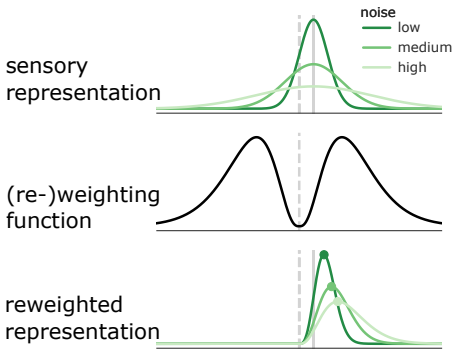

Figure 1.7: Encoding-decoding model of reference repulsion: The reweighted representations are the results of combining sensory representations with the reweighting function. Sensory representations are Gaussian functions with three noise levels. The solid gray lines represent the values of the true stimulus. The reweighting function is a mixture of two symmetric Gamma density functions that center around the reference boundary at the dashed gray line. The green dots in the bottom figures indicate the reweighted representation.

Parallel to the behavioral measurements of the reference repulsion phenomenon, several studies have adopted modeling approaches to uncover the underlying mechanisms. Jazayeri and Movshon (2007) introduced the first model to explain reference repulsion, which was based on a preceding hypothesis about how sensory information was decoded from neural population codes (Jazayeri and Movshon, 2006). The theory of population coding posits that sensory information is encoded by populations of neurons (Pouget et al., 2000). To decode the information, the brain needs to compute the likelihood of the stimuli that are consistent with the sensory response. The model in Jazayeri and

Movshon (2006)'s study considers the likelihood function as a weighted sum of sensory neuron responses, in which the activity of each neuron is weighted by the log of its own tuning function. The model was able to explain various psychophysical data and predict the underlying neuronal contributions. Notably, in a fine discrimination task where two alternative stimuli are similar, the model predicts that discrimination depends more on the contribution of neurons tuned away from the two alternatives than on neurons with preferences near the two alternatives.

Based on these predictions, Jazayeri and Movshon (2007) proposed that reference repulsion results from a strategy for decoding sensory information, where the responses of sensory neurons are weighted based on their contribution to discrimination (Fig. 1.7). Specifically, the neurons with direction preferences moderately shifted towards the sides of a reference boundary are given the highest weight in this strategy. The corresponding decoding model thus plays the role of a reweighting function, with a profile that peaks moderately shifted towards the sides of the boundary and can be implemented, for example, as a gamma probability density function. The brain uses the product of the reweighting function and the sensory representation of a stimulus to estimate a stimulus, resulting in estimates that are biased away from the boundary. The model successfully predicted the psychophysical data in multiple experiments, although with different interpretations of the underlying processes (Jazayeri and Movshon, 2007, Zamboni et al., 2016).

Recent studies have proposed alternative models to explain reference repulsion. For example, Luu and Stocker (2018) adopted a Bayesian model of conditioned perception (Stocker and Simoncelli, 2007), based on the assumption that perception is conditioned on the preceding decision and follows self-consistency. This Bayesian observer model suggests that the brain infers an estimate by combining a categorical prior formed in the preceding discrimination with the sensory representation of a stimulus. Another study (Ye and Liu, 2020) explained the reference repulsion bias with a variable-precision encoding model, in which the encoding precision linearly decreases with increasing the difference between the stimulus and reference orientation. These two models could account for the repulsive bias in corresponding results, although they may subject to particular premises such as an explicit discrimination choice (Luu and Stocker, 2018) or particular stimulus settings (Ye and Liu, 2020).

1.5 Aim of the thesis

As discussed above, contexts can bias visual percepts, as observed in various types of contexts and explained by different computational models. Examining how context induces bias has shed light on how the brain processes sensory information. However, there are still unanswered questions about the mechanisms of contextual information processing and the commonalities of contextual biases across different visual features. This thesis aims to address some of these issues through behavioral and modeling findings, focusing on two visual features, color and orientation, and two specific types of biases arising respectively from natural or instructive contexts.

The first study presented in Chapter 2 aims to reveal the perceptual bias of color discrimination and explain color perceptual properties using Bayesian models. The study extends the notion of natural prior from other visual perception domains to color perception. The hypothesis is that observers may utilize color information of natural environments and form a prior that favors particular hues, such as those occurring predominantly under natural conditions, leading to a systematic perceptual bias. Therefore, we measured the perceptual properties of hue discrimination to recover an internal prior for hue perception.

The other two studies focus on reference repulsion, a controversial task-specific bias. The study in Chapter 3 assesses at which stage of contextual information processing reference repulsion occurs. We adopted a paradigm where an orientation reference was presented successively to the disappearance of an orientation stimulus. If reference repulsion arises from an early sensory process, such a post-stimulus reference would not bias the subject's estimate of orientation stimulus. Moreover, we designed two task conditions to compare the effects between implicit and explicit processes and sought explanations from an encoding-decoding observer model.

In Chapter 4, we examined whether reference repulsion is a common phenomenon of contextual bias for orientation perception and color perception. We designed an experiment to measure the subject's estimates of hue stimuli following an explicit comparison between the stimulus and a color reference. Another goal of this study is to assess the non-uniformity in hue perception by comparing the effects among different hues. The expectation is that, in line

with the other visual features, an encoding-decoding model could explain the repulsion effects and predict perceptual non-uniformities.

2 A Bayesian observer model reveals a prior for natural daylights in hue perception

Publication: *Su, Y., Shi, Z., & Wachtler, T. (2024). A Bayesian observer model reveals a prior for natural daylights in hue perception. Vision Research, 220, 108406. https://doi.org/10.1016/j.visres.2024.108406*

Vision Research 220 (2024) 108406

Contents lists available at ScienceDirect

Vision Research

journal homepage: www.elsevier.com/locate/visres

A Bayesian observer model reveals a prior for natural daylights in hue perception

Yannan Su [a,b,*,1], Zhuanghua Shi [c,2], Thomas Wachtler [a,d,3]

[a] Faculty of Biology, Ludwig-Maximilians-Universität München, Planegg-Martinsried, Germany
[b] Graduate School of Systemic Neurosciences, Ludwig-Maximilians-Universität München, Planegg-Martinsried, Germany
[c] General and Experimental Psychology, Ludwig-Maximilians-Universität München, Munich, Germany
[d] Bernstein Center for Computational Neuroscience Munich, Planegg-Martinsried, Germany

ARTICLE INFO

Keywords:
Color vision
Hue perception
Perceptual bias
Natural daylights
Bayesian perception model
Perceptual prior
Sensory information processing

ABSTRACT

Incorporating statistical characteristics of stimuli in perceptual processing can be highly beneficial for reliable estimation from noisy sensory measurements but may generate perceptual bias. According to Bayesian inference, perceptual biases arise from the integration of internal priors with noisy sensory inputs. In this study, we used a Bayesian observer model to derive biases and priors in hue perception based on discrimination data for hue ensembles with varying levels of chromatic noise. Our results showed that discrimination thresholds for isoluminant stimuli with hue defined by azimuth angle in cone-opponent color space exhibited a bimodal pattern, with lowest thresholds near a non-cardinal blue-yellow axis that aligns closely with the variation of natural daylights. Perceptual biases showed zero crossings around this axis, indicating repulsion away from yellow and attraction towards blue. These biases could be explained by the Bayesian observer model through a non-uniform prior with a preference for blue. Our findings suggest that visual processing takes advantage of knowledge of the distribution of colors in natural environments for hue perception.

1. Introduction

The dynamic and statistical nature of the sensory environment poses challenges for sensory processing and perception. Sensory responses to the same stimulus can differ, and different stimuli can cause similar sensory stimulation. However, the natural sensory world is not entirely random but exhibits regularities, and exploiting such regularities can help an organism make useful decisions and efficient actions. Achieving this, however, requires that knowledge about the sensory environment is incorporated in sensory processing.

That sensory processing might utilize knowledge about regularities of the world can be traced back to von Helmholtz's idea of 'unconscious inference' (von Helmholtz, 1867). In recent decades, the development of the Bayesian inference framework suggests that incorporating prior knowledge can significantly enhance the reliability of perceptual estimation, especially when the input signals are corrupted by noise (Knill & Pouget, 2004; Shi et al., 2013). The Bayesian inference framework has successfully accounted for perceptual performance in object perception (Kersten et al., 2004), multi-sensory integration (Ernst & Banks, 2002), sensorimotor learning (Körding & Wolpert, 2004), visual speed perception (Stocker & Simoncelli, 2006), visual orientation perception (Girshick et al., 2011; Su et al., 2023), and time perception (Shi & Burr, 2016; Glasauer & Shi, 2022).

In the case of orientation perception, Bayesian approaches have revealed that human observers' perceptual judgments are systematically biased towards cardinal orientations (Girshick et al., 2011). The corresponding prior matched the non-uniform distribution of orientation in natural scenes, where orientations near the cardinals have a higher incidence than oblique orientations (Girshick et al., 2011). Non-uniformities in the statistics of natural sensory signals also exist in the domain of color. For example, distributions of cone-opponent signals in natural scenes show a correlation between S-(L + M) and (L-M) coordinates (Webster & Mollon, 1997; Wachtler et al., 2001; Nascimento et al., 2002; Webster et al., 2007), indicating a dominance of contrasts

* corresponding author.
E-mail addresses: su@bio.lmu.de (Y. Su), strongway@psy.lmu.de (Z. Shi), wachtler@bio.lmu.de (T. Wachtler).
[1] ORCID: 0009-0007-7764-7039
[2] ORCID: 0000-0003-2388-6695
[3] ORCID: 0000-0003-2015-6590

https://doi.org/10.1016/j.visres.2024.108406
Received 29 November 2023; Received in revised form 20 March 2024; Accepted 25 March 2024
Available online 15 April 2024

along an oblique color space axis that corresponds to the variation of natural daylights. Analyzing human color perception in a Bayesian framework may provide insights into how human color perception is adapted to such non-uniformities in the chromatic properties of the natural environment.

In the Bayesian framework, an observer's statistical inference is influenced by two key components: the likelihood, which is the probability of sensory measurements given a stimulus, and the prior, which reflects the observer's prior knowledge about stimulus probabilities (Knill & Pouget, 2004). Optimal integration of the two components results in a posterior density function that represents the probability of the stimulus given the measurements. Common choices for an optimal observer when selecting a point estimate of the posterior include the mode (maximum a posterior, MAP) or the mean (Stocker & Simoncelli, 2006).

A common difficulty encountered in the Bayesian inference framework lies in measuring likelihood and prior, which are not directly accessible. Stocker and Simoncelli (2006) proposed a method to recover likelihood and prior from psychophysical measurements of perceptual bias and variability. Specifically, these measurements were obtained from discrimination between stimuli with different noise levels, corresponding to different widths of the likelihood. According to the Bayesian inference framework, this results in different posterior distributions. When the likelihood does not align with the prior, the larger the noise, the larger the shift in the posterior induced by the prior (Fig. 1). Girshick et al. (2011) used this approach to investigate orientation perception and revealed a prior that peaked at the cardinal orientations, suggesting that visual perception may involve prior information regarding the regularities of natural scene structures.

To investigate how prior knowledge is integrated into color processing, we closely followed the approach by Stocker and Simoncelli (2006) and Girshick et al. (2011), applying the Bayesian framework in hue perception. We measured perceptual variability and biases of observers in the discrimination of noisy hue ensembles and used a Bayesian model to recover their priors.

2. Methods

2.1. Participants

Six observers, (two males and four females), ranging in age from 23 to 56 years, participated in the experiments. Four of the subjects had no knowledge with respect to the purpose of the study, while two were authors. All had normal or corrected-to-normal vision. Participants signed informed consent prior to the experiment and received a compensation of 10 Euros per hour. The study was conducted in accordance with the Declaration of Helsinki.

2.2. Stimuli

Stimuli were presented on a ViewPixx Lite 2000A display (VPixx, Saint-Bruno, QC, Canada), calibrated by a PR-655 spectroradiometer (PhotoResearch, Chatsworth, CA, USA) and controlled by a Radeon Pro WX 5100 graphics card (AMD, Santa Clara, CA, USA) in a HP Compaq Elite 8300 desktop computer running Ubuntu Linux 20.04. The screen resolution was set to 1920 × 1200 pixels at a refresh rate of 120 Hz. Stimuli were generated using PsychoPy 2020.1.2 (RRID:SCR_006571, Peirce et al., 2019) based on Python 3.6 (RRID:SCR_008394).

Chromaticities of the stimuli were defined in an opponent cone contrast color space, similar to the one used by Derrington et al. (1984), but with the polarity of the y-axis defined such that positive values corresponded to increasing S-cone stimulation, in line with MacLeod and Boynton (1979). The x-axis corresponded to increasing L-cone excitation and decreasing M-cone excitation (L-M), such that the sum of L and M remained constant. Cone excitations were estimated based on the Stockman and Sharpe (2000) cone fundamentals. Cone contrasts were calculated with respect to a neutral gray (CIE [x, y] = [0.307, 0.314], 106.7 cd/m^2), which also served as the display background on which stimuli were presented and to which subjects were adapted. The cone excitations corresponding to this reference gray served as starting values from which resulting cone excitations for a given stimulus were calculated according to its cone contrasts. L-M cone contrasts were measured as the sum of the contrast of L and M cones. S-cone contrasts were scaled by a factor of 2.6, yielding approximately equally salient stimuli for all hues at a given cone contrast (Teufel & Wehrhahn, 2000).

To account for individual differences in luminance perception, the color space plane that each subject perceived as isoluminant with the reference gray was determined using the method of Teufel and Wehrhahn (2000). Isoluminance points for 16 stimuli of different hues were determined using heterochromatic flicker photometry (Kaiser & Boynton, 1996). Fitting a plane through the reference gray to these data yielded an estimate of the individual isoluminant plane for the respective observer. The individual luminance corrections relative to the nominal isoluminant plane were less than 4%.

All stimuli used were isoluminant and had a fixed cone contrast of c = 0.12 with respect to the neutral gray background. Thus, stimuli varied only in azimuth angle, corresponding to hue (Fig. 2a). Note that scaling the S axis with respect to the L-M axis will affect the numerical values of hue angles for stimuli not aligned with a coordinate axis, but will not change their respective quadrants in the isoluminant plane. Each stimulus presentation consisted of a reference stimulus, a comparison stimulus, and a color gradient bar as a hue sequence reference (Fig. 2b). This color gradient was introduced to provide a direction of hue change, because, in contrast to orientation judgments, for hue there is no perceptual quality corresponding to clockwise vs. counterclockwise rotation. The gradient bar indicated from left to right increasing hue

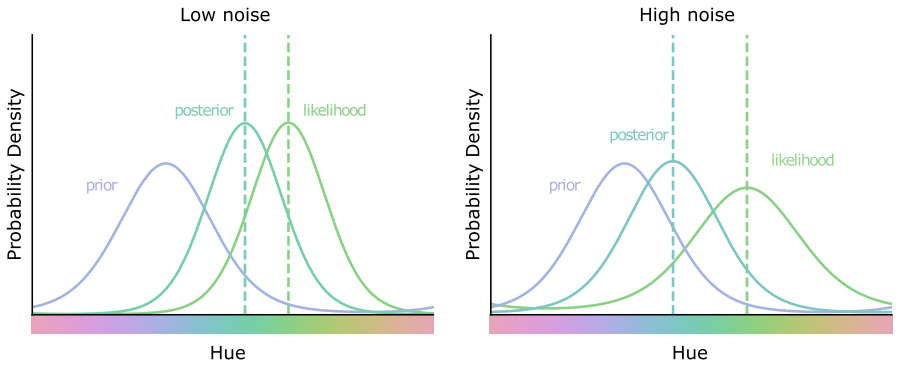

Fig. 1. Illustration of Bayesian inference in hue perception (after Stocker and Simoncelli, 2006). The same prior integrates with the likelihoods for two stimuli with different noise levels. Left: A stimulus with a low level of noise results in a narrow likelihood and thus a small shift of the posterior. Right: A stimulus with a high level of noise results in a wide likelihood and thus a large shift of the posterior.

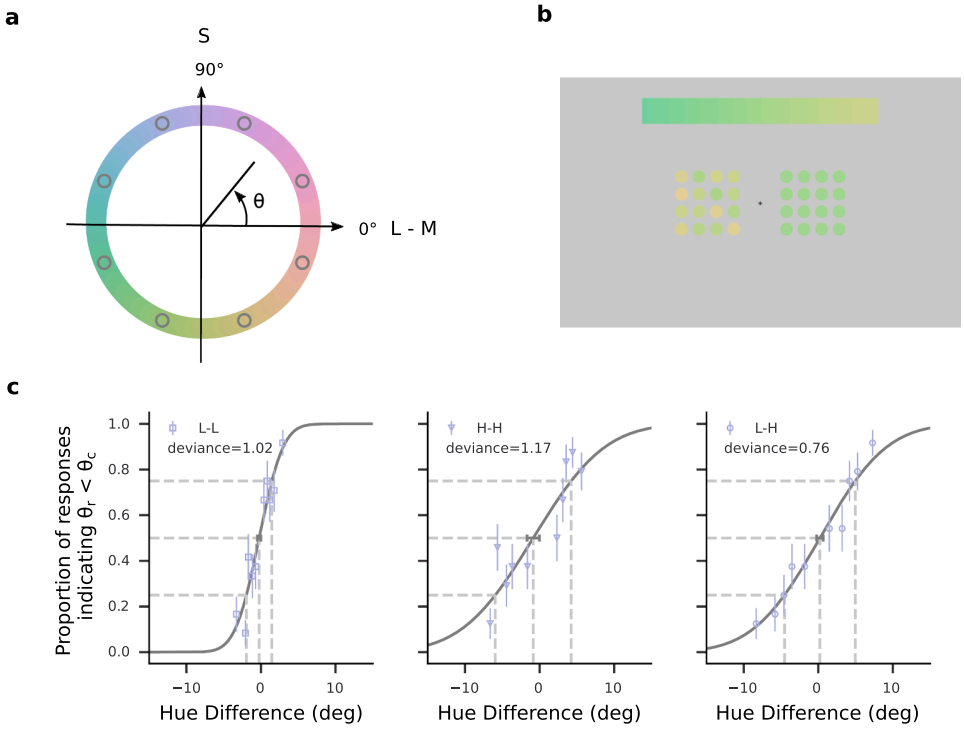

Fig. 2. Stimuli and psychometric functions. (a) Stimulus chromaticities. All stimuli were defined in the isoluminant plane with fixed chromatic contrast and thus varied only in azimuth angle, corresponding to hue (colored circle). Eight hues with equidistant azimuth angles θ (gray open dots) were defined as reference hues. (b) Example of a stimulus display. Participants were asked to compare two arrays of color patches, presented on the left and right sides of fixation, and to indicate whether their respective average hues matched the direction of hue changes that was indicated by the color gradient bar at the top of the display. (For this example, the correct response should be 'No', given that the hue averages of the arrays from left to right do not match the direction of hue changes indicated by the color gradient bar). The figure shows the cross-noise condition with a high-noise array on the left and a low-noise array on the right. Note that hue differences have been exaggerated in the figure for illustrative purposes. (c) Examples of psychometric functions for the three noise conditions. Proportions of responses indicating the subject perceived the hue angle of the comparison stimulus (θ_c) as larger than the hue angle of the reference stimulus (θ_r) are plotted as a function of the difference between the hue angles θ_c and θ_r. Data are from a single subject's responses with $\theta_r = 112.5°$ for the three noise conditions L-L (left), H-H (center), and L-H (right). Error bars of the data points denote standard error. Solid lines show cumulative Gaussian functions fitted to the data. Dashed lines denote 25%, 50%, and 75% values. Horizontal error bars around the estimated 50% points denote 68% confidence intervals. Deviance values represent the goodness of fit.

changes along the color space azimuth (Fig. 2a-b). Both reference and comparison stimuli consisted of arrays of 16 circular patches with diameters of 0.75° of visual angle, evenly spaced on a 4 × 4 grid extending 3° × 3° of visual angle. Within each stimulus, the circular patches were randomly positioned on the grid of the array. The color gradient bar had an extent of 12° × 1.5° of visual angle.

On a neutral gray background (46.01° × 29.68°), a fixation cross (0.6° × 0.6°) was presented at the screen center. The color gradient bar was presented on the upper part of the screen, 5° above the center. Reference and comparison stimuli were placed 3° left and right from the fixation cross, with the sides of reference and comparison stimulus assigned trial-by-trial in a pseudo-random fashion such that their positions were balanced within each session.

For both reference and comparison stimuli, the hues of the circular patches either were identical (low-noise stimuli) or were drawn from a uniform distribution with a range (noise level) that was individually predetermined for each subject to yield thresholds twice as large as the low-noise stimuli (high-noise stimuli, see below). The reference hues, θ_r, were evenly spaced along the azimuth of color space at 45° intervals from 22.5° to 337.5°. For each θ_r, the corresponding color gradient bar was filled by 45 evenly spaced hue angles from θ_r - 30° to θ_r + 30°.

2.3. Procedures

During the experiment, the participant sat in a dimly lit room and viewed the display binocularly from a viewing distance of 57 cm. A central fixation cross was displayed and participants had to maintain their eyes on the fixation throughout the entire trial.

Each trial started with the presentation of the color gradient bar to indicate the range of hues to be tested. After 500 ms, the reference stimulus and the comparison stimulus were presented simultaneously for 500 ms, followed by a 500-ms full-screen checkerboard pattern of random chromatic squares (1.3° × 1.2°) to prevent afterimages of the stimuli. Participants were instructed to compare the two stimuli and indicate whether the ensemble hue averages of the arrays from left to right matched the direction of color change shown by the color gradient bar. Responses were given by pressing the up or down arrow key with the right hand. There was no time constraint on the response. Average response times were within one second.

For a given reference stimulus, its average hue and corresponding color gradient bar remained unchanged across trials, while the absolute hue difference between the reference hue and the average hue of the comparison stimulus was adjusted by a 1-up/2-down staircase that increased the absolute hue difference after every incorrect response and decreased the absolute hue difference after every two consecutive correct responses. Note that, for a given reference, there were two independent 1-up/2-down staircases to adjust the comparison stimuli whose average hues were smaller and larger than the reference, respectively. Two same-noise conditions, low-noise versus low-noise (L-L) and high-noise versus high-noise (H-H), and one cross-noise condition, low-noise versus high-noise (L-H), were tested in the experiments. In the cross-noise condition, the reference stimulus was always the low-noise stimulus.

Following the approach of Girshick et al. (2011), prior to the main

experiment, we determined each participant's level of hue variance for the high-noise stimulus, ensuring the H-H discrimination thresholds were about twice as large as L-L discrimination thresholds. We selected a reference hue angle of 135°, as thresholds for this hue were at intermediate levels. For each participant, we measured the discrimination threshold (d_L) of this stimulus in the L-L condition by fitting a cumulative Gaussian function to the psychophysical data. Next, we fixed the reference and comparison stimuli at 135° and 135° + $2d_L$, respectively, adjusting the hue noise of both stimuli using a 1-up/2-down staircase to achieve 75% accuracy based on the psychometric function. The determined noise levels (21.2°,20.1°,24.5°,20.1°,22.2°, and 24.4° for the six subjects, respectively) were used for the high-noise stimuli in the main experiment. Note that these measurements were only used to determine the hue variances and excluded from other analyses.

In the main experiment, each session consisted of 128 trials, in which the first 8 trials were warm-up trials with random hues and were excluded from further analysis. Within each session, two reference stimuli with 180° difference in their mean hue angles, were randomly interleaved. Prior to the formal experiment, participants completed four practice sessions with feedback about the correctness of their responses given as text emojis (":)" or ": (" for correct and incorrect responses, respectively). The feedback was only given in the practice sessions but not in the formal experiment. Each participant performed 5760 trials divided into 24 conditions (8 reference stimuli × 3 comparison conditions) over 48 sessions.

2.4. Data analysis

2.4.1. Estimation of perceptual variability and bias

The psychophysical data were analyzed separately for each subject. In addition, data for a hypothetical average observer were obtained by pooling all subjects' data. For the data of each condition, we fitted a cumulative Gaussian function (Fig. 2c) using non-linear least square minimization with the Nelder-Mead algorithm (Gao & Han, 2012) and determined its mean, representing the point of subjective equality (PSE) and the standard deviation, representing the just noticeable difference (JND). PSE and JND thus reflected perceptual bias and perceptual variability, respectively.

2.4.2. Estimation of the measurement distributions and the likelihood functions

The measurement distribution is the conditional distribution $p(m|\theta)$ and corresponds to the likelihood of a sensory measurement m given a particular stimulus hue angle θ. For each stimulus θ we estimated the measurement distribution as a von Mises distribution with a peak at θ and the concentration parameter κ_θ, thus

$$p(m|\theta) = \frac{e^{(\kappa_\theta \cos(\theta - m))}}{2\pi i_0(\kappa_\theta)}, \tag{1}$$

where $i_0(\kappa_\theta)$ is the modified Bessel function of order 0. The concentration parameter κ_θ represents the measurement noise and is converted from the corresponding perceptual variability $J(\theta)$ by $\kappa_\theta = J^{-2}(\theta)$. For each same-noise condition (L-L and H-H),we estimated $J(\theta)$ by fitting each subject's JNDs as a sine mixture function of the hue angle θ:

$$J(\theta) = a(\sin\theta + \sin 2\theta) + b. \tag{2}$$

With periods of 180° and 360°, the two sine functions allow capturing both the periodicity and asymmetry of the JND patterns. The parameters a and b were estimated using non-linear least squares minimization.

To avoid any constraint of predefined shapes in estimating the likelihood, we adopted a sampling method based on representing the measurement distribution and the likelihood function as a two-dimensional function (Girshick et al., 2011), where the vertical dimension represented measurement distributions centered on particular stimulus hue angles θ, and the horizontal dimension represented likelihood functions of θ given particular measurements m. Thus, a single measurement from the measurement distribution resulted in a likelihood given by the corresponding horizontal slice of the two-dimensional function.

2.4.3. Estimation of the priors

To estimate the prior, we considered unimodal as well as alternative multimodal models. As model of the unimodal prior $p(\theta)$ we chose a von Mises function (Eq. 1), which guarantees that the prior had a period of 360° and an integral of 1. We determined the prior by fitting the estimation of a Bayesian observer to the behavioral data under the cross-noise condition (Girshick et al., 2011). We assumed that the Bayesian observer encodes with sensory noise and gives distributed measurements $m(\theta)$ for repeated presentation of the same stimulus θ. Each measurement leads to a likelihood function, which is multiplied by the prior to obtain a maximum a posterior (MAP) estimate at the decoding phase. Note that, an alternative to the MAP estimate is the mean of the posterior; however, we opted for the MAP estimate in alignment with the approach outlined by Girshick et al. (2011). The MAP estimate thus represents the observer's estimate $\widehat{\theta}$ of the stimulus θ. Therefore, the measurement distribution of a stimulus results in a distribution of MAP estimates. The discrimination task was simulated by comparing two MAP estimate distributions according to signal detection theory (Green & Swets, 1966), yielding a single point on the simulated psychometric function.

According to the Bayesian inference framework, non-negligible biases reflecting the prior should only be observed in the cross-noise condition in our experiments (Fig. 1). Thus, we fitted the observer model to the cross-noise biases to obtain the optimal parameters of the prior. For each participant, we simulated 1000 trials for each stimulus pair of the cross-noise comparison data. For every paired low-noise and high-noise stimuli, 1000 samples each were drawn from two corresponding measurement distributions with centers at m_L and m_H, and concentration parameters κ_L and κ_H, respectively. Each sample generated a likelihood function that was combined with the prior and led to an estimate of the stimulus. The two distributions formed by the 1000 estimates each were compared, resulting in a response probability given the corresponding stimulus pair. We then obtained a model-generated psychometric function by fitting a cumulative Gaussian function to the simulated data.

We evaluated the prior model by computing the likelihood of the cross-noise data given the model-generated psychometric function. The optimal parameters of the prior for each subject were estimated by maximizing the overall likelihood. We performed bootstrapping on each subject's binary responses for each stimulus pair 100 times and estimated the priors given the bootstrapped data. The point-wise standard deviation of the 100 estimated priors was taken as the uncertainty of the estimates. We further assessed the model by comparing its performance with the performance of a model with a uniform prior. We evaluated the performance of the model by a normalized difference of log-likelihood to the model with the uniform prior,

$$L = \frac{L_{\text{est}} - L_{\text{uni}}}{L_{\text{raw}} - L_{\text{uni}}}, \tag{3}$$

where L_{est} and L_{uni} represent the log likelihoods of the models with the estimated prior and the uniform prior, respectively, and L_{raw} represents the log likelihoods of the raw psychometric fits. Thus, $L = 0$ corresponds to the model with a uniform prior and $L = 1$ corresponds to the raw psychometric fits. Given the difference in the degrees of freedom between the estimated prior and the uniform prior, we also calculated the Akaike Information Criterion (AIC) scores (Akaike, 1998) of the models.

To validate the unimodality of the prior model, we also modeled two alternative priors by normalized sine functions with periods of 360° and 180°, respectively, and determined the prediction performance of the

observer models with these priors. While we cannot exclude the possibility of other forms of alternative priors, the 180° sine model enables describing multimodal priors while keeping the number of parameters well below the number of sample points in our data. Furthermore, perceptual quantities such as thresholds and biases often show symmetries in color space (Danilova & Mollon, 2010; Klauke & Wachtler, 2015), and our data of variability and bias (see Results) were in line with such symmetry. Therefore, a prior with 180° periodicity seems the most promising model for a multimodal prior.

3. Results

3.1. Behavioral results

We used two-alternative forced-choice discrimination experiments to measure perceptual variability and bias in hue perception. We tested three conditions for each measured hue: two same-noise conditions (low-noise versus low-noise, L-L, and high-noise versus high-noise, H-H), and one cross-noise condition (low-noise versus high-noise, L-H). The purpose of adopting these conditions was grounded in the Bayesian inference framework, which posits that, assuming the same prior, biases would not differ between stimuli with the same noise level but would increase with the noise level (Fig. 1). Thus, the same-noise conditions enabled measuring the perceptual variability of stimuli with specific noise levels, while the data in the cross-noise condition could potentially reveal the effect of a prior through a cross-noise bias, that is, a difference between the low- and the high-noise bias.

We fitted the psychometric data for hue discrimination across varying noise conditions with cumulative Gaussian functions (see Fig. 2c for examples). The goodness of the psychometric fit was measured by deviance (Wichmann & Hill, 2001) and was comparable across subjects (0.94 ± 0.38 for the L-L condition, 1.03 ± 0.34 for the H-H condition, and 1.17 ± 0.61 for the L-H condition). Based on the estimated psychometric function, we used the standard deviation of the cumulative Gaussian function as the just noticeable difference (JND) and calculated the point of subjective equality (PSE) at the threshold of 50%. These values reflected the discrimination thresholds and bias of each participant, respectively. In addition, we determined the results for a hypothetical average subject whose data were from pooled trials of all subjects. This average subject showed an average performance: there was no significant difference between the average subject's psychophysical estimates and the mean values of all subjects' psychophysical measurements (sign test $p = 0.44$ for discrimination thresholds, sign test $p = 0.68$ for biases).

3.1.1. Discrimination thresholds

Under the same-noise conditions, discrimination thresholds as a function of hue angle typically exhibited a bimodal pattern (Fig. 3a). On average, across subjects, the L-L condition had two local minima at hue angles of $101.3° \pm 22.5°$ and $298.1° \pm 28.8°$ (see Figs. S1 and S2), and two local maxima occurred at $49.5° \pm 24.6°$ and $170.4° \pm 21.9°$. Fitting a sine mixture model to the discrimination thresholds yielded similar hue angles corresponding to these extrema (local minima at $97.3° \pm 28.4°$ and $290.7° \pm 18.1°$, and local maxima at $39.4° \pm 47.1°$ and $186.7° \pm 23.6°$, averaged across subjects; Fig. 4a-b, also see Fig. S4a).

The bimodal pattern of discrimination thresholds, with the lowest thresholds near an oblique blue-yellow axis, is in line with the results of previous studies (Danilova & Mollon, 2010; Witzel & Gegenfurtner, 2013). In the H-H condition, thresholds were significantly higher than in the L-L condition (sign test $p < .001$) but the bimodal pattern persisted, however two of the subjects (S2 and S6) showed inconsistent maxima and minima between the conditions (Fig. S1). The cross-noise condition (L-H) typically yielded intermediate discrimination thresholds (Fig. 3b). Of the L-H discrimination thresholds, 82.5% were higher (sign test $p < .001$) than the corresponding L-L discrimination thresholds, and 90.0% were lower (sign test $p < .001$) than the H-H discrimination thresholds.

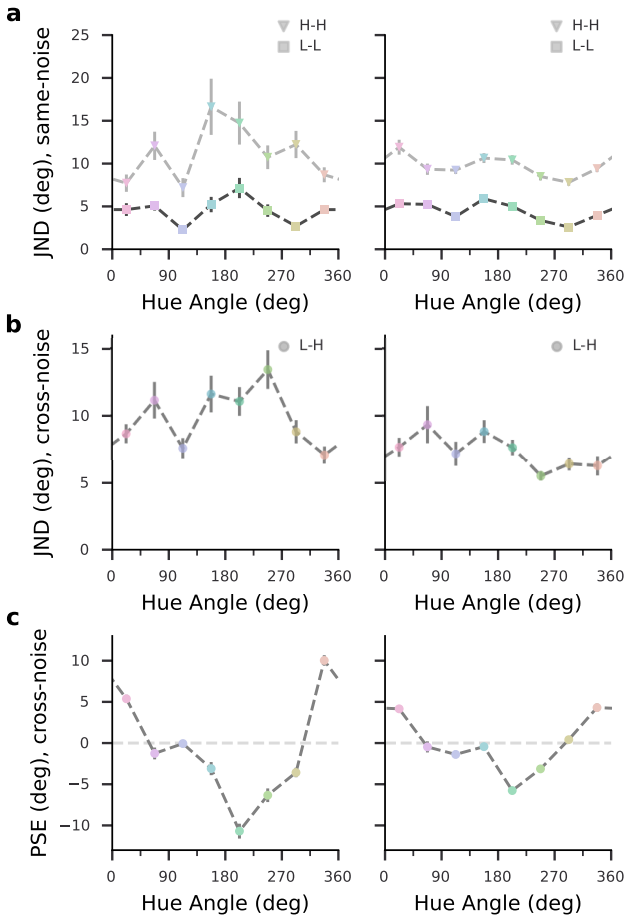

Fig. 3. Experimental data for subject S3 (left) and the average subject (right). (a) Hue discrimination thresholds (JNDs) under the same-noise condition. (b) Hue discrimination thresholds under the cross-noise condition. (c) Biases under the cross-noise condition, measured as hue angle differences between the high-noise and low-noise stimuli at the PSE. Bars denote one standard error of the estimates.

3.1.2. Biases

We observed non-negligible bias only under the cross-noise condition (L-H) for all subjects (Fig. 3c; also see Fig. S3 for the same-noise bias results), which matches our prediction based on the Bayesian inference framework: assuming the same prior for perceptual inference, biases would only differ among stimuli with different noise levels. Given that in the cross-noise condition the low-noise stimulus always served as the reference stimulus, with fixed hue across trials, the cross-noise bias shown in Fig. 3c represents the perceptual bias of the high-noise stimulus relative to the low-noise stimulus. Averaged across subjects, the biases showed a minimum of $-5.6° \pm 3.1°$ and a maximum of $5.5° \pm 2.9°$. Among the biases, 88.9% of the negative values corresponded to hue angles within the range of 112.5° to 292.5°, and 85.7% of the positive values were at the hue angles smaller than or equal to 112.5°, or larger than or equal to 292.5°, which indicated bias zero-crossings along an oblique blue-yellow axis. Specifically, zero-crossings occurred at the hue angles within 45° around 112.5° and within 45° around 292.5°, except for one subject whose zero-crossings did not fall within the hue angles of $112.5° \pm 45°$. Around the zero-crossings, biases were attractive towards blue hues (near 112.5°) and repulsive away from yellow hues (near 292.5°). Most subjects exhibited two zero-crossings, around 112.5° and 292.5°, respectively. The two

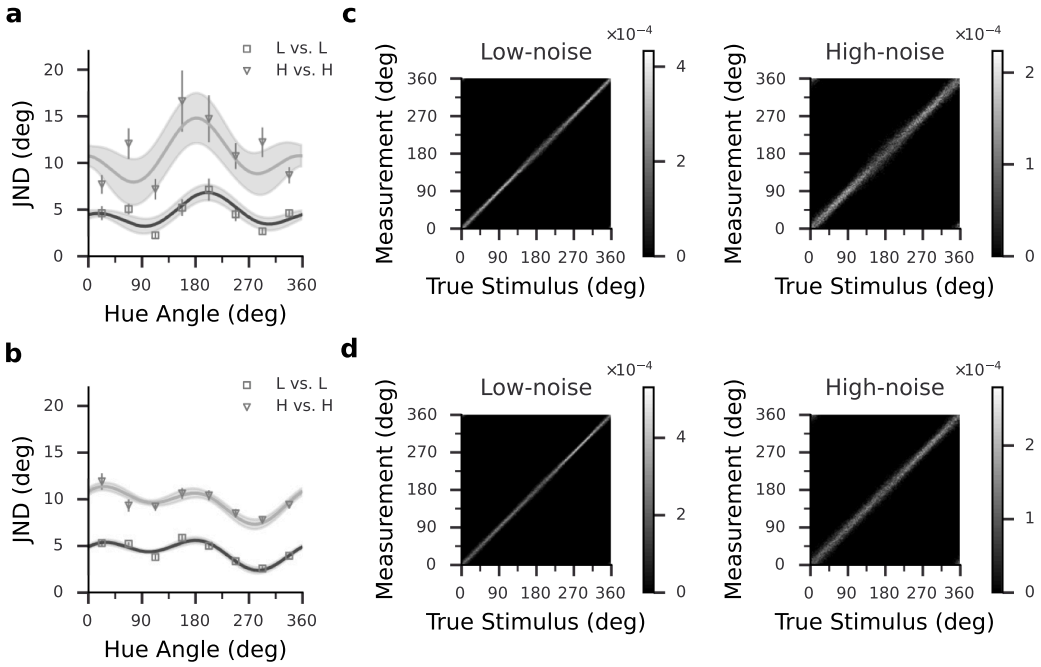

Fig. 4. Threshold fits and estimated likelihood functions in the same-noise conditions. (a and b) Fitted JNDs of subject S3 (a) and the average subject (b). JND estimates are from the data shown in Fig. 3, error bars indicate one standard error. The dark and light gray lines are the fitted JNDs for the L-L and the H-H conditions, respectively. The gray shaded area indicates 68% confidence intervals of fitted JNDs. (c and d) Estimated likelihood functions of subject S3 (c) and the average subject (d). Each horizontal slice of the two-dimensional function represents a likelihood function of stimulus hue angle θ given a particular measurement m, and each vertical slice represents a measurement distribution centered on a particular θ. The gray level represents corresponding probability densities.

subjects that had inconsistent discrimination thresholds across conditions showed additional bias zero-crossings around 157.5° (see S2 and S6 in Fig. S1). According to the Bayesian observer model, perceptual bias arises when the prior is non-uniform over the stimulus space and misaligned with sensory measurements. This prediction matches our observations of non-zero cross-noise bias, suggesting non-uniformity of the perceptual prior.

Since our color space is not perceptually uniform, we expect some bias to arise from the variation of discrimination thresholds. If changes in thresholds occur over a scale of hue angles comparable to the hue range of the noisy stimulus arrays, then the perceived ensemble average for a given stimulus may vary depending on the noise level. To determine the contribution of threshold non-uniformities to observed bias, we simulated the effect of non-uniform thresholds when the paired cross-noise stimuli had identical central hues of the ensemble. For each subject, we multiplied the hue angle differences between the hues in the high-noise stimuli and the central hue of the ensemble by the inverse of the fitted JNDs (see Modeling Results and Fig. 4a-b). Thus, we mapped the stimuli to a scale where hue differences were represented as multiples of discrimination thresholds and then computed the hue averages of the scaled stimuli. This resulted in biases that varied systematically with hue angle, corresponding to the variation in discrimination thresholds. However, their magnitudes were considerably smaller than the observed cross-noise bias (Fig. S1). Averaged across observers, the biases arising from threshold non-uniformities showed maximal magnitudes of $0.91° \pm 0.78°$, that is, less than 20% of the magnitudes of the experimentally measured biases. Thus, the variation of discrimination thresholds had a negligible influence on the cross-noise biases.

Taken together, we found that hue discrimination thresholds followed a bimodal pattern, with observers showing the best discrimination for bluish and yellowish stimuli. The introduction of chromatic noise resulted in increases in discrimination thresholds and cross-noise biases. The observed biases were attractive towards blue and repulsive from yellow, indicative of non-uniform priors.

3.2. Modeling results

To determine priors employed by observers, we used a Bayesian ideal observer model and optimized prior parameters to predict behavioral hue judgments. The model connects two behavioral measurements—discrimination threshold and bias—to two Bayesian components—likelihood and prior. Specifically, the stimulus uncertainty was propagated from the measurement distribution to the posterior distribution, resulting in perceptual variability (Girshick et al., 2011). In line with this model, measurement distributions and likelihood functions were computed from the fitted same-noise variabilities. When stimulus noise increased the threshold, the widths of the corresponding measurement distribution and likelihood function were also increased (Fig. 4, see also Fig. S4). We assumed the ideal observer's estimates of a particular stimulus θ corresponded to maximum a posteriori (MAP) estimates $\widehat{\theta}$ resulting from multiplying the likelihood function with a prior at the Bayesian decoding stage. We simulated each subject's cross-noise data by comparing each pair of MAP estimate distributions ($\widehat{\theta}_L$ and $\widehat{\theta}_H$). The prior was modeled as a von Mises function, and the prior parameters were obtained by maximizing the likelihood of the experimental data given the simulation-generated psychometric function.

Most individual subjects' priors, as well as the prior of the average subject, peaked in the second quadrant, corresponding to positive S and M cone contrasts and negative L cone contrast, that is, colors that appear bluish. These priors were large and had comparatively narrow peaks with standard deviations between 19.3° and 33.1° (Fig. 5 and Fig. S5). The two subjects whose discrimination thresholds were inconsistent across noise levels and whose biases showed more than two zero crossings had priors that peaked in the fourth quadrant (Fig. S5). These priors were shallow and relatively broad, with standard deviations of 37.7° and 48.4°. None of the priors peaked in the first or third quadrant.

The confinement of priors to the second and fourth quadrants is in line with both the distribution of natural spectra and perceptual properties. Natural spectra vary mainly along the daylight locus, which

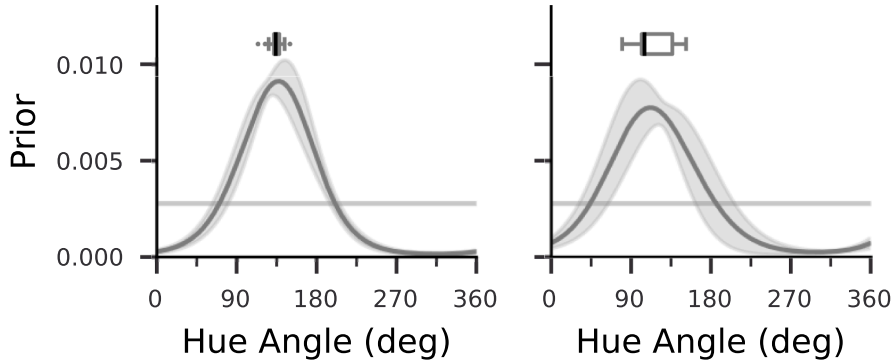

Fig. 5. Estimated prior for subject S3 (left) and the average subject (right). The gray shaded area indicates the point-wise standard deviation of 100 bootstrapped estimates. The boxes above the curves indicate the first quartile to the third quartile of the peak locations of the 100 bootstrapped estimates, with the black line at the median. The whiskers extend from the box by 1.5× the inter-quartile range (IQR). Flier points indicate values beyond the range of the whiskers. The light gray horizontal line represents the uniform prior.

covers the range from long-wavelength-dominated sunlight to short-wavelength-dominated light from the blue sky (Wyszecki & Stiles, 1982). The daylight locus aligns closely with a perceptual blue-yellow axis connecting wavelengths of 476 nm and 576 nm on the spectral locus (Mollon, 2006). This axis has an angle of 112° in our color space. The cross-subject average of the hue angles of prior peaks was 107.3° ± 26.7° (SE). The estimated prior for the average subject had its peak at 115.2° ± 19.9° (Fig. 5, right).

The elongation of the distribution of natural colors along an oblique axis in color space is paralleled by a perceptual non-uniformity: Discrimination thresholds are higher along this axis than perpendicular to it. This relation between natural stimulus statistics and perception is nicely illustrated by comparing the color gamut of natural scenes and colors from the Munsell palette plotted in the same color space (see Fig. 5 in Webster, 2020). The distribution of our priors is in line with this picture, while at the same time emphasizing an asymmetry in favor of blue over yellow.

To assess the effectiveness of the encoding–decoding model with the estimated prior, we compared its performance in predicting the cross-noise bias against a model with a uniform prior. The model with the estimated prior was found to be better at predicting both the sign and amplitude of the cross-noise bias than the model with the uniform prior (Fig. 6a-b). Across all subjects, the normalized log-likelihoods indicated that the estimated prior outperformed the uniform prior (Fig. 6c). Furthermore, when comparing the two prior models using Akaike Information Criterion (AIC) scores (Akaike, 1998), we found that the estimated prior consistently performed better than the uniform prior (Table S1). Additionally, modeling the prior as a normalized sine function yielded similar results, with the estimated prior peaking around the blue hue (119.1° ± 28.6° (SE), averaged across subjects, see Fig. S7). Note that the sine function had a constrained period of 360° and thus exhibited a single peak over the hues. Its prediction performance was better than a bimodal sine function with period 180° (Fig. S7), which confirmed the unimodality of the prior.

In summary, these results indicate that the observers used a non-uniform prior related to the oblique blue-yellow axis. Specifically, the average prior showed the highest probability at blue and the lowest probability at yellow.

4. Discussion

Our study aimed to investigate the perceptual characteristics of hue discrimination and identify an internal prior that contributes to hue perception. The experimental results showed that the lowest discrimination thresholds and smallest biases occurred for stimuli near a perceptual blue-yellow hue axis. In addition, cross-noise perceptual biases were attractive towards blue and repulsive from yellow, which was explained by a Bayesian observer model with a prior that favored blue. Our study extends the Bayesian perspective on perception to the domain of color and provides evidence of a systematic bias in color perception related to natural daylights. In contrast to previous attempts, where it had turned out difficult to determine adequate priors to explain human performance in color judgments (Brainard et al., 2006), our study presents an approach that recovers a prior that explains hue

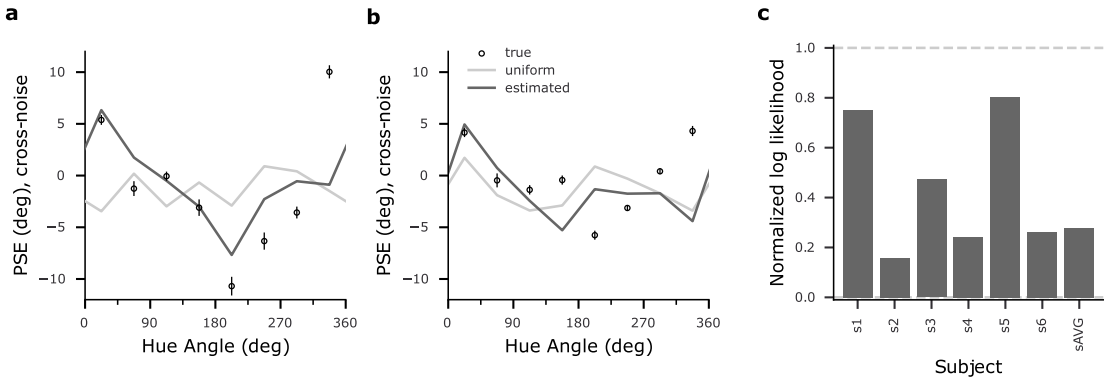

Fig. 6. Comparison of priors. (a and b) Cross-noise biases with predictions from estimated prior (black lines) and uniform prior (gray lines) for subject S3 (a) and the average subject (b). Circles represent the cross-noise biases shown in Fig. 3. (c) Normalized log-likelihoods of predictions using the estimated prior for all subjects, including the average subject (sAVG). Values greater than 1 indicate prediction better than raw psychometric fits, and values greater than 0 indicate prediction better than the model with uniform priors.

perceptual bias and can be related to natural color statistics.

Our investigation focused on the hue aspect of color perception, using an isoluminant hue circle with fixed cone contrast. However, color perception also includes brightness and saturation, which vary along the luminance axis and with radial distance in the isoluminant plane, respectively. Thus, our results should be seen as reflecting a one-dimensional aspect of a broader multi-dimensional prior for color perception. For context-induced biases, there is a consistent generalization from one dimension to higher dimensions in color space (Klauke & Wachtler, 2015; Vattuone et al., 2021; Vattuone & Samengo, 2023), and we expect the same for biases arising from a prior and the prior itself. While it may be difficult to practically determine the prior distribution along the saturation dimension (i.e., the radial direction in the color space), it is quite possible that the actual three-dimensional prior has a peak at a luminance level different from isoluminance. The main axes of variation of natural spectra vary in elevation, but not systematically with hue (Webster & Mollon, 1997). Therefore, had we included stimuli with luminance variations and recovered the two-dimensional distribution of the projection of the prior onto the unit sphere, its actual peak might lie outside the horizontal isoluminance plane. However, we would not expect a significant difference in the azimuth value.

4.1. Ensemble hue perception and interindividual variability

Our psychophysical results showed that subjects could effectively integrate the information over noisy hue ensembles, which agrees with previous findings on ensemble hue perception (Maule et al., 2014; Webster et al., 2014; Maule & Franklin, 2015; Virtanen et al., 2020). Specifically, our data confirm that hue averaging does not require a spatial configuration with abutting hue elements (Virtanen et al., 2020).

Previous studies have indicated that categorical effects may influence the percept of hue ensembles (Maule et al., 2014). However, discrimination thresholds in our experiments were approximately equal between yellow and blue ($p = 0.35$), despite their categories spanning different hue angle ranges (Webster et al., 2000; Hansen et al., 2007; Witzel & Gegenfurtner, 2013). Moreover, observers were instructed to discriminate hue using an external physical reference instead of internal criteria, minimizing potential categorical effects from subjective color naming. Nevertheless, to identify any relationship of the priors with individual specifics in color vision, we compared the locations of priors and unique hue percepts of the individual subjects. We determined the unique hue locations in five subjects (see Supplementary Methods) and found the standard deviation in unique hue locations ($5.31° \pm 2.05°$, averaged across four unique hues) was much smaller than that in the prior peak locations ($70.46°$). For one observer (S1) whose blue and yellow unique hue locations deviated from other subjects' settings towards larger hue angles, the corresponding prior peaked at a hue angle close to the average peak location of all subjects' priors. An observer (S6) with a prior peaking at the largest hue angle among subjects did not show pronounced deviations from the other subjects in unique hue categories. Overall, we did not find evidence for covariation between the prior peak location and any of the unique hue locations (Pearson correlation $r = -0.33, p = 0.59$ for unique blue, $r = -0.77, p = 0.12$ for unique yellow, $r = -0.09, p = 0.88$ for unique red, $r = -0.42, p = 0.47$ for unique green). Thus, it is unlikely that the biases we observed could be attributed to categorical effects.

The lack of covariation between priors and unique hue settings may suggest different underlying mechanisms. Recently, Rezeanu et al. (2023) suggested that the basis for unique hues lies in retinal opponency. The model considered by these authors assumed adaptation to equal-energy spectra. However, under changes in macular pigment density, which would have a similar effect as deviations from equal-energy white along the daylight locus, the model's loci of unique blue and unique yellow were fairly stable. Thus, it seems likely that the unique blue and yellow predictions of the model would not have been substantially different if adaptation to some other phase of natural daylights had been assumed.

Even if the visual systems of different observers are adapted to the same natural stimulus statistics, some interindividual variability is expected. Unique hue percepts are influenced by chromatic context (Klauke & Wachtler, 2016), which suggests that, even if the basis for unique hues is established early in the visual system (Rezeanu et al., 2023), cortical mechanisms may fine-tune color computations for perception. This implies that individual experience during ontogeny may affect perceptual priors, leading to interindividual differences. Moreover, the use of artificial primary spectra in experiments may cause variations in results among individuals. This is because differences in cone spectral sensitivities or pre-receptoral filters can result in different conditions for metamery and thus different results, even when the observers' perceptions of specific broad-band natural spectra would be the same.

4.2. Relation between perceptual variability and bias

The two primary psychophysical measures – perceptual variability and bias – covaried in our experiments: both discrimination thresholds and biases were lowest near the blue-yellow axis and largest orthogonal to the blue-yellow axis. This finding is consistent with previous studies on orientation perception, which have shown a similar relation between threshold and bias minima occurring at cardinal orientations (Tomassini et al., 2010; Girshick et al., 2011).

However, as previous studies have reported, orientation stimuli with high discrimination thresholds or high variability, such as oblique orientations, can also be perceived with minimal bias (Tomassini et al., 2010; Girshick et al., 2011). Wei and Stocker (2017) presented a mathematical description of the relation between variability and bias, suggesting a proportional relationship between bias and the derivative of the square of the discrimination threshold, and found that the relation holds for many visual features, including orientation, motion direction, magnitude, and spatial frequency (Wei & Stocker, 2017). The relationship predicts that bias is minimal at the extrema of discrimination thresholds, with attraction towards the maxima and repulsion bias away from the minima of discrimination thresholds. According to this prediction, one would expect that the bias of perceived hues in our study would show four zero-crossings, corresponding to the number of maxima and minima in the bimodal pattern of discrimination thresholds. Specifically, the hue percept should be biased away from the blue-yellow axis, where discrimination thresholds are minimal, and attracted towards colors with high discrimination thresholds, such as reddish and greenish hues (Fig. S8). However, the measured cross-noise biases showed repulsion from yellow and attraction towards blue.

Potentially, our measurements might have missed to consistently identify some zero crossings, particularly around $157.5°$ where inter-subject variability occurred in biases (Fig. 3c) and some subjects showed more than two zero-crossings (Fig. S1). Even if this were the case, the attraction bias around blue in our results is nevertheless inconsistent with the prediction of the Wei-Stocker relation, which would predict that the bias should be repulsive away from blue. An alternative possibility that could explain the deviation of our results from the relation is a strongly skewed likelihood function. Intuitively, one would expect the bias to be zero when the prior of a Bayesian observer is uniformly distributed across the entire range of stimuli. However, the model with a uniform prior predicted non-negligible bias for some of our subjects (Fig. 6, see also S2 and S6 in Fig. S6). These results are likely related to the asymmetry of the likelihood function in the observer model (Wei & Stocker, 2015), which resulted from estimating the likelihood directly from the experimental data by sampling from a measurement distribution, a method also employed by Girshick et al. (2011). While it might be feasible to simultaneously model the likelihood and prior (Stocker & Simoncelli, 2006), we relied on the measurement distribution to ensure reliable likelihoods that captured the perceptual variability for stimuli with specific noise levels. A heavy-

tailed likelihood might lead to a deviation of the posterior from the true stimulus, such that both likelihood shape and prior could contribute to perceptual bias (Stocker & Simoncelli, 2006; Wei & Stocker, 2015; Prat-Carrabin & Woodford, 2021). However, the asymmetric likelihood with a uniform prior generated less accurate predictions than the model with a non-uniform prior (Fig. S6). Thus, the key factor in yielding the systematic bias in our study is likely the non-uniformity of the prior.

Could the marked deviation from the Wei-Stocker relation indicate that the perception of color is governed by fundamentally different principles than other visual features? Wei and Stocker derived their relation under assumptions of efficient coding, specifically, that stimulus encoding maximizes the mutual information between stimuli and sensory representations. How such efficient coding principles would generalize from the univariate case as considered by Wei and Stocker (2017) to higher-dimensional stimulus spaces, like for three-dimensional color space, has not been fully worked out yet (Yerxa et al., 2020). Therefore, it is unclear whether the Wei-Stocker relation applies to univariate manifolds in higher-dimensional stimulus spaces as in our case of a hue circle in three-dimensional color space. Moreover, given the multiple transformations of color signals in the visual system, perceptual judgments in the chromatic domain may be subject to more complex constraints than visual features with simple stimulus correspondence, such as spatial features including orientation or motion direction. Different criteria of efficiency may apply to different aspects or at different stages of visual processing (von der Twer & MacLeod, 2001; Lee et al., 2002; Manning et al., 2024), which would imply deviations from the conditions considered by Wei and Stocker (2017). In particular, sensory signals for color vision are encoded first in a cone-opponent fashion by the retinal circuitry. The resulting representation is the basis for the color space that is commonly used (MacLeod & Boynton, 1979; Derrington et al., 1984), including in our study. Retinal cone opponency decorrelates the photoreceptor signals and thus reduces redundancy (Ruderman et al., 1998; Lee et al., 2002). However, it does not capture the distribution of natural chromatic signals to achieve maximal information (Wachtler et al., 2001; Kellner & Wachtler, 2013). Specifically, retinal cone opponency does not align with the variation of natural illumination, as is reflected by the non-cardinal orientation of the daylight axis in cone-opponent color space (Mollon, 2006). A sensory representation better matched to the distribution of natural chromatic signals appears only at a later stage, by the transformation of color signals in the visual cortex, where the precortically separated cone-opponent signals (Chatterjee & Callaway, 2003) are mixed and a distributed code is achieved (Lennie et al., 1990; Wachtler et al., 2003; Kuriki et al., 2015; Li et al., 2022) that captures the oblique axis of variation of natural daylights (Wachtler et al., 2003; Lafer-Sousa et al., 2012). At least at early cortical stages, neural activity shows features of both kinds of representations (Kaneko et al., 2020). While color appearance judgments are likely based on the cortical representation, perceptual variability may be reasonably assumed to be influenced considerably by the signal-to-noise ratios at precortical stages (Vorobyev & Osorio, 1998). These different influences may result in thresholds and biases inconsistent with the Wei-Stocker relation.

4.3. Hue perceptual non-uniformity and blue-yellow asymmetries

Our study reveals the non-uniformity in perceptual quantities in the present color space. Specifically, discriminability and variability vary in this cone-opponency based color space (Boynton et al., 1986; Krauskopf & Gegenfurtner, 1992; Danilova & Mollon, 2010; Bosten et al., 2015; Klauke & Wachtler, 2015). Our results verified that such non-uniform discriminability also exists for hue ensembles with chromatic noise. Moreover, we found that biases in hue judgments varied with hue, showing minima near blue and yellow, which further reflected the non-uniformity. Notably, the non-uniformity arises not along the cardinal axes of precortical cone opponency, but with respect to the oblique blue-yellow axis that aligns with the variation of natural daylight. The variance of chromaticity in natural outdoor scenes is also high along this axis (Webster & Mollon, 1997; Webster, 2014; Webster, 2020). This axis has been found special for color vision in many respects, from the distribution of natural chromatic signals (Webster & Mollon, 1997; Wachtler et al., 2001; Webster, 2020) to neural processing (Wachtler et al., 2003; Lafer-Sousa et al., 2012) and perception including discrimination (Danilova & Mollon, 2010; Bosten et al., 2015), color induction (Klauke & Wachtler, 2015), color constancy (Delahunt & Brainard, 2004; Pearce et al., 2014; Gegenfurtner et al., 2015; Lafer-Sousa et al., 2015; Weiss et al., 2017), and, as our results show, priors for hue perception. These prominent features suggest a role of this axis as a perceptual cardinal axis for color vision.

While blue and yellow appear symmetrical, in terms of their similarities in perceptual quantities and the coincidence with the daylight locus (Mollon, 2006; Webster, 2020), the bias in our results was attractive towards blue and repulsive from yellow, confirming asymmetries between blue and yellow (Webster, 2020). A previous study has demonstrated a systematic deviation towards blue when subjects adjusted yoked blue-green hue pairs to achieve an equal perceived mixture of binary hues (Webster et al., 2014). The deviation occurred for unique blue settings and not for other unique hues, which matches the unimodality of the systematic prior revealed in our results. Moreover, the deviation only occurred in the blue-green settings, while no conspicuous bias arose in the mixture consisting of yellow hues, which strongly evidenced asymmetries between blue and yellow.

A special role of blue has been observed previously in color constancy: bluish illumination results in higher color constancy than other chromatic illuminations (Delahunt & Brainard, 2004; Pearce et al., 2014; Winkler et al., 2015; Radonjic et al., 2016; Weiss et al., 2017; Aston et al., 2019). An explanation for this so-called “blue bias” was that the illumination sensitivity threshold is higher for blue than for other colors (Pearce et al., 2014; Radonjic et al., 2016), which would be in line with the hypothesis that the visual system may adapt to the natural environment and be least sensitive to the illumination changes that are most likely to occur (Aston et al., 2019). Additionally, such reduced sensitivity may be attributed to innate physiological factors: short-wavelength-sensitive cones have shown relatively poorer detection of changes in ratios of cone excitations due to illuminant changes (Nascimento & Foster, 1997). Alternatively, given the color distribution of lighting and shadows in natural scenes, the blue bias may emerge from the observer’s tendency to infer blue tints as illuminants (Winkler et al., 2015). Although these explanations do not reconcile, most of them commonly imply an environmental account of the blue-yellow asymmetry: color vision may be adapted to natural spectra and expect blue illumination as a dominant feature in natural conditions.

In line with these interpretations, our observer model attributes the blue-yellow asymmetries at the behavioral level to a unimodal prior that peaks at blue. Notably, the unimodal prior outperforms bimodal or uniform priors in predicting the perceptual biases (Fig. S7). Our model is in line with the notion that perception, and in particular color perception, is shaped by the regularities of the sensory environment (Shepard, 1992), but also suggests an asymmetry in natural daylight. As Mollon (2006) has pointed out, the clear sky appears unique blue, which suggests that the light of the sky, resulting from the fundamental physical process of Rayleigh scattering, might provide a stable reference to which color perception is anchored. Thus, in keeping with other Bayesian approaches, our results suggest that human perception internalizes the natural sensory statistics and incorporates prior knowledge into the processing of sensory information.

CRediT authorship contribution statement

Yannan Su: Methodology, Software, Formal analysis, Investigation, Data curation, Visualization, Writing – original draft, Writing – review & editing. **Zhuanghua Shi:** Writing – review & editing, Supervision. **Thomas Wachtler:** Conceptualization, Methodology, Writing – review

& editing, Supervision.

Declaration of competing interest

The authors declare that they have no known competing financial interests or personal relationships that could have appeared to influence the work reported in this paper.

Data availability

The data and code underlying this study is available at G-Node: https://doi.org/10.12751/g-node.rp2ft3.

Acknowledgments

Supported by DFG (RTG 2175 “Perception in Context and its Neural Basis”) and Bernstein Center for Computational Neuroscience Munich. We thank all participants for participating in the experiments.

Appendix A. Supplementary data

Supplementary data associated with this article can be found in the online version at https://doi.org/10.1016/j.visres.2024.108406.

References

Akaike, H. (1998). Information theory and an extension of the maximum likelihood principle. In E. Parzen, K. Tanabe, & G. Kitagawa (Eds.), *Selected Papers of Hirotugu Akaike* (pp. 199–213). New York, NY: Springer New York.
Aston, S., Radonjic, A., Brainard, D. H., & Hurlbert, A. C. (2019). Illumination discrimination for chromatically biased illuminations: Implications for color constancy. *Journal of Vision, 19*(3), 15.
Bosten, J. M., Beer, R. D., & MacLeod, D. I. A. (2015). What is white? *Journal of Vision, 15*(16), 5.
Boynton, R. M., Nagy, A. L., & Eskew, R. T., Jr (1986). Similarity of normalized discrimination ellipses in the constant-luminance chromaticity plane. *Perception, 15*(6), 755–763.
Brainard, D. H., Longère, P., Delahunt, P. B., Freeman, W. T., Kraft, J. M., & Xiao, B. (2006). Bayesian model of human color constancy. *Journal of Vision, 6*(11), 1267–1281.
Chatterjee, S., & Callaway, E. M. (2003). Parallel colour-opponent pathways to primary visual cortex. *Nature, 426*(6967), 668–671.
Danilova, M. V., & Mollon, J. D. (2010). Parafoveal color discrimination: a chromaticity locus of enhanced discrimination. *Journal of Vision, 10*(1), 4.1–9.
Delahunt, P. B., & Brainard, D. H. (2004). Does human color constancy incorporate the statistical regularity of natural daylight? *Journal of Vision, 4*(2), 57–81.
Derrington, A. M., Krauskopf, J., & Lennie, P. (1984). Chromatic mechanisms in lateral geniculate nucleus of macaque. *The Journal of Physiology, 357*, 241–265.
Ernst, M. O., & Banks, M. S. (2002). Humans integrate visual and haptic information in a statistically optimal fashion. *Nature, 415*(6870), 429–433.
Gao, F., & Han, L. (2012). Implementing the Nelder-Mead simplex algorithm with adaptive parameters. *Computational Optimization and Applications, 51*(1), 259–277.
Gegenfurtner, K. R., Bloj, M., & Toscani, M. (2015). The many colours of ‘the dress’. *Current Biology, 25*(13), R543–R544.
Girshick, A. R., Landy, M. S., & Simoncelli, E. P. (2011). Cardinal rules: Visual orientation perception reflects knowledge of environmental statistics. *Nature Neuroscience, 14*(7), 926–932.
Glasauer, S., & Shi, Z. (2022). Individual beliefs about temporal continuity explain variation of perceptual biases. *Scientific Reports, 12*(1), 10746.
Green, D. M., & Swets, J. A. (1966). *Signal detection theory and psychophysics*. New York: Wiley.
Hansen, T., Walter, S., & Gegenfurtner, K. R. (2007). Effects of spatial and temporal context on color categories and color constancy. *Journal of Vision, 7*(4), 2.
Kaiser, P. K., & Boynton, R. M. (1996). *Human color vision*. Washington: Optical Society of America.
Kaneko, S., Kuriki, I., & Andersen, S. K. (2020). Steady-State visual evoked potentials elicited from early visual cortex reflect both perceptual color space and Cone-Opponent mechanisms. *Cerebral Cortex Communications, 1*(1), Article tgaa059.
Kellner, C. J., & Wachtler, T. (2013). A distributed code for color in natural scenes derived from center-surround filtered cone signals. *Frontiers in Psychology, 4*(661), 1–11.
Kersten, D., Mamassian, P., & Yuille, A. (2004). Object perception as Bayesian inference. *Annual Review of Psychology, 55*, 271–304.
Klauke, S., & Wachtler, T. (2015). “Tilt” in color space: Hue changes induced by chromatic surrounds. *Journal of Vision, 15*(13), 17,1–11.
Klauke, S., & Wachtler, T. (2016). Changes in unique hues induced by chromatic surrounds. *Journal of The Optical Society of America A: Optics, Image Science, and Vision, 33*(3), A255–9.
Knill, D. C., & Pouget, A. (2004). The Bayesian brain: The role of uncertainty in neural coding and computation. *Trends in Neurosciences, 27*(12), 712–719.
Körding, K. P., & Wolpert, D. M. (2004). Bayesian integration in sensorimotor learning. *Nature, 427*(6971), 244–247.
Krauskopf, J., & Gegenfurtner, K. (1992). Color discrimination and adaptation. *Vision Research, 32*(11), 2165–2175.
Kuriki, I., Sun, P., Ueno, K., Tanaka, K., & Cheng, K. (2015). Hue selectivity in human visual cortex revealed by functional magnetic resonance imaging. *Cerebral Cortex, 25*, 4869–4884.
Lafer-Sousa, R., Hermann, K. L., & Conway, B. R. (2015). Striking individual differences in color perception uncovered by ‘the dress’ photograph. *Current Biology, 25*(13), R545–546.
Lafer-Sousa, R., Liu, Y. O., Lafer-Sousa, L., Wiest, M. C., & Conway, B. R. (2012). Color tuning in alert macaque V1 assessed with fMRI and single-unit recording shows a bias toward daylight colors. *Journal of the Optical Society of America A: Optics, Image Science, and Vision, 29*(5), 657–670.
Lee, T.-W., Wachtler, T., & Sejnowski, T. J. (2002). Color opponency is an efficient representation of spectral properties in natural scenes. *Vision Research, 42*(17), 2095–2103.
Lennie, P., Krauskopf, J., & Sclar, G. (1990). Chromatic mechanisms in striate cortex of macaque. *The Journal of Neuroscience, 10*(2), 649–669.
Li, P., Garg, A. K., Zhang, L. A., Rashid, M. S., & Callaway, E. M. (2022). Cone opponent functional domains in primary visual cortex combine signals for color appearance mechanisms. *Nature Communications, 13*(1), 6344.
MacLeod, D. I., & Boynton, R. M. (1979). Chromaticity diagram showing cone excitation by stimuli of equal luminance. *Journal of The Optical Society of America A: Optics, Image Science, and Vision, 69*(8), 1183–1186.
Manning, T. S., Alexander, E., Cumming, B. G., DeAngelis, G. C., Huang, X., & Cooper, E. A. (2024). Transformations of sensory information in the brain suggest changing criteria for optimality. *PLoS Computational Biology, 20*(1), e1011783.
Maule, J., & Franklin, A. (2015). Effects of ensemble complexity and perceptual similarity on rapid averaging of hue. *Journal of Vision, 15*(4), 6.
Maule, J., Witzel, C., & Franklin, A. (2014). Getting the gist of multiple hues: metric and categorical effects on ensemble perception of hue. *Journal of The Optical Society of America A: Optics, Image Science, and Vision, 31*(4), A93–102.
Mollon, J. (2006). Monge: The Verriest lecture, Lyon, July 2005. *Visual Neuroscience, 23*(3–4), 297–309.
Nascimento, S. M., & Foster, D. H. (1997). Detecting natural changes of cone-excitation ratios in simple and complex coloured images. *Proceedings of the Royal Society B: Biological Sciences, 264*(1386), 1395–1402.
Nascimento, S. M. C., Ferreira, F. P., & Foster, D. H. (2002). Statistics of spatial cone-excitation ratios in natural scenes. *Journal of The Optical Society of America A: Optics, Image Science, and Vision, 19*(8), 1484–1490.
Pearce, B., Crichton, S., Mackiewicz, M., Finlayson, G. D., & Hurlbert, A. (2014). Chromatic illumination discrimination ability reveals that human colour constancy is optimised for blue daylight illuminations. *PLoS One, 9*(2), e87989.
Peirce, J., Gray, J. R., Simpson, S., MacAskill, M., Höchenberger, R., Sogo, H., Kastman, E., & Lindeløv, J. K. (2019). PsychoPy2: Experiments in behavior made easy. *Behavior Research Methods, 51*(1), 195–203.
Prat-Carrabin, A., & Woodford, M. (2021). Bias and variance of the Bayesian-mean decoder. In M. Ranzato, A. Beygelzimer, Y. Dauphin, P. S. Liang, & J. W. Vaughan (Eds.), *Advances in Neural Information Processing Systems* (Vol. 34, pp. 23793–23805). Curran Associates Inc.
Radonjic, A., Pearce, B., Aston, S., Krieger, A., Dubin, H., Cottaris, N. P., Brainard, D. H., & Hurlbert, A. C. (2016). Illumination discrimination in real and simulated scenes. *Journal of Vision, 16*(11), 2.
Rezeanu, D., Neitz, M., & Neitz, J. (2023). From cones to color vision: A neurobiological model that explains the unique hues. *Journal of The Optical Society of America A: Optics, Image Science, and Vision, 40*(3), A1–A8.
Ruderman, D., Cronin, T., & Chiao, C. (1998). Statistics of cone responses to natural images: implications for visual coding. *Journal of The Optical Society of America A: Optics, Image Science, and Vision, 15*(8), 2036–2045.
Shepard, R. N. (1992). The perceptual organization of colors: An adaptation to regularities of the terrestrial world?. In J. H. Barkow (Ed.), *The adapted mind: Evolutionary psychology and the generation of culture* (Vol. 666, pp. 495–532) New York: Oxford University Press.
Shi, Z., & Burr, D. (2016). Predictive coding of multisensory timing. *Current Opinion in Behavioral Sciences, 8*, 200–206.
Shi, Z., Church, R. M., & Meck, W. H. (2013). Bayesian optimization of time perception. *Trends in Cognitive Sciences, 17*(11), 556–564.
Stocker, A. A., & Simoncelli, E. P. (2006). Noise characteristics and prior expectations in human visual speed perception. *Nature Neuroscience, 9*(4), 578–585.
Stockman, A., & Sharpe, L. T. (2000). The spectral sensitivities of the middle- and long-wavelength-sensitive cones derived from measurements in observers of known genotype. *Vision Research, 40*(13), 1711–1737.
Su, Y., Wachtler, T., & Shi, Z. (2023). Reference induces biases in late visual processing. *Scientific Reports, 13*(1), 18624.
Teufel, H. J., & Wehrhahn, C. (2000). Evidence for the contribution of S cones to the detection of flicker brightness and red-green. *Journal of The Optical Society of America A: Optics, Image Science, and Vision, 17*(6), 994–1006.
Tomassini, A., Morgan, M. J., & Solomon, J. A. (2010). Orientation uncertainty reduces perceived obliquity. *Vision Research, 50*(5), 541–547.
Vattuone, N. and Samengo, I. (2023). The predictive power of the geometry of colour space. https://doi.org/10.1101/2023.09.16.557954. bioRxiv preprint.

Vattuone, N., Wachtler, T., & Samengo, I. (2021). Perceptual spaces and their symmetries: The geometry of color space. *Mathematical Neuroscience and Applications, 1*.
Virtanen, L. S., Olkkonen, M., & Saarela, T. P. (2020). Color ensembles: Sampling and averaging spatial hue distributions. *Journal of Vision, 20*(5), 1.
von der Twer, T., & MacLeod, D. I. (2001). Optimal nonlinear codes for the perception of natural colours. *Network, 12*(3), 395–407.
von Helmholtz, H. (1867). Handbuch der physiologischen Optik. *Voss*.
Vorobyev, M., & Osorio, D. (1998). Receptor noise as a determinant of colour thresholds. *Proceedings of the Royal Society B: Biological Sciences, 265*(1394), 351–358.
Wachtler, T., Lee, T. W., & Sejnowski, T. J. (2001). Chromatic structure of natural scenes. *Journal of The Optical Society of America A: Optics, Image Science, and Vision, 18*(1), 65–77.
Wachtler, T., Sejnowski, T. J., & Albright, T. D. (2003). Representation of color stimuli in awake macaque primary visual cortex. *Neuron, 37*(4), 681–691.
Webster, J., Kay, P., & Webster, M. A. (2014). Perceiving the average hue of color arrays. *Journal of The Optical Society of America A: Optics, Image Science, and Vision, 31*(4), A283–92.
Webster, M. (2014). Environmental influences on color vision. In R. Luo (Ed.), *Encyclopedia of Color Science and Technology* (pp. 1–6). Berlin, Heidelberg: Springer Berlin Heidelberg.
Webster, M. A. (2020). The Verriest lecture: Adventures in blue and yellow. *Journal of The Optical Society of America A: Optics, Image Science, and Vision, 37*(4), V1–V14.
Webster, M. A., Miyahara, E., Malkoc, G., & Raker, V. E. (2000). Variations in normal color vision. II. Unique hues. *Journal of The Optical Society of America A: Optics, Image Science, and Vision, 17*(9), 1545–1555.
Webster, M. A., Mizokami, Y., & Webster, S. M. (2007). Seasonal variations in the color statistics of natural images. *Network, 18*(3), 213–233.
Webster, M. A., & Mollon, J. D. (1997). Adaptation and the color statistics of natural images. *Vision Research, 37*(23), 3283–3298.
Wei, X.-X., & Stocker, A. A. (2015). A Bayesian observer model constrained by efficient coding can explain 'anti-Bayesian' percepts. *Nature Neuroscience, 18*(10), 1509–1517.
Wei, X.-X., & Stocker, A. A. (2017). Lawful relation between perceptual bias and discriminability. *Proceedings of the National Academy of Sciences of the United States of America, 114*(38), 10244–10249.
Weiss, D., Witzel, C., & Gegenfurtner, K. (2017). Determinants of colour constancy and the blue bias. *i-Perception, 8*(6), 2041669517739635.
Wichmann, F. A., & Hill, N. J. (2001). The psychometric function: I. Fitting, sampling, and goodness of fit. *Perception & Psychophysics, 63*(8), 1293–1313.
Winkler, A. D., Spillmann, L., Werner, J. S., & Webster, M. A. (2015). Asymmetries in blue-yellow color perception and in the color of 'the dress'. *Current Biology, 25*(13), R547–R548.
Witzel, C., & Gegenfurtner, K. R. (2013). Categorical sensitivity to color differences. *Journal of Vision, 13*(7), 1.
Wyszecki, G., & Stiles, W. S. (1982). *Color science: Concepts and methods, quantitative data and formulae*. New York: Wiley.
Yerxa, T. E., Kee, E., DeWeese, M. R., & Cooper, E. A. (2020). Efficient sensory coding of multidimensional stimuli. *PLoS Computational Biology, 16*(9), e1008146.

Supplementary Materials

Data Availability

The data and code can be found at G-Node: https://doi.org/10.12751/g-node.rp2ft3.

Supplementary Methods

Unique Hue Measurements

We measured unique hue locations to investigate whether the priors were related to the participants' color categories. Five of the recruited participants participated in this supplementary experiment. The stimulus was a $10° \times 10°$ colored rectangle presented on a neutral gray background. Participants were instructed to adjust the hue of the stimulus by moving the mouse until the color appeared a unique hue. For example, in a trial measuring subjective unique blue, the task was to make the color appear "blue and neither reddish nor greenish". Participants adjusted the stimulus along the azimuth of the color space. There was no time constraint on the response. Participants confirmed the adjustment and terminated the trial by pressing the space bar on the keyboard. Four unique hues (red, blue, green, and yellow) were tested with 30 repeated trials each. The initial hue angle of the stimulus color was randomly chosen from a range of 40° around a guessed value of the unique color (0°, 110°, 220°, and 315° for red, blue, green, and yellow, respectively) based on previous studies (Webster et al., 2000). To prevent after-image and adaption, a full-screen 500-ms checkerboard pattern of chromatic squares was presented after the subject's response, and all trials were randomly interleaved.

Supplementary Figures and Tables

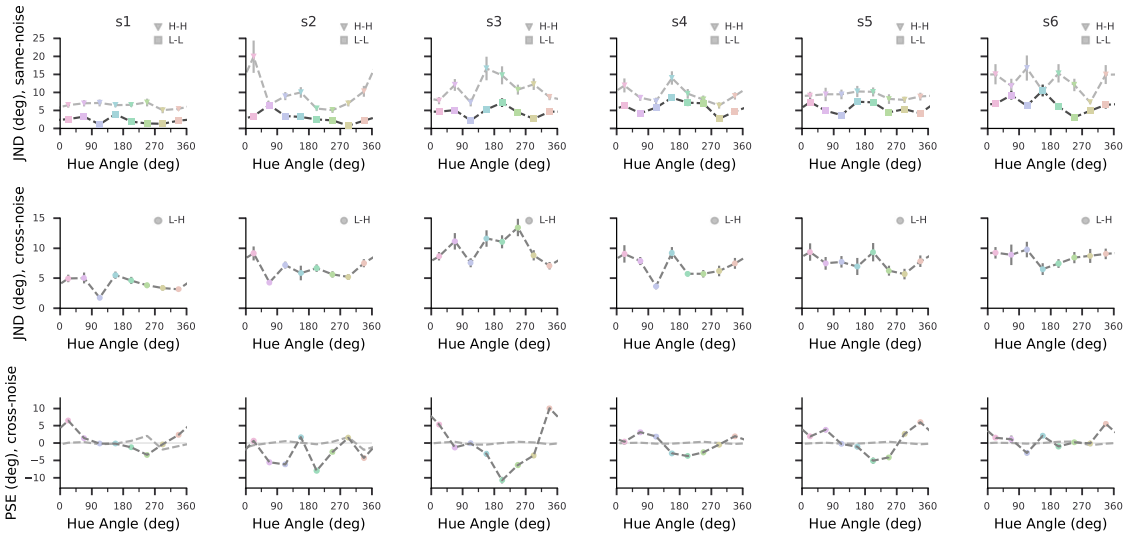

Figure S1: Experimental data for each subject (each column, respectively). Top: hue discrimination thresholds (JNDs) under the same-noise condition. Middle: hue discrimination thresholds under the cross-noise condition. Bottom: biases under the cross-noise condition, measured as hue angle differences between the high-noise and low-noise stimuli at the PSE. Bars denote one standard error of the estimates. Light gray dashed lines represent the bias induced by local non-uniformity of discrimination (see Results).

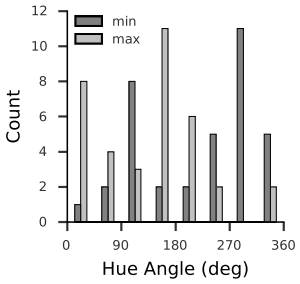

Figure S2: Distribution of stimulus hue angles corresponding to the two local minima (dark gray bars) and two local maxima (light gray bars) of the discrimination thresholds. Data are from all subjects and all conditions.

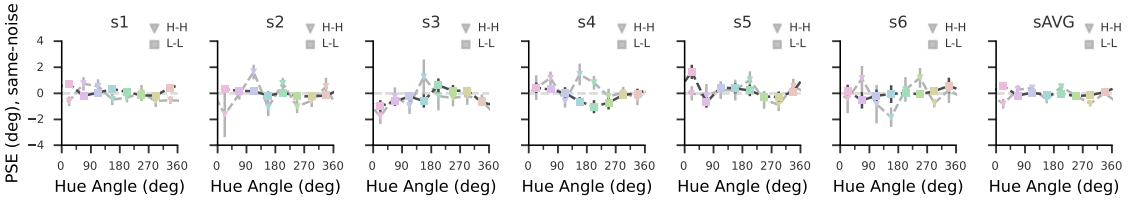

Figure S3: Same-noise bias for each subject (each column, respectively). Bars denote one standard error of the estimates.

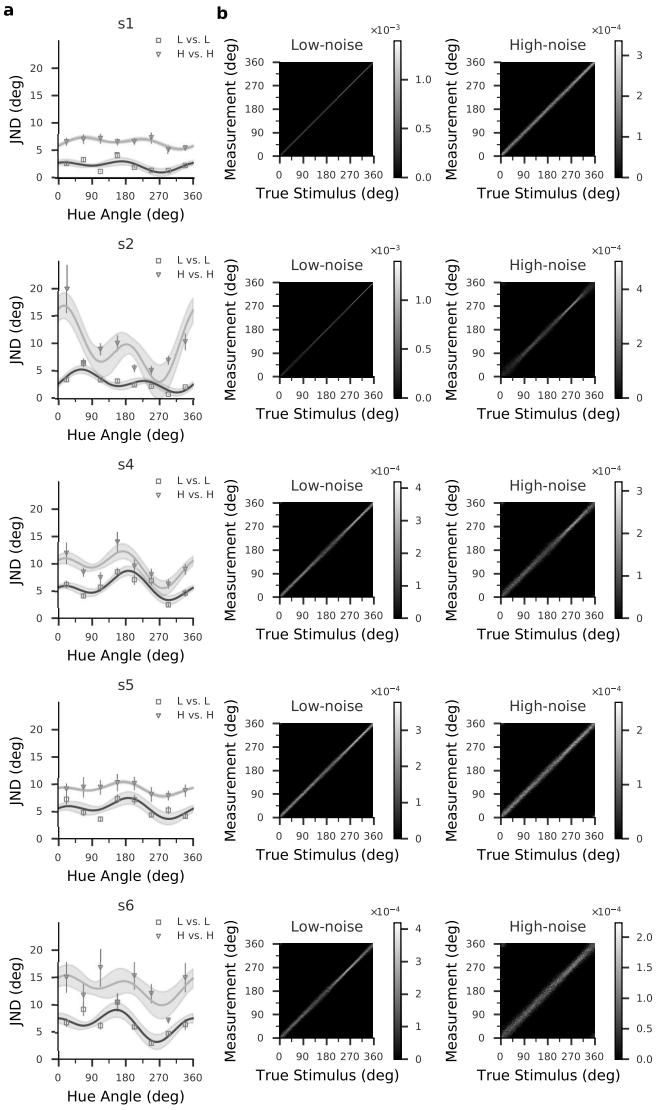

Figure S4: Threshold fits and estimated likelihood functions in the same-noise conditions for subjects S1, S2, S4, S5, and S6 (five rows, respectively). (a) Fitted JNDs of the subjects. JND estimates are from the data shown in Fig. S1, error bars indicate one standard error. The dark and light gray lines are the fitted JNDs for the L-L and the H-H conditions, respectively. The gray shaded area indicates 68% confidence intervals of fitted JNDs. (b) Estimated likelihood functions of the subjects. Each horizontal slice of the two-dimensional function represents a likelihood function of stimulus hue angle θ given a particular measurement m, and each vertical slice represents a measurement distribution centered on a particular θ. The gray level represents corresponding probability densities in the L-L condition("Low-noise", left) and in the H-H condition ("High-noise", right).

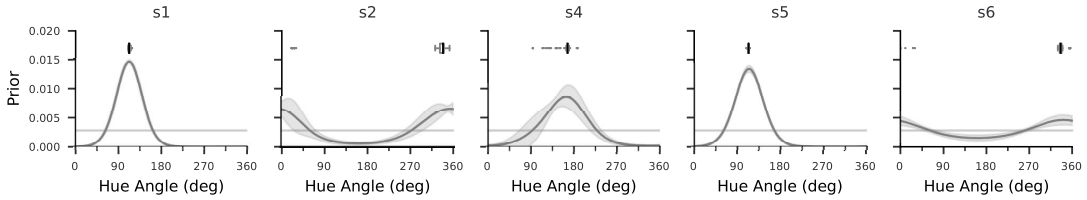

Figure S5: Estimated priors for subjects S1, S2, S4, S5, and S6 (five columns, respectively). The gray shaded area indicates the point-wise standard deviation of 100 bootstrapped estimates. The boxes above the curves indicate the first quartile to the third quartile of the peak locations of the 100 bootstrapped estimates, with the black line at the median. The whiskers extend from the box by 1.5× the interquartile range (IQR). Flier points indicate values beyond the range of the whiskers. The light gray horizontal line represents the uniform prior.

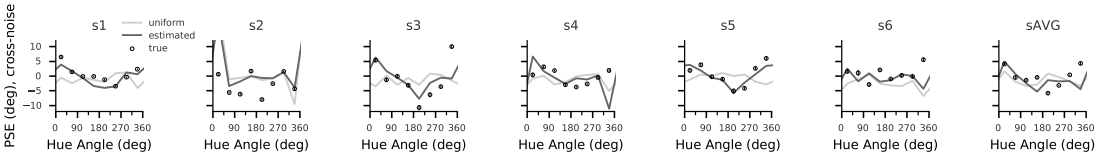

Figure S6: Cross-noise biases with predictions from estimated priors (black lines) and uniform prior (gray lines) for all subjects and the average subject S1, S2, S4, S5, and S6 (5 columns, respectively). Circles represent the cross-noise biases shown in Fig. S1.

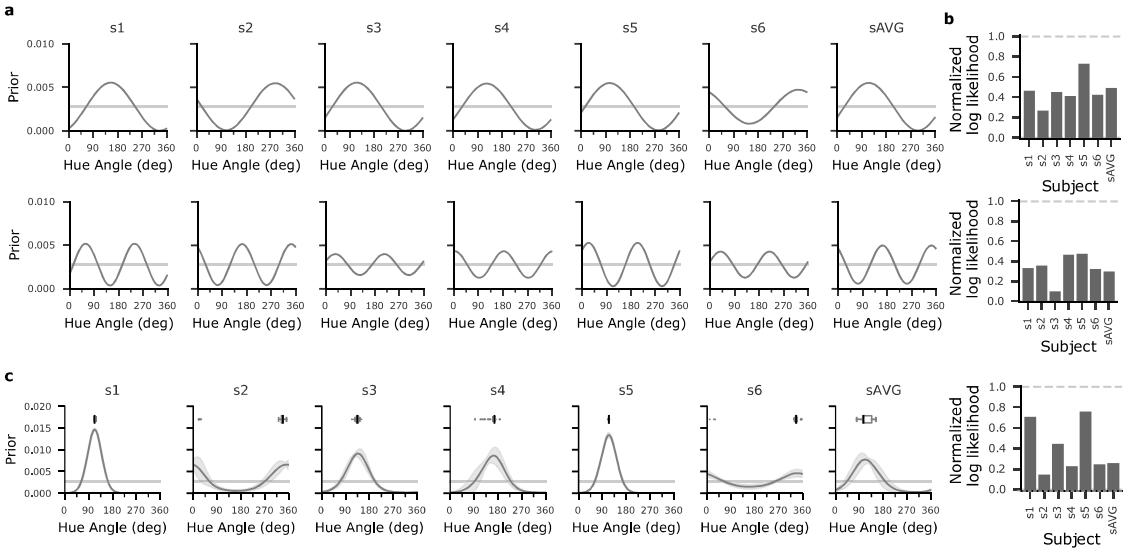

Figure S7: Alternative prior models. Estimated priors as sine functions for all subjects (including the average subject, sAVG). The periods of the estimated sine-shape priors were 360° (top) and 180° (bottom), respectively. (a) Estimated sine-shaped priors for all subjects (7 columns, respectively). The light gray line represents the uniform prior. (b) Normalized log-likelihoods of predictions using the estimated sine-shape prior for all subjects. (c) For ease of comparison, replicates of Fig. 5 and Fig. S5 representing the estimated priors using in the main experiment and corresponding normalized log-likelihoods of predictions (replicates of Fig. 6c).

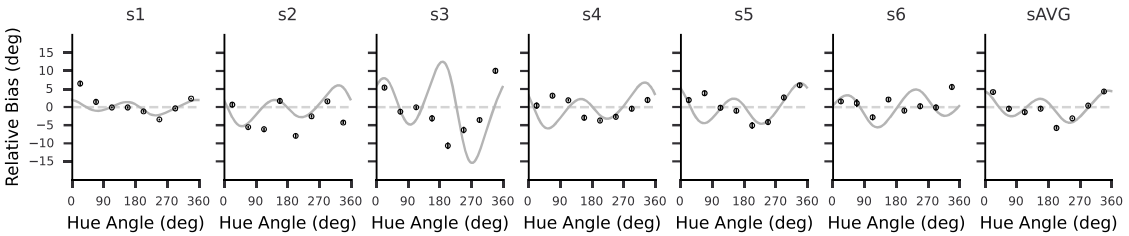

Figure S8: Cross-noise bias predicted according to the Wei and Stocker (2017) relation. Bias curves (gray) were calculated using the mathematical relation between perceptual variability and bias described by Wei and Stocker (2017). Black dots represent the measured cross-noise biases (same data as in Fig. 3 and Fig. S1).

Subject	Estimated Prior	Uniform Prior
s1	2097	2724
s2	2473	2560
s3	2365	2633
s4	2311	2388
s5	2421	2988
s6	2318	2379
sAVG	2458	2539

Table S1: Akaike Information Criterion (AIC) scores of the estimated and uniform priors for all subjects.

3 Reference induces biases in late visual processing

Publication: *Su, Y., Wachtler, T., & Shi, Z. (2023). Reference induces biases in late visual processing. Scientific Reports, 13(1), 18624. https://doi.org/10.1038/s41598-023-44827-8*

scientific reports

Check for updates

OPEN

Reference induces biases in late visual processing

Yannan Su[1,2]✉, Thomas Wachtler[1,3] & Zhuanghua Shi[4]

How we perceive a visual stimulus can be influenced by its surrounding context. For example, the presence of a reference skews the perception of a similar feature in a stimulus, a phenomenon called reference repulsion. Ongoing research so far remains inconclusive regarding the stage of visual information processing where such repulsion occurs. We examined the influence of a reference on late visual processing. We measured the repulsion effect caused by an orientation reference presented after an orientation ensemble stimulus. The participants' reported orientations were significantly biased away from the post-stimulus reference, displaying typical characteristics of reference repulsion. Moreover, explicit discrimination choices between the reference and the stimulus influenced the magnitudes of repulsion effects, which can be explained by an encoding-decoding model that differentiates the re-weighting of sensory representations in implicit and explicit processes. These results support the notion that reference repulsion may arise at a late decision-related stage of visual processing, where different sensory decoding strategies are employed depending on the specific task.

The world around us is filled with a wealth of visual stimuli, where objects are arranged in a contextual setting. Our perception of the world, thus, is not merely a collection of individual isolated objects, but is susceptible to the surrounding context. This susceptibility to context has been recognized since ancient times, such as the observation in ancient China 400 BC that the moon looks bigger when it rises on the horizon than when it is overhead[1]. Context-based perceptual biases typically appear in the form of repulsion. When two similar objects or features are placed together, they appear more distinct or dissimilar than if presented separately. The repulsion effect has been widely observed in basic visual features, including motion direction[2], orientation[3,4], brightness and color[5,6], numerosity[7], and even in higher cognitive judgments[8].

Recent studies have shown that the repulsion bias can be amplified through explicit comparison with an external reference, so-called reference repulsion[9–12]. Jazayeri & Movshon[10] have demonstrated a classic example of reference repulsion using a dual-task paradigm, where participants reproduced the motion direction of a moving random-dot pattern after comparing it with a reference boundary. In contrast to classical contextual effects such as the tilt effect or the tilt after-effect[3], the results revealed a systematic bias away from the reference that was strongest when the stimulus aligned with the reference. The authors concluded that the bias in the reproduction task was a result of the first discrimination that caused preferentially weighted signals from neurons tuned away from the reference in decoding. This weighted representation of sensory likelihoods 'repels' from the reference, resulting in better discrimination[10]. An alternative account proposes that the repulsion bias arises from the sensory encoding rather than the decoding process[13]. It posits that the encoding precision of measurement varies according to the difference between the stimulus and the reference. During decoding, this variable-precision encoding is integrated with a uniform prior to form a posterior distribution[13]. The prediction based on that posterior distribution could produce a similar reference repulsion effect. Both accounts, despite applying different underlying mechanisms, concur in that the reference repulsion originates from the perceptual stage.

Several recent studies, however, have challenged the notion that reference repulsion is solely a perceptual process. For instance, Zamboni et al.[11] have shown that the presence of the reference during the reproduction task is crucial in eliciting the repulsion effect. When the reference orientation shifted slightly (±6°) during the reproduction task, the repulsive bias also shifted accordingly with the reference. Similarly, Fritsche & de Lange[14] let participants first judge whether a grating stimulus was clockwise or counterclockwise relative to a previously presented reference boundary. Subsequently, participants indicated whether the stimulus had the same orientation as a comparison stimulus. The researchers found that the perceptual bias that occurred in a successive comparison task had distinct characteristics from those of the reference repulsion bias, suggesting that reference repulsion does not directly alter the appearance of the stimulus, but acts at a late decision stage.

[1]Faculty of Biology, Ludwig-Maximilians-Universität München, Munich, Germany. [2]Graduate School of Systemic Neurosciences, Ludwig-Maximilians-Universität München, Munich, Germany. [3]Bernstein Center for Computational Neuroscience, Munich, Germany. [4]General and Experimental Psychology, Ludwig-Maximilians-Universität München, Munich, Germany. ✉email: su@biologie.uni-muenchen.de

This idea also aligns with the self-consistent Bayesian observer model[12,15], which posits that an optimal observer seeks self-consistency in representations across the hierarchy of inference. In a series of tasks, the decision in one task is influenced by the preceding task, and a prior categorical judgment biases downstream processes, such as reproduction, based on working memory[12,15]. These findings suggest that the repulsion effect may emerge at the late decision stage.

Despite the ongoing debate surrounding the processing stage of the reference repulsion continues, most studies commonly used the reference throughout the trial, starting before or concurrently with the target stimulus. However, the timing of the reference plays a crucial role in determining the processing stage involved in the reference repulsion effect. For example, by presenting the reference after the sensory encoding of the stimulus, early encoding of the reference can be effectively avoided.

Another crucial factor influencing the repulsion effect is the distinction between explicit and implicit processes[16]. Many studies investigating reference repulsion employ an explicit discrimination task before the primary measurement[10,12]. In some cases, participants are exposed to an explicit categorical discrimination task, even if they are not asked to make explicit judgments[9,11,13,14], potentially causing the categorical decision to influence the main task. Therefore, it is crucial to directly compare the repulsion effect under explicit and implicit instructions to gain deeper insights into the nature of reference repulsion.

On this ground, we conducted a study using an ensemble orientation averaging paradigm to investigate the impact of the reference orientation and task conditions on the repulsion effect. Notably, we presented the reference after the stimulus. Our reasoning was twofold: if reference repulsion primarily occurs during early sensory processing, a post-stimulus reference would have no influence on the observer's judgment; however, if the reference does affect judgment, we would observe judgment biased away from the reference. In addition, we introduced different task conditions to assess the impact of explicit and implicit processes on the repulsion effect directly.

We found that the post-stimulus reference indeed induced repulsion, but the effect differed between explicit and implicit processes. We attribute the findings to variations in weighting between implicit and explicit processes within an encoding-decoding model.

Methods

Participants

Five volunteers, one male and four females, ranging from 21 to 26 years old, participated in the experiments. All participants had normal or corrected-to-normal vision and were right-handed and naive with respect to the purpose of the experiment. Participants signed informed consent prior to the experiment and received a compensation of 10 Euros per hour. The study was approved by the ethics committee of the LMU Munich and carried out in accordance with the Declaration of Helsinki.

Stimuli

All visual stimuli were generated using the software Psychopy 2020.1.2 [RRID:SCR_006571, Ref.[17]] based on Python 3.7, presented on a ViewPixx Lite 2000A display, with a resolution of 1920 × 1200 pixels at a refresh rate of 120 Hz, controlled by a Radeon Pro WX 5100 graphics card.

All stimuli were presented on a neutral gray background (106.7 cd/m^2). The fixation dot (radius 0.6°), if presented, was always shown at the screen center (Fig. 1). A reference consisted of a pair of line segments (length:

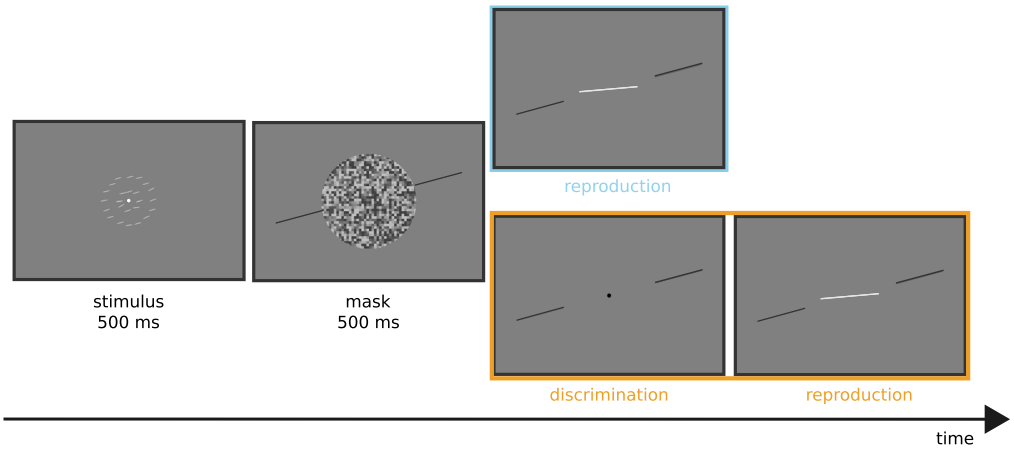

Figure 1. Experiment paradigm. A 500-ms presentation of the ensemble display was followed by a 500-ms circular white noise mask. A reference was presented simultaneously with the mask display and lasted until the end of the trial. Observers had to reproduce the mean orientation of the ensemble with a computer mouse, with (the dual-task blocks, colored orange) or without (the single-task blocks, colored blue) a preceding discrimination task. The task required them to indicate whether the mean orientation was CW or CCW of the reference orientation.

5°, line width: 0.074°), both positioned 5° from the screen center and were colinear, indicating a reference orientation. The ensemble display consisted of 24 tilted bars (length 0.6°, width 0.1°), arranged on a grid of two concentric circles, 8 bars positioned on an inner circle with a diameter of 1.0°, 16 bars positioned on an outer circle with a diameter of 2.5°. Small independent variations were applied to the positions of the bars by adding random shift values (sampled from $\mathcal{N}(0, 0.1°)$) on x-y coordinates. The mask display was a circular patch of white noise (contrast 0.5, spatial frequency 0.03 c/deg). The mask display was positioned at the screen center, with a diameter of 10° for masking the entire ensemble stimuli, or a diameter of 15° for masking the entire display after the trial.

The reference orientations were randomly chosen from 15°, 45°, 75°, 105°, 135°, and 165° (note the 0° is the vertical). The averaged orientation of the tilted bars was randomly probed around the corresponding reference orientation, with a step of 3° in a range of $[-18°, 18°]$. The variation of the orientations within the ensemble display had two versions: a low-noise version, in which all bars had the same orientation (i.e., 0° of orientation noise), and a high-noise version, in which the orientations randomly varied according to a normal distribution with a standard deviation of 9°.

Procedures

During the experiment, the subject sat in a dimly lit room and viewed the display binocularly from a distance of 57 cm. The fixation dot was present during the stimulus presentation and response waiting period. Participants were instructed to maintain their eyes on the fixation dot during the trial.

A trial started with a white fixation dot, shown in the center of the screen for 500 ms. Then, an ensemble display with 24 tilted bars appeared for 500 ms, followed by a 500-ms mask display with circular white noise, preventing any afterimage effects. After the ensemble display vanished, a reference was presented simultaneously with the mask display, remaining visible until the final response.

Participants were given two types of block-wise tasks: a single-task and a dual-task. To minimize explicitly using the reference in the single-task condition, the dual-task condition was introduced only after participants completed all required single-task blocks. The single task involved an orientation reproduction, where participants adjusted the orientation of a white line (length 3.0°, initial orientation randomly chosen from 0° to 180°) at the screen center to indicate the perceived average orientation of the ensemble bars. By moving a computer mouse up or down, they could adjust the line's orientation. Participants had to confirm the final orientation judgment by pressing the space key. Following the response, a mask display appeared for 500 ms to minimize cross-trial carryover effects.

The dual-task consisted of the orientation reproduction from the single task and a discrimination task. In the discrimination task, participants had to judge whether the averaged orientation was clockwise (CW) or counterclockwise (CCW) relative to the reference orientation by pressing the left or right key of the mouse. The discrimination task was conducted before the reproduction task, with a black fixation dot indicating the discrimination task. If the response time exceeded 4 seconds for discrimination or 8 seconds for reproduction, the corresponding trial was discarded and repeated at the end of the same block. Discarded trials were rare, on average 0.43%. The average response time was 2.04 ± 0.96 seconds.

Each block consisted of 156 trials, resulting from the full combination of the reference orientations (6 levels), the corresponding stimulus orientations (13 levels per reference orientation), and the two noise levels (high vs. low). The combination was randomized within each block. In total, there were ten blocks: five blocks for the single task, and five blocks for the dual task, yielding 1560 valid trials in total. Before the main experiment, participants completed a practice block (156 trials) with feedback texts showing the error value of the reproduction (single-task) or the correctness of the discrimination judgment (dual-task).

Data analysis

Data analysis was performed for individual participants' datasets as well as for the pooled data. For the discrimination task, we fitted a cumulative Gaussian function to the binary responses using the Psignifit package[18], and estimated lapse and guess rates, the point of subjective equality (PSE), and the standard deviation of the function. The PSE corresponds to the 50% threshold of the psychometric function, and the standard deviation of the cumulative Gaussian function corresponds to the reciprocal of the psychometric function slope.

For the reproduction task, we first measured the reproduced orientation relative to the reference, $\Delta\omega$, as

$$\Delta\omega = \bar{\omega} - \omega_{ref}, \tag{1}$$

where $\bar{\omega}$ was the reproduced stimulus orientation and ω_{ref} was the reference orientation, and we plotted the histogram of the estimates $\Delta\omega$ (Fig. 3). To compare the distributions of estimates between conditions quantitatively, we fitted a symmetric Gamma mixture model to the data. The model can capture and describe the potential bimodality and skewness of the distribution. The model is a mixture of two identical Gamma density functions, denoted as $\Gamma(\alpha, \theta)$, each characterized by a shape parameter α and a scale parameter θ. The variance of each density function is thus $\alpha\theta^2$. The model parameters were optimized by minimizing the non-linear least squares, and the optimized parameters with 95% confidence intervals were compared within participants.

To compute the repulsive bias, we selected the trials with the estimates indicating correct orientation judgment. Note that, given there was no direct measurement of judgment correctness in the single-task condition, we classified the correctness of judgment based on the subject's estimates in the reproduction task rather than the explicit judgment responses in the discrimination task. A reproduction response was deemed correct when the estimate fell on the same CW/CCW side of the reference as the true stimulus orientation. Approximately 83.14% of the total trials were selected for the analysis (49.73% were from the single-task condition, and the rest

were from the dual-task condition). The repulsive bias was determined as the bias of the estimate, with a positive sign indicating repulsive bias away from the reference.

Modeling

We used a two-component encoding-decoding model based on previous studies[10,11], which included two main components: a measurement distribution and a weighting function. The measurement distribution represented the noisy encoding of stimulus orientation. It was modeled as a Gaussian $N(\mu, \sigma)$, with mean μ and variance σ, where σ represented the variability of sensory representations and thus could vary between stimulus noise levels. At the decoding stage, the sensory representations were re-weighted by multiplying the measurement distribution with a weighting function. We modeled this weighting function as a symmetric gamma mixture of two identical Gamma density functions that integrate to 1:

$$f(\omega; \alpha, \theta, \delta) = \frac{1}{2} \cdot g(\omega; \alpha, \theta, \delta) + \frac{1}{2} \cdot g(\omega; \alpha, \theta, -\delta),$$

where ω represents orientation in measurement distribution and g is a Gamma density function

$$g(\omega; \alpha, \theta, \delta) = \frac{1}{\theta^{\alpha} \cdot \Gamma(\alpha)} \cdot (\omega - \delta)^{\alpha - 1} \cdot e^{\left(-\frac{\omega - \delta}{\theta}\right)},$$

with parameters of shape α, scale θ, and shift δ, and with a Gamma function $\Gamma(\alpha)$. To capture changes due to explicit judgment at the decoding stage, we allowed for different weighting functions between two task conditions (single-task and dual-task). The model also included a constant motor bias term ϵ independent of conditions. Altogether, the model had two parameters σ_l and σ_h for the noise levels, six parameters defining the weighting functions (α_s, θ_s and δ_s for the single-task condition; α_d, θ_d and δ_d for the dual-task condition), and a motor bias term ϵ.

The optimal parameters were estimated by maximizing the likelihood of measured data given the model using the Nelder-Mead algorithm[19]. All trials were included for the optimization. The optimization was performed with bootstrapping 100 times for each subject's data and for the pooled data. Our model was designed to account for both the mean and full distribution of the participants' estimates. Therefore, for each stimulus orientation, 500 samples were randomly drawn from the combination of the measurement distribution and the weighting function. This resulted in a set of predicted estimates, rather than mean or mode, that were analyzed in the same way as the experimental data.

Results

Behavioral results

To examine whether a reference orientation could bias the subject's estimate of a preceding stimulus orientation, we analyzed and compared the estimates under different noise and task conditions.

We first evaluated the discriminability of reference and stimulus by fitting psychometric functions to the explicit judgment responses in the dual-task condition. Discrimination data under this condition showed that all participants were able to perform the task (Fig. 2a, see Fig. S1 for individual data). For the pooled data, the discrimination threshold increased from $5.16° \pm 0.30°$to $6.39° \pm 0.44°$ with increasing stimulus noise levels. Likewise, stimulus noise elevated the discrimination thresholds for all individuals (sign test $p = .031$, Fig. 2b). There was no difference in the PSEs between the two noise conditions (sign test $p = .999$).

We then evaluated the bimodality of the distribution of estimates, a characteristic that previous research has identified as a crucial aspect of the reference repulsion effects[10]. Fig. 3 shows the distributions of estimates under different noise and task conditions. We applied Hartigan's dip test of unimodality[20] to examine the multimodality of the distributions. For the pooled data, the distribution of estimates did not show multimodality under the single-task condition (dip test $p = .120$ for low noise stimuli, $p = .682$ for high noise stimuli), while the estimates of the dual-task condition followed bimodal distributions (dip test $p < .001$ for both low and high noise stimuli).

To further compare the distributions under the two task conditions, we fitted a symmetric mixed Gamma distribution to the distribution of estimates and subsequently compared scale (θ) and shape (α) parameters, which characterize the spread and skewness of the fit, respectively. For four out of five participants, both parameters were significantly different, with lower values of the scale parameter and higher values of the shape parameter under the dual-task condition compared to the values under the single-task condition (Fig. 4a,b, see Fig. S2 for individual's parameters with 95% confidence intervals). This resulted in the variance of the fitted Gamma distribution, derived as $\alpha\theta^2$, being lower under the dual-task condition than under the single-task condition (Fig. 4c). The comparison results did not depend on the specific fitting method. Similar results were obtained by fitting the distribution with a mixture of two identical Gaussian density functions or a mixture of two identical Gamma density functions with shifts.

Correspondingly, we compared the variability of all estimates under different conditions. As Fig. 4d shows (see Fig. S3 for individual data), the estimates showed larger standard deviations in the single-task condition than in the dual-task condition for most individuals (four out of five participants), while participants did not show consistent differences in standard deviations between noise conditions.

For all participants, the estimates were biased away from the reference when the stimulus orientation was close to the reference orientation (Fig. 5a). The repulsion effect was more pronounced in the dual-task than in the single-task condition. In line with previous findings[10–12,15], the repulsion effects weakened with increasing difference between stimulus and reference orientation (Fig. 5b, also see Fig. 8a for individual data). Stimulus noise elevated the repulsive bias of most stimulus orientations (82.8% of individual's repulsive biases under the

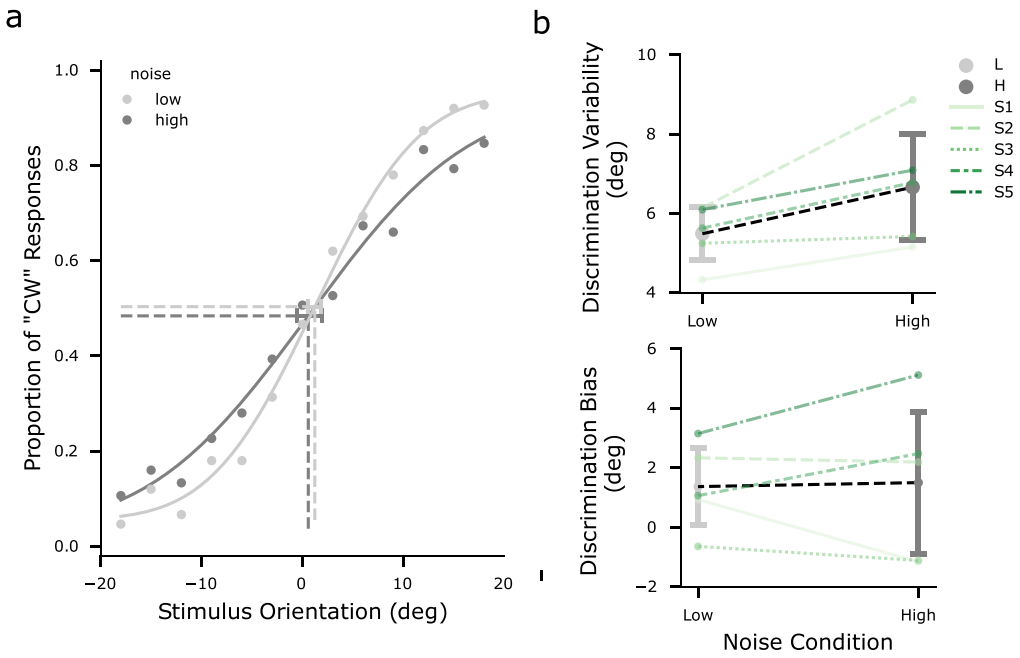

Figure 2. Discrimination data in the dual-task condition. (**a**) Mean proportion of clockwise (CW) responses and associated cumulative Gaussian psychometric functions, separated for low (light gray) and high (dark gray) noise levels. The x-axis represents the stimulus orientation relative to the reference orientation. Positive values indicate orientations clockwise to the reference line. Data points were pooled from the dual-task condition of all participants' data. Vertical dashed lines denote PSEs for the two conditions. The error bar denotes one standard error of the associated PSE. (**b**) Estimated parameters of the psychometric function. Top: Discrimination variability; Bottom: Discrimination bias (PSE). Data points denote averages across all participants, error bars denote standard deviations. Dashed lines connect individual's estimates of each noise condition.).

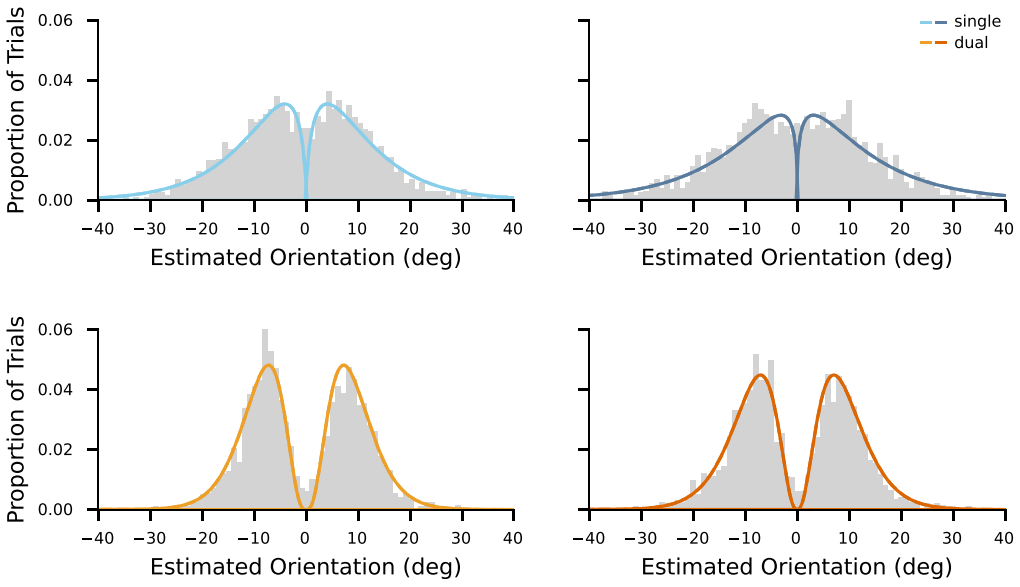

Figure 3. Distributions of all participants' pooled estimates under different conditions. The x-axis represents the estimated orientation relative to the reference orientation. Curves denote the symmetric mixed Gamma density functions fitted to the distributions of estimates. The four colors of the lines represent the four conditions, where hues correspond to task conditions and shades correspond to noise levels (darker shades correspond to higher stimulus noise).

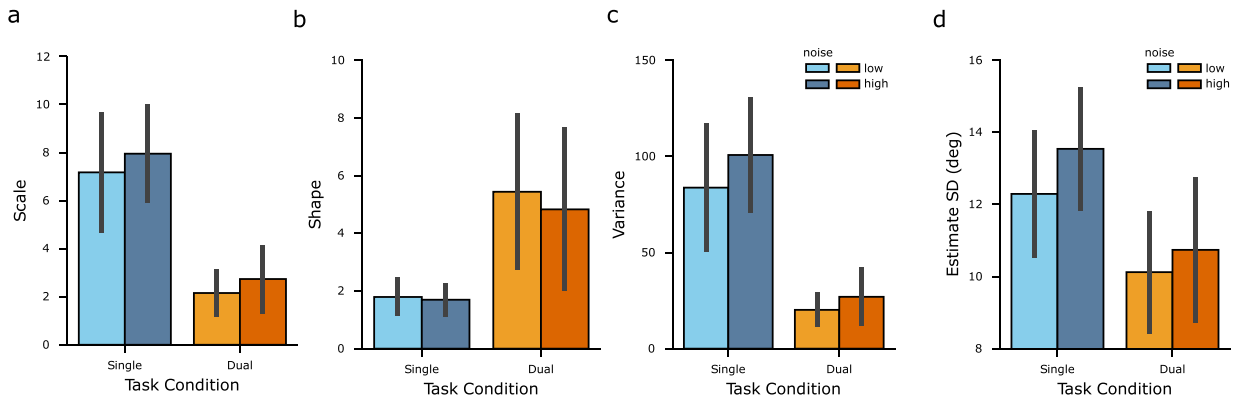

Figure 4. Characteristics of the distributions of estimates. (**a**–**c**) Parameters of the fitted symmetric mixed Gamma density functions. (**a**): scale parameter; (**b**): shape parameter; (**c**): derived variance. Error bars denote ±1 standard deviation across participants. (**d**) Standard deviations of participants' estimates. Error bars denote ±1 standard deviation across participants. The four colors represent the four conditions, where hues correspond to task conditions and shades correspond to noise levels.

single-task condition and 71.4% of individual's repulsive biases under the dual-task condition). Interestingly, for stimulus orientations with larger differences (above 6°) from the reference orientation, the repulsive biases were smaller under the dual-task condition compared to those under the single-task condition. Note that these repulsive biases were negative, indicating that for these stimuli the reference induced larger attraction effects under the dual-task condition compared to the single-task condition.

The overall results demonstrate that in the dual-task paradigm, participants' estimates were biased away from a post-stimulus reference, presenting characteristic features of reference repulsion. Moreover, the distribution of these estimates was quantitatively distinct compared to those observed in tasks that did not require an explicit discrimination response.

Modeling results

Reference repulsion has been hypothesized as a consequence of a decoding strategy in which sensory neurons are weighted according to their contributions to the discrimination between reference and stimuli. This strategy is mathematically described by an encoding-decoding model[10]. However, it remains unclear whether this model could account for the repulsion induced not only by simultaneously presented reference and the stimulus but also by a post-stimulus reference. Furthermore, the distinction between implicit and explicit discrimination and its impact on reference repulsion is still under investigation. To address these questions, we adopted an encoding-decoding model.

We assumed that the post-stimulus reference influences discrimination choices by re-weighting representations in working memory. In probabilistic terms, inferring an estimate involves combining a measurement distribution derived from sensory encoding with a re-weighting profile during the late stage of decision-making. Based on this assumption, we developed a two-component encoding-decoding model, consisting of a measurement distribution centered on the true stimulus orientation and a weighting function featuring a profile that was symmetrical around the reference boundary and had a mixed Gamma density function.

We derived the parameters of the model by maximizing the likelihood of the subject's estimates. It is important to note that the variability of measurements was influenced by both external and internal noise during stimulus encoding. Consequently, we compared the measurement distributions across noise conditions. Furthermore, since the two task conditions differed in terms of whether they involved an explicit choice at a late stage, we compared the weighting functions between the conditions to investigate any potential difference. As Fig. 6a shows, the spreads of the measurement distributions increased with increasing the noise level of the stimulus (a sign test of $p < .001$). The estimated weighting functions showed different profiles between the task condition (Fig. 6b). While the averaged weighting functions among participants peaked at similar positions (around ±7°) in both task conditions, the weighting functions displayed a lower degree of concentration in the single-task condition compared to the dual-task condition for all participants, represented by larger means and broader ranges (both with a sign test of $p < .001$). The models accurately predicted the entire distribution of the estimates (Fig. 7a), the explicit judgment responses (Fig. 7b), as well as the repulsive biases (Fig. 7c, and see Fig. 8 for individual's results).

In light of these results, we conclude that an encoding-decoding model can account for orientation estimates in the presence of a post-stimulus reference orientation, suggesting that participants use the reference-relevant information to derive an estimate by re-weighting the preceding sensory information. This re-weighting strategy appeared relevant for an explicit discrimination judgment, as evidenced by re-weighting profiles that showed a higher degree of concentration when an explicit choice was required.

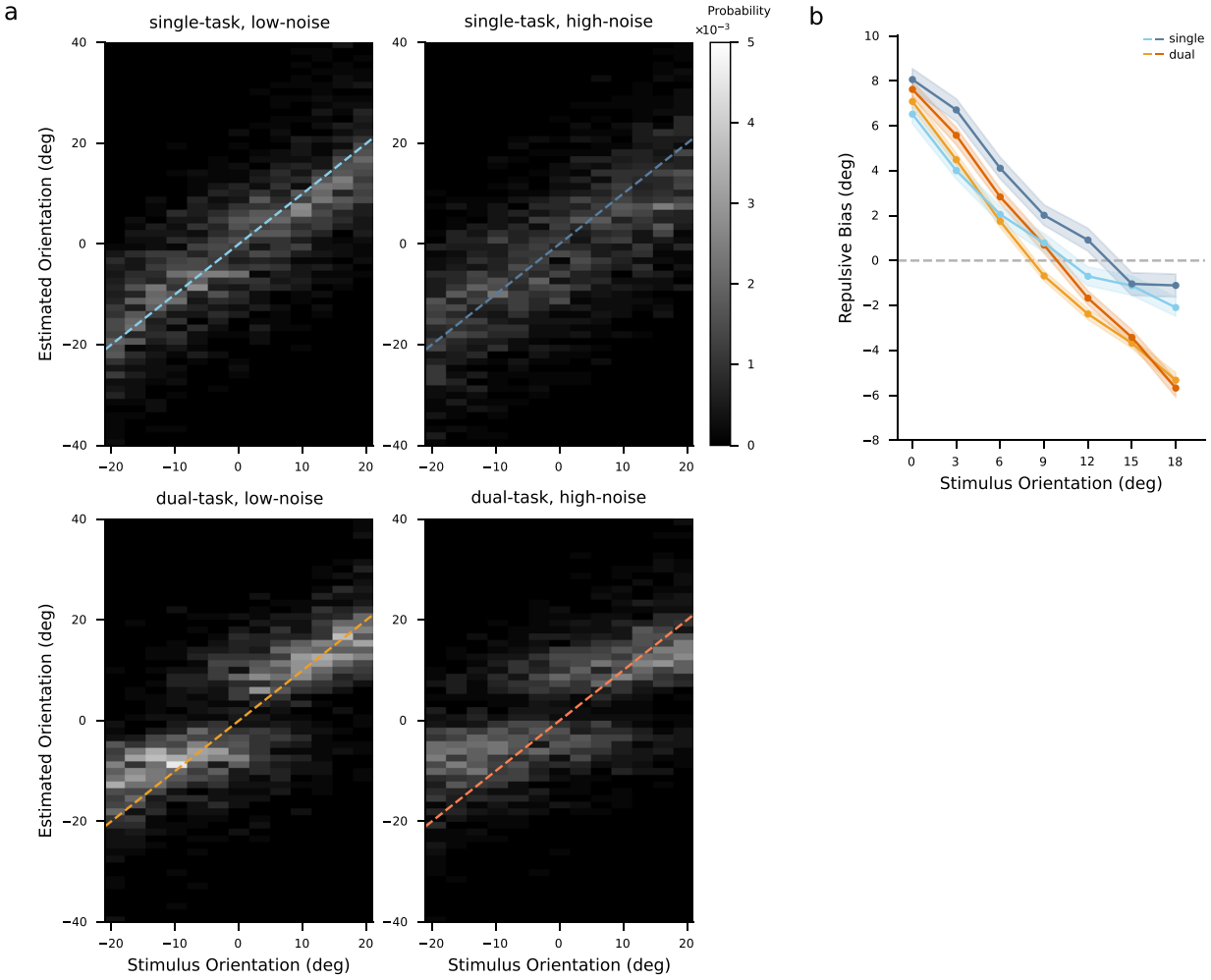

Figure 5. Estimates distribution and repulsive bias. (**a**) Distributions of all participants' pooled estimates for each particular stimulus orientation. Probability is presented by gray level. Values on the x-axis and y-axis are orientations relative to the reference orientation. The dashed lines indicate where estimated orientations are equal to stimulus orientations. (**b**) Repulsive bias of all participants' pooled data. Data are from trials where the subject's estimates indicated that the subject correctly judged the side (CW/CCW) of the reference orientation on which stimulus orientation fell. The x-axis represents the absolute difference between the stimulus orientation and the reference orientation. Shades denote one standard error of the mean. The four colors represent the four conditions, where hues correspond to task conditions and shades correspond to noise levels.

Discussion

The perception of visual stimuli is susceptible to the context in which they are presented, and specifically, judgments of a stimulus feature tend to be biased away from a reference that shares a similar feature. The present study investigated whether such repulsion effects can be induced by a reference presented after the stimulus. We found that participants' estimates of the mean orientation of ensemble stimuli were biased away from a post-stimulus reference. These repulsive biases showed the typical characteristics of the reference repulsion effect, which indicates that the repulsive bias occurred during a late stage of visual decision-making. Moreover, the explicit discrimination judgment made by participants between the stimulus and reference impacted on the magnitude and direction of these biases. This impact can be explained by an observer model that accounted for the differential re-weighting of sensory representations between implicit and explicit processes.

A novel paradigm with a post-stimulus reference

Our experimental paradigm complements previous studies that used a reference simultaneously presented with the stimulus [9-11]. Instead, we employed a post-stimulus reference, which we demonstrated can induce repulsion effects on the judgment of the preceding stimulus. It is important to note that while the reference influenced the participant's estimates of the preceding stimulus, it is unlikely to reflect backward masking effects induced by the reference[21]. In contrast to the brief stimulus presentations (typically less than 50 ms) that have

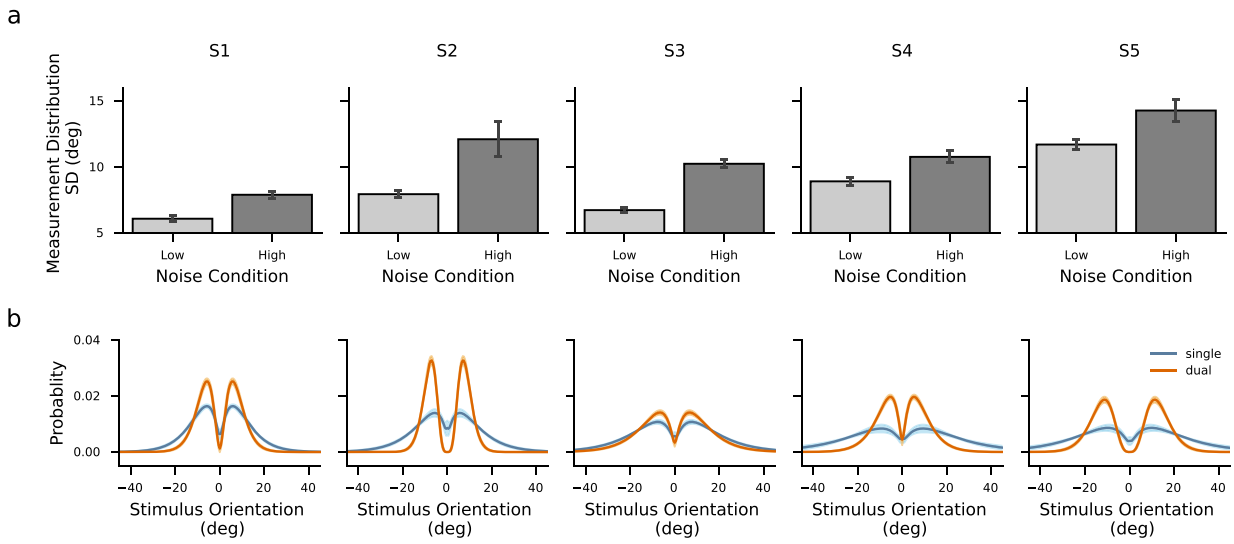

Figure 6. Recovered models for individual participants. (**a**) Standard deviations of estimated measurement distributions. Error bars denote ±1 standard deviation of 100 bootstrapped estimates. (**b**) Estimated weighting functions. Shaded areas around the curves denote ±1 standard deviation of 100 bootstrapped estimates.

been used to induce backward masking effects[22], the stimulus in our study had a presentation duration of 500 ms, which was sufficiently long for conscious visual processing of the stimulus.

Similarly, it is unlikely that the stimulus biased the perception of the subsequent reference. If the reference was systematically biased by the stimulus, we would expect consistent biases across individuals and noise conditions in the discrimination data. However, this was not observed (Fig. 2b). Moreover, considering that reference repulsion effects typically involve working memory[15], it is unlikely that the reference presented throughout the tasks would be memorized and then biased by the stimulus. Nevertheless, our results are based on the comparison of reference-induced repulsion effects across the two task conditions. Even if any of the effects considered above were present, they would have been consistent across both conditions and thus would not substantially influence our conclusions.

Reference repulsion as a late decision-related bias

Our findings show that the presence of a reference during the target stimulus presentation is not necessary for reference repulsion effects to occur. This provides compelling evidence that reference repulsion bias can be a late decision-related bias[11,12,14,15], as opposed to an exclusive early-stage bias resulting from encoding or even decoding at the time of stimulus presentation[10,13], particularly when considering the impact of the post-stimulus reference on the reproduction of a preceding stimulus.

Thus, our findings align with existing theories on information integration during late-stage perceptual inference processes[11,12,15]. Specifically, our dual-task results agree with the self-consistency theory, which posits that categorical judgments generate top-down expectations that serve as a categorical prior[12,15]. Our results extend this theory by suggesting that these categorical priors can not only reflect expectations before the exposure to sensory evidence, but can also be formed in a subsequent event, updating sensory representations in working memory.

Our results suggest that the reference repulsion effect results from the combination of contextual information and sensory representations in the perceptual inference process. However, it remains unclear whether this combined probabilistic information directly replaced the representation in working memory. According to Luu & Stocker[15], categorical judgments introduce biases in a downstream process from working memory. In their study, participants flexibly recombined probabilistic information in working memory recall, based on feedback about their categorical judgments, maintaining self-consistency. Further research could explore whether judgments directly modify working memory representations, with a particular focus on the necessity of explicit judgment in these interactions.

Biases in the dual-task condition

Our results showed that reference repulsion displayed the typical characteristics previously reported, such as consistency with preceding discrimination choices, increased biases for stimulus orientation closer to the reference, and a systematic influence from stimulus noise[10]. In the dual-task condition, our findings clearly aligned with these characteristics, while we also found that, for some subjects, the estimates for the stimulus orientation dissimilar to the reference displayed a greater attraction towards the reference than previously reported[12,15].

To examine whether these attraction biases resulted from the post-stimulus reference, we conducted a control experiment with two participants under the dual-task condition. Unlike the main experiment, where the reference was presented after the stimulus, in this control experiment, the reference and the ensemble stimulus were presented simultaneously. For the participant who exhibited fairly large attraction biases in the main experiment

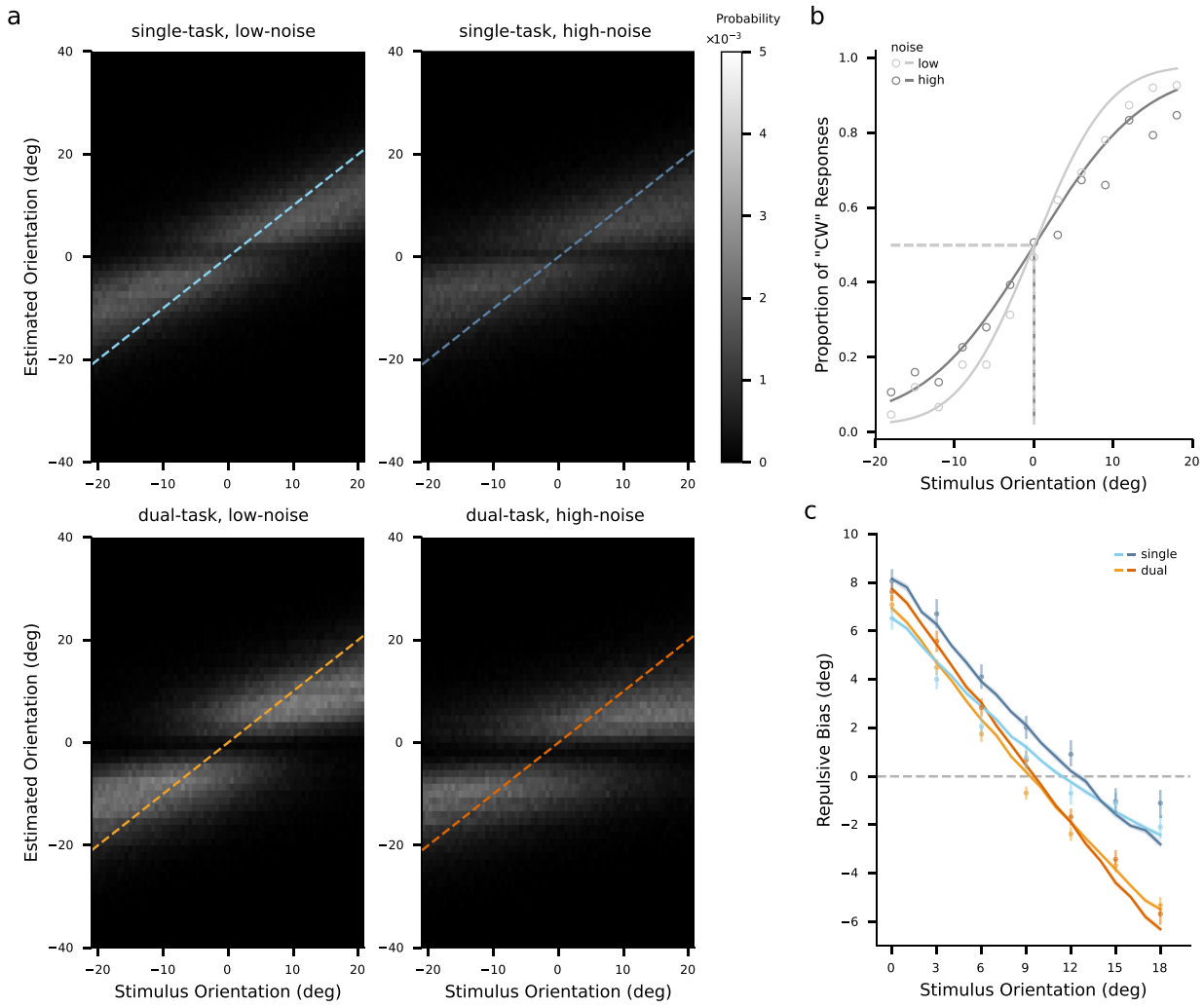

Figure 7. Pooled model prediction for all participants. (**a**) Distributions of estimates predicted by the estimated model for each particular stimulus orientation. The density was presented with a lightness scale. All the values on the x-axis and y-axis are orientations relative to the reference orientation. The dashed lines indicate where estimated orientations are equal to stimulus orientations. (**b**) Psychometric functions of predicted explicit judgment as "the stimulus orientation is more clockwise than the reference orientation". The x-axis represents the stimulus orientation relative to the reference orientation. Data are from all participants' pooled judgment responses under the dual-task condition (open circle; same as the data in Fig. 2). Solid lines denote the cumulative Gaussian function fitted to the model prediction. Dashed lines denote the 50% threshold of discrimination. The error bar denotes one standard error of the estimated 50% threshold. (**c**) Repulsive bias predicted by the model (solid lines). Data are repulsive bias of all participants' pooled data (dots; same as the data in Fig. 5b). The x-axis represents the absolute difference between the stimulus orientation and the reference orientation. Shades denote one standard error of the mean of 100 bootstrapped model predictions.

(S1), the simultaneous presentation significantly reduced the attraction biases (ANOVA tests $p < .001$ for all stimuli with a distance larger than 9°). However, there was no significant difference between the main and control experiments for the other participant (S3), likely due to this participant displaying relatively small attraction biases (Fig. S4). Therefore, it is plausible that the post-stimulus reference introduced greater attraction compared to a reference presented simultaneously with the stimulus, as participants may rely more on decision categories when sensory representations decayed in working memory[23].

An alternative explanation for the attraction bias is that participants might form and utilize prior expectations regarding the range of the stimuli[24,25]. This notion is supported by the observations of attraction biases when participants were given explicit cues about the stimulus range (see Experiment 2 in[12]). In our study, we chose the reference orientations from eight fixed values, leading to a less stochastic stimulus sampling compared to previous studies[10,12]. As participants were exposed to these stimulus orientations across trials, they may have become familiar with the statistical regularities of the reference orientations and implicitly learned that the stimulus orientations consistently fell within a certain CW/CCW range (±18°) around the reference. Consequently,

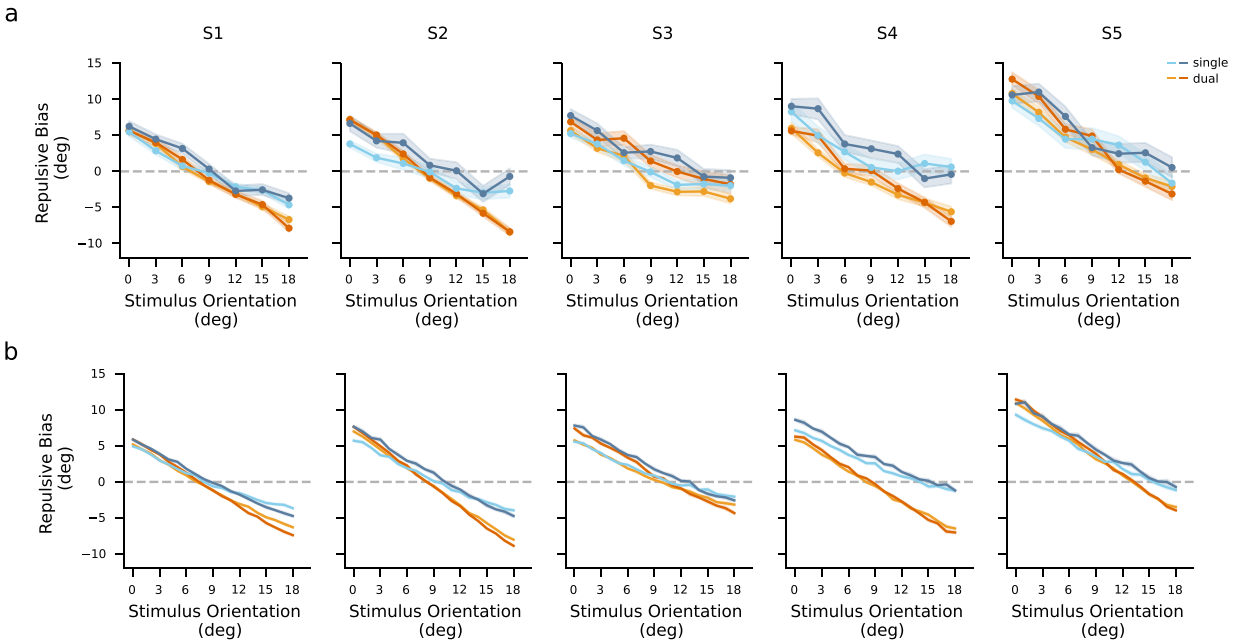

Figure 8. Measured and predicted repulsive bias of individuals. (**a**) Measured repulsive bias of individual participants. Data are from trials where the subject's estimates indicated that the subject correctly judged stimulus orientation relative to the reference orientation. (**b**) Model prediction of individual's repulsive bias. The x-axis represents the absolute difference between the stimulus orientation and the reference orientation. Shades denote one standard error of the mean. The four colors represent the four conditions, where hues correspond to task conditions and shades correspond to noise levels.

participants may have formed prior beliefs corresponding to the stimulus range, resulting in estimates being attracted toward the center of these expectations (i.e. around 9° CW/CCW to the reference).

Biases in the implicit process

We observed reference repulsion effects even in the absence of an explicit task directly related to the reference. This distinguishes our study from previous studies that employed an explicit discrimination task in the paradigm[10,12]. Instead, we employed a paradigm where the reference was only presented after the target stimulus, avoiding any contextual modulation of the reference during stimulus encoding, which excludes the classic tilt effect[3] that occurs when the stimulus and reference are presented simultaneously, or the tilt after-effect if the reference precedes the target stimulus. Therefore, our results provide further confirmation of earlier evidence of repulsion biases that arise during passive viewing of the reference and involve the implicit processing of reference-related information[11,14,15].

Similarly, implicit repulsion effects have also been observed in studies focusing on working memory[26–29]. Although these studies did not explicitly employ a stimulus as a reference, participants implicitly compared the memorized stimuli, resulting in repulsive interactions. Various theories have attempted to explain these repulsion effects. For example, Ding et al.[28] suggested that the heightened difference between the stimuli yielded a temporal repulsion effect when participants performed a successive reproduction task involving two orientations. These findings indicate that the implicit use of ordinal information constrains the decoding of working memory representations. Alternatively, an adaptive perspective of inter-item bias proposes that repulsion occurs between similar stimuli[27,29], while attraction occurs between dissimilar stimuli, thereby balancing accurate and distinct representations.

Despite the diversity of interpretations and methodologies, previous studies, in line with our findings, consistently demonstrate implicit repulsive exaggeration between similar stimulus representations in working memory. In our study, even though the reference was not a memorized item, these exaggerations may have helped participants to implicitly avoid overlapping representations.

Comparison between the single-task and dual-task conditions

We found distinct reference repulsion effects between the two task conditions and proposed a re-weighting account that differentiated between implicit and explicit processes as a plausible explanation for the observed behavior. However, it is important to consider alternative explanations for these differences.

One possibility is that, during the reproduction phase of the dual-task condition, participants intentionally adjusted the probe further away from the reference due to the forced discrimination choice. This adjustment may have exaggerated the orientation difference between the stimulus and the reference. Such a strategy could be adopted to maintain the participant's self-consistency[12] when the difference between the stimulus and the

reference was too small or near zero. Consistent with this expectation, we found that the magnitude of the repulsion bias when the stimulus orientation aligned with the reference orientation (7.35° ± 2.47°, averaged across subjects and noise levels in the dual-task condition) matched the just noticeable difference (7.37° ± 2.11°, averaged across subjects and noise levels) in the discrimination task. However, this explanation fails to account for the attraction bias towards the reference observed for stimuli with orientations that were significantly different from the reference orientation.

Another difference between the two task conditions is the memory delay before the reproduction phase. If the stimulus representations were held in working memory until the reproduction phase and read out specifically for the reproduction task, one would expect a larger variance in participant's estimates due to larger internal memory-related noise[30–32]. However, our results do not support this hypothesis. In fact, the total time to complete was not significantly different between the dual-task and the single-task (repeated measure ANOVA, $p = .025$, see Fig. S5). Moreover, participants spent more time with the high noise stimulus when the task involved explicit judgment (interaction between noise and task conditions, repeated measure ANOVA $p = 0.002$). Additionally, the reaction times were shorter under the dual-task condition than the single-task condition for most participants, although a repeated measure ANOVA test showed a significant difference only for the interaction between the task and noise conditions ($p = .025$). These comparisons of the reaction times suggest that the explicit discrimination response sped up the following reproduction task, indicating that the readout of the stimulus representation occurred at the first relevant task. Thus, the memory decay account cannot fully explain our results. However, it remains unclear whether the readout would be equivalent in terms of representation quantities and neural mechanisms to the readout for the following accurate reproduction.

Furthermore, it is also unlikely that the differential effects observed are attributable to learning over experiment blocks and task conditions. Perceptual learning has been shown to occur over trials and blocks, reducing perceptual variability[33–35]. Therefore, one might expect a decrease in the variance of the estimates over blocks, especially considering the possibility that participants learned to use the reference. Data from two participants who repeated the experiment under the single-task condition after completing the main experiment (Fig. S6) showed sharp transitions between the dual-task and single-task blocks, suggesting that the variability of the participants' estimates was immediately reduced by the explicit discrimination, rather than gradually decreased over time through learning (Fig. S6a). These results also imply that participants were unlikely to learn to use the discrimination judgment before being exposed to the instruction of the explicit discrimination task. Interestingly, the effects of explicit discrimination were reversible and anchored to the relevant task for both participants, evidenced by no significant difference in the standard deviations of estimates between the first and repeated single-task conditions (Levene's test $p > .05$ for both participants, see Fig. S6b).

Therefore, our results strongly support genuine distinctions between explicit and implicit processes, which may reflect the employment of different strategies for utilizing sensory information in visual perception, depending on the availability of categorical context. The re-weighting model we adopted is not limited to early visual processing or specific behavioral paradigms[10], suggesting a fundamental disparity in information utilization between explicit and implicit processes, which may apply to other findings on sensory information processing. Studies across various topics have reported non-normative patterns of information integration in explicit processes. For example, in visual search, Hansmann et al.[16] found that the explicit encoding of ensemble representations is based on summary statistics, whereas the implicit assessment encodes ensembles with rich details. Similarly, Chen et al.[36] found differences in the use of category information between implicit and explicit processes in category-based induction. When predicting the direction of moving geometric figures that were categorized by learning, participants were more likely to integrate information across categories in the implicit process, whereas the explicit process was dominated by single-category information. Consistent with these theories, our model suggests that the explicit process prioritizes the coarse information about statistical and categorical representations, while the implicit process tends to utilize rich sensory representations.

Finally, the role of explicit choices in contextual information processing remains an open question. Explicit choices may lead to feature-oriented attention and allocate more cognitive resources to the reference[37]. Top-down attentional guidance directs limited cognitive resources towards task-relevant signals for optimal performance[38,39]. Therefore, it is possible that in the present study, participants paid more attention to the reference in the dual-task condition compared to the single-task condition, as they were aware of its relevance to the task. This increased attention to the reference could potentially result in distinct biases between the two conditions. Moreover, explicit choices may alter decision-making, suggested by a recent study showing that explicit choices induce the down-weighting of late evidence in the accumulation of decision-relevant information, which is reflected by pupil-linked arousal[7]. Another possibility is that explicit choices increase the gain of neurons encoding the reference, resulting in contextual modulation of the representation of the stimulus in working memory. Population coding models have extensively explained contextual biases, which posit modulations on the responses of neuronal populations in the visual cortex[6,40–44]. For example, neurons in population codes may adjust their gains to different degrees as a consequence of the context, leading to biases[42,44]. It is conceivable that explicit choices increase the gain around the reference and thus enhance the repulsion effect. However, the traditional population coding model has limitations in explaining the reference-induced attraction effect. Our results suggest a strategy for extending the model to account for the effects of explicit choices by incorporating the reweighting components we identified.

Conclusion

Reference repulsion is a well-known phenomenon that demonstrates how contextual information influences visual perception. Such repulsion may occur at an early, sensory-related stage, or a late, decision-related stage of visual processing. To investigate the influence of the reference during late visual processing, we conducted an

experiment using an ensemble stimulus of orientation, followed by the presentation of a reference orientation. We found strong repulsion effects induced by the post-stimulus reference, as evidenced by the significant bias in participants' reported stimuli. Moreover, the explicit discrimination made between the reference and the stimulus had a notable impact on the magnitude of repulsion effects. This impact can be effectively explained by an encoding-decoding model that differentiates the re-weighting of sensory representations between implicit and explicit processes. In summary, our findings provide evidence that reference repulsion can occur during late visual processing, indicating distinct sensory decoding between implicit and explicit tasks.

Data availibility

The data and code can be found at the G-Node GIN platform: https://doi.org/10.12751/g-node.46h2gl.

Received: 26 July 2023; Accepted: 12 October 2023
Published online: 30 October 2023

References

1. Ross, H. & Plug, C. *The Mystery of the Moon Illusion: Exploring Size Perception* (Oxford University Press, 2002).
2. Rauber, H. J. & Treue, S. Revisiting motion repulsion: Evidence for a general phenomenon?. *Vision. Res.* **39**, 3187–3196 (1999).
3. Gibson, J. J. & Radner, M. Adaptation, after-effect and contrast in the perception of tilted lines. I. Quantitative studies. *J. Exp. Psychol.* **20**, 453 (1937).
4. O'Toole, B. & Wenderoth, P. The tilt illusion: Repulsion and attraction effects in the oblique meridian. *Vision. Res.* **17**, 367–374 (1977).
5. Whittle, P. Brightness, discriminability and the "crispening effect". *Vis. Res.* **32**, 1493–1507 (1992).
6. Klauke, S. & Wachtler, T. "Tilt" in color space: Hue changes induced by chromatic surrounds. *J. Vis.* **15**, 17–17 (2015).
7. Talluri, B. C. *et al.* Choices change the temporal weighting of decision evidence. *J. Neurophysiol.* **125**, 1468–1481 (2021).
8. Spicer, J., Zhu, J.-Q., Chater, N. & Sanborn, A. N. Perceptual and cognitive judgments show both anchoring and repulsion. *Psychol. Sci.* **33**, 1395–1407 (2022).
9. Rauber, H. J. & Treue, S. Reference repulsion when judging the direction of visual motion. *Perception* **27**, 393–402 (1998).
10. Jazayeri, M. & Movshon, J. A. A new perceptual illusion reveals mechanisms of sensory decoding. *Nature* **446**, 912–915 (2007).
11. Zamboni, E., Ledgeway, T., McGraw, P. V. & Schluppeck, D. Do perceptual biases emerge early or late in visual processing? Decision-biases in motion perception. *Proc. Biol. Sci.* **283**, 20160263 (2016).
12. Luu, L. & Stocker, A. A. Post-decision biases reveal a self-consistency principle in perceptual inference. *Elife* **7**, e33334 (2018).
13. Ye, R. & Liu, X. How the known reference weakens the visual oblique effect: A Bayesian account of cognitive improvement by cue influence. *Sci. Rep.* **10**, 20269 (2020).
14. Fritsche, M. & de Lange, F. P. Reference repulsion is not a perceptual illusion. *Cognition* **184**, 107–118 (2019).
15. Luu, L. & Stocker, A. A. Categorical judgments do not modify sensory representations in working memory. *PLoS Comput. Biol.* **17**, e1008968 (2021).
16. Hansmann-Roth, S., Kristjánsson, Á., Whitney, D. & Chetverikov, A. Dissociating implicit and explicit ensemble representations reveals the limits of visual perception and the richness of behavior. *Sci. Rep.* **11**, 3899 (2021).
17. Peirce, J. *et al.* PsychoPy2: Experiments in behavior made easy. *Behav. Res. Methods* **51**, 195–203 (2019).
18. Schütt, H. H., Harmeling, S., Macke, J. H. & Wichmann, F. A. Painfree and accurate Bayesian estimation of psychometric functions for (potentially) overdispersed data. *Vis. Res.* **122**, 105–123 (2016).
19. Gao, F. & Han, L. Implementing the Nelder-Mead simplex algorithm with adaptive parameters. *Comput. Optim. Appl.* **51**, 259–277 (2012).
20. Hartigan, J. A. & Hartigan, P. M. The dip test of unimodality. *Ann. Statist.* **13**, 70–84 (1985).
21. Breitmeyer, B. & Ogmen, H. *Visual Masking: Time Slices Through Conscious and Unconscious Vision* (Oxford University Press, 2006).
22. Breitmeyer, B. G. & Ogmen, H. Recent models and findings in visual backward masking: A comparison, review, and update. *Percept. Psychophys.* **62**, 1572–1595 (2000).
23. Zang, X. *et al.* Duration reproduction under memory pressure: Modeling the roles of visual memory load in duration encoding and reproduction. *bioRxiv*https://doi.org/10.1101/2022.02.10.479853 *(2022).*
24. Teghtsoonian, R. & Teghtsoonian, M. Range and regression effects in magnitude scaling. *Percept. Psychophys.* **24**, 305–314 (1978).
25. Petzschner, F. H. & Glasauer, S. Iterative Bayesian estimation as an explanation for range and regression effects: A study on human path integration. *J. Neurosci.* **31**, 17220–17229 (2011).
26. Kang, M.-S. & Choi, J. Retrieval-induced inhibition in short-term memory. *Psychol. Sci.* **26**, 1014–1025 (2015).
27. Bae, G.-Y. & Luck, S. J. Interactions between visual working memory representations. *Attent. Percept. Psychophys.* **79**, 2376–2395 (2017).
28. Ding, S., Cueva, C. J., Tsodyks, M. & Qian, N. Visual perception as retrospective Bayesian decoding from high- to low-level features. *Proc. Natl. Acad. Sci. U. S. A.* **114**, E9115–E9124 (2017).
29. Chunharas, C., Rademaker, R. L., Brady, T. F. & Serences, J. T. An adaptive perspective on visual working memory distortions. J. Experim. Psychol. Gen. (2022).
30. Wei, X.-X. & Stocker, A. A. A Bayesian observer model constrained by efficient coding can explain 'anti-Bayesian' percepts. *Nat. Neurosci.* **18**, 1509 (2015).
31. Shin, H., Zou, Q. & Ma, W. J. The effects of delay duration on visual working memory for orientation. *J. Vis.* **17**, 10 (2017).
32. Rademaker, R. L., Park, Y. E., Sack, A. T. & Tong, F. Evidence of gradual loss of precision for simple features and complex objects in visual working memory. *J. Experim. Psych. Hum. Percept. Perform.* **44**, 925–940 (2018).
33. Goldstone, R. L. Perceptual learning. *Annu. Rev. Psychol.* **49**, 585–612 (1998).
34. Kattner, F., Cochrane, A. & Green, C. S. Trial-dependent psychometric functions accounting for perceptual learning in 2-AFC discrimination tasks. *J. Vis.* **17**, 3 (2017).
35. Seitz, A. R. Perceptual learning. *Curr. Biol.* **27**, R631–R636 (2017).
36. Chen, S. Y., Ross, B. H. & Murphy, G. L. Implicit and explicit processes in category-based induction: Is induction best when we don't think?. *J. Exp. Psychol. Gen.* **143**, 227–246 (2014).
37. Treue, S. & Martínez Trujillo, J. C. Feature-based attention influences motion processing gain in macaque visual cortex. *Nature* **399**, 575–579 (1999).
38. Folk, C. L., Remington, R. W. & Johnston, J. C. Involuntary covert orienting is contingent on attentional control settings. *J. Exp. Psychol. Hum. Percept. Perform.* **18**, 1030–1044 (1992).
39. Corbetta, M. & Shulman, G. L. Control of goal-directed and stimulus-driven attention in the brain. *Nat. Rev. Neurosci.* **3**, 201–215 (2002).

40. Gilbert, C. D. & Wiesel, T. N. The influence of contextual stimuli on the orientation selectivity of cells in primary visual cortex of the cat. *Vision. Res.* **30**, 1689–1701 (1990).
41. Clifford, C. W., Wenderoth, P. & Spehar, B. A functional angle on some after-effects in cortical vision. *Proc. Biol. Sci.* **267**, 1705–1710 (2000).
42. Schwartz, O. & Simoncelli, E. P. Natural signal statistics and sensory gain control. *Nat. Neurosci.* **4**, 819–825 (2001).
43. Jazayeri, M. & Movshon, J. A. Optimal representation of sensory information by neural populations. *Nat. Neurosci.* **9**, 690–696 (2006).
44. Schwartz, O., Sejnowski, T. J. & Dayan, P. Perceptual organization in the tilt illusion. *J. Vis.* **9**, 19 (2009).

Acknowledgements
Supported by DFG (RTG 2175 "Perception in Context and its Neural Basis"). We thank all participants for participating in the experiments.

Author contributions
All authors designed the study. Y.S. conducted the experiments and performed the data analysis. Y.S., T.W., and Z.S. curated the data. Y.S. wrote the first draft of the manuscript. All authors reviewed and edited the manuscript.

Funding
Open Access funding enabled and organized by Projekt DEAL.

Competing interests
The authors declare no competing interests.

Additional information
Supplementary Information The online version contains supplementary material available at https://doi.org/10.1038/s41598-023-44827-8.

Correspondence and requests for materials should be addressed to Y.S.

Reprints and permissions information is available at www.nature.com/reprints.

Publisher's note Springer Nature remains neutral with regard to jurisdictional claims in published maps and institutional affiliations.

Supplementary Information

Supplementary Methods

Two of five participants completed supplementary experiments after completing the main experiment.

To examine any potential learning effect, we asked two participants to repeat the experiment under the single-task condition after the main experiment. The stimuli and procedures were the same as those in the single-task condition of the main experiment.

To measure the repulsion effect from a reference that is presented throughout the experiment trial, we asked two participants to repeat the experiment under the dual-task condition. The stimuli and procedures remained compared to those in the dual-task condition of the main experiment, while the reference was presented simultaneously with the ensemble and lasted until the final response.

Supplementary Figures

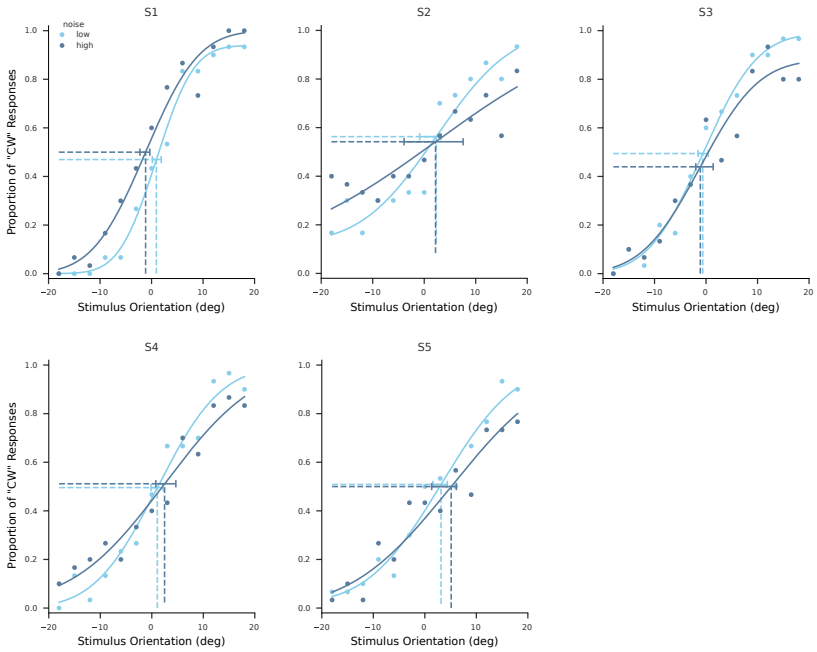

Figure S1: Individual's discrimination data in the dual-task condition: mean proportion of clockwise (CW) responses and associated cumulative Gaussian psychometric functions, separated for the low and high noise levels. The x-axis represents the stimulus orientation relative to the reference orientation. Positive values mean the orientation clockwise to the reference line. Data points were pooled from the dual-task condition of all participants' data. Vertical dashed lines denote PSEs for two conditions respectively, and the error bar denotes one standard error of the associated PSE.

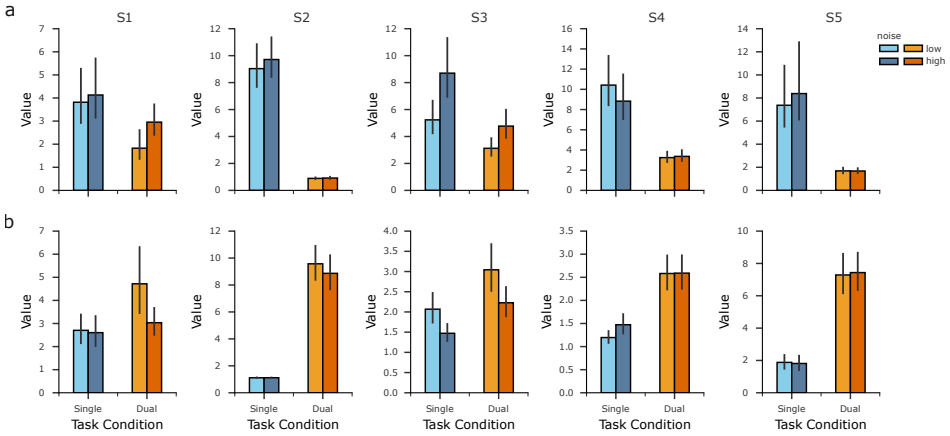

Figure S2: Estimated parameters of fitted symmetric mixed Gamma density functions for individuals. (a): scale parameter; (b): shape parameter. Error bars denote 95% confidence intervals of the estimates. The four colors represent the four conditions, where hues correspond to task conditions and shades correspond to noise levels.

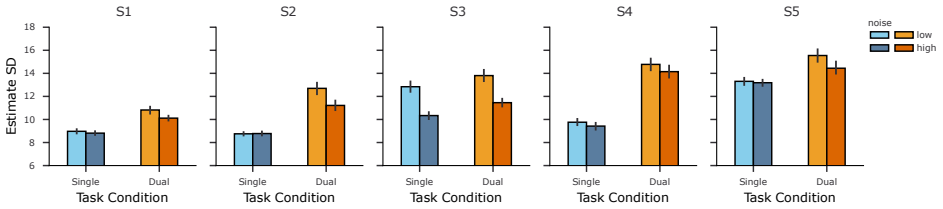

Figure S3: Standard deviations of individual's estimates. Error bars denote 95% confidence intervals of 100 bootstrapping resamples. The four colors represent the four conditions, where hues correspond to task conditions and shades correspond to noise levels.

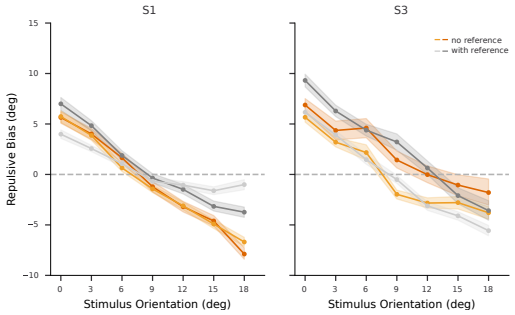

Figure S4: Repulsive bias of two participants' estimates. Data are from trials where the subject's estimates indicated that the subject correctly judged stimulus orientation relative to the reference orientation. The orange colors represent the data under the dual-task condition in the main experiment, where the reference was absent in the stimulus presentation. The gray colors represent the data of a control experiment where the reference was present simultaneously with the stimulus in the dual-task condition. The shades of colors correspond to the noise level. The x-axis represents the absolute difference between the stimulus and reference orientations. Shades denote one standard error of the mean.

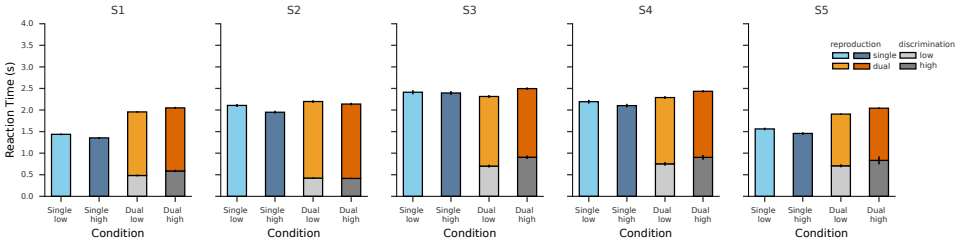

Figure S5: Individual's reaction times for all tasks. The four blue and orange colors represent the four conditions of reproduction reaction time, where hues correspond to task conditions and shades correspond to noise levels. The gray colors represent the noise conditions of discrimination reaction time in the dual-task condition.

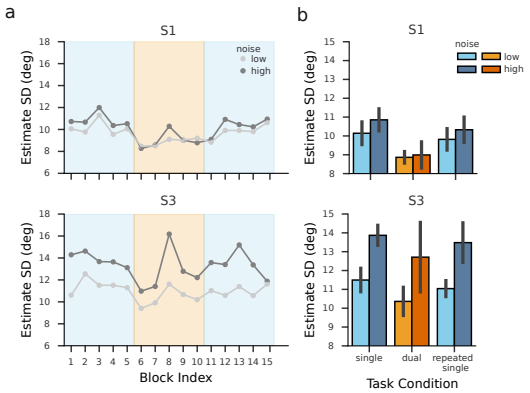

Figure S6: Variations of two participants' estimate standard deviations. (a) The standard deviations of estimates varied over blocks. The shade represents the task condition of the corresponding block (blue: single-task, orange: dual-task). (b) The standard deviations of estimates varied over task conditions. Error bars denote ±1 standard deviation.

4 Reference repulsion effects in hue perception

Manuscript (in preparation for submission): *Su, Y. & Wachtler, T. (2024). Reference repulsion effects in color perception.*

Reference repulsion effects in color perception

Yannan Su[1,2] and Thomas Wachtler[1,4]

[1]Faculty of Biology, Ludwig-Maximilians-Universität München, Planegg-Martinsried, Germany
[2]Graduate School of Systemic Neurosciences, Ludwig-Maximilians-Universität München, Planegg-Martinsried, Germany
[4]Bernstein Center for Computational Neuroscience Munich, Planegg-Martinsried, Germany

Abstract

Visual perception can be biased by contextual information. One phenomenon of contextual influence is reference repulsion: the visual estimates of stimuli are biased away from an explicit reference that shares features with the stimuli, which has been observed in perception of motion direction or orientation. In color vision, while repulsion effects are known to result from colored surrounds, a systematic examination of the repulsion from an explicit color reference is still missing. We used a dual-task paradigm where the subjects were asked to estimate the average hue of a noisy color ensemble after discrimination between the average hue of the ensemble and an explicit reference hue. The estimated hues showed systematic biases away from the reference hues, demonstrating characteristic features of reference repulsion effects. An encoding-decoding model successfully predicted the repulsion effects and explained the nonuniformities that blue and yellow references showed the largest overall repulsion effects. These results suggest a general mechanism for contextual information processing and visual decision-making.

1 Introduction

Our visual percept does not solely depend on the feature of the physical stimulus but is susceptible to contextual information. For example, the color appearance of an apple relies on the color of a fruit bowl: a red apple appears less reddish in a red fruit bowl than in a green fruit bowl. This example also evidences a significant and mysterious feature of contextual biases: visual estimates can be biased and repelled away from the context. Such repulsive biases have been found occurring in temporal, spatial, or instructive contexts (see Schwartz et al. (2007) for a review), across a variety of visual features including orientation (Gibson and Radner, 1937; Fritsche et al., 2020), motion direction (Rauber and Treue, 1998; Jazayeri and Movshon, 2007), and color (Webster et al., 2002; Klauke and Wachtler, 2015).

Among the repulsive biases, one specific repulsion effect, so-called reference repulsion, has been reported arising in the subject's estimate following a discrimination choice. Such repulsion

effects can be measured in a dual-task paradigm including a discrimination task and a succeeding estimation task. When subjects report the feature of a stimulus after comparing it with an explicit reference, the reported feature is systematically biased away from the reference. Such effects are featured with conspicuous characteristics. For example, the reported estimates are usually consistent with the preceding discrimination choices. Moreover, the magnitude of the effect decreases with increasing the feature difference between the stimulus and the reference, and it increases with increasing the stimulus noise (Jazayeri and Movshon, 2007). Reference repulsion was first revealed by studies on the perception of motion directions (Rauber and Treue, 1998; Jazayeri and Movshon, 2007; Zamboni et al., 2016), and then was found in orientation perception (Luu and Stocker, 2018, 2021), numerical decision-making (Talluri et al., 2018, 2021), and cognitive judgment (Spicer et al., 2022). The effects thus seem common across a wide range of processes of perception and cognition. However, it remains little known whether reference repulsion exists for various visual features, such as colors.

In color vision, repulsion effects are known to result from colored surrounds (Klauke and Wachtler, 2015). When subjects adjusted the hue of a stimulus in a neutral gray surround to match it to a test hue embedded in a chromatic surround, the chromatic surround induced hue changes that were repulsive from it. The magnitudes of the repulsion effects increased until reaching a maximum and then decreased with increasing the hue difference between the stimulus and the surround. The effects do not only show similarities to the tilt effect in orientation perception (Gibson and Radner, 1937; O'Toole and Wenderoth, 1977; Smith et al., 2001), but also imply the possibility of resembling the reference repulsion effects. The surround might implicitly play a role as a reference, which could induce repulsive biases without instructing subjects to generate or explicitly report any discrimination choice (Rauber and Treue, 1998; Zamboni et al., 2016; Fritsche and de Lange, 2019; Ye and Liu, 2020). Yet, much less is known about whether an explicit color reference can induce systematic repulsion effects.

A non-negligible characteristic of color perception is the non-unifomity among different hues. Such non-uniformity has been widely reported in hue perceptual variability (Boynton et al., 1986; Krauskopf and Gegenfurtner, 1992; Danilova and Mollon, 2010; Witzel and Gegenfurtner, 2013), chromatic contextual modulation (Klauke and Wachtler, 2015), and color working memory (Bae et al., 2014, 2015). Specifically, studies have consistently addressed the special features of some colors, such as blue and yellow. These colors have been shown lower discrimination thresholds and higher perceptual sensitivity (Boynton et al., 1986; Krauskopf and Gegenfurtner, 1992; Danilova and Mollon, 2010; Witzel and Gegenfurtner, 2013). In a perceptual cone-opponent color space, the contextual biases induced by colored surrounds have shown the largest magnitudes along an oblique, blue-yellow axis (Klauke and Wachtler, 2015). Taken together, it begs the question that, if color reference induces repulsion effects, whether these effects are different for distinct colors. Thus, another aim of our study was to compare the reference repulsion effects among colors.

In the present study, we examined the reference repulsion effects in color perception, by measuring the subject's estimates of the hue ensemble following an explicit comparison between the ensemble and a color reference. We observed that hue estimates were biased away from the reference, along with characteristic features of the reference repulsion effects. Despite similar patterns of the effects for different hue references, the strongest overall repulsion occurred around blue

and yellow hues. Such non-uniform repulsion biases were explained by an encoding-decoding model, indicating that both encoding precision and reweightings of sensory representations were different for different colors.

2 Methods

2.1 Subjects

Nine subjects, two males and seven females, ranging in age from 18 to 30 years, participated in the experiments. All observers had normal or corrected-to-normal vision. Participants signed informed consent prior to the experiment and received a compensation of 10 Euros per hour. The study was conducted in accordance with the Declaration of Helsinki.

2.2 Stimuli

Stimuli were presented on a ViewPixx Lite 2000A display, calibrated by a PhotoResearch (Chatsworth, CA) PR-655 spectroradiometer, and controlled by a Radeon Pro WX 5100 graphics card. The screen resolution was 1920×1200 pixels at a refresh rate of 120 Hz.

Chromaticities of the stimuli were defined in an opponent cone-contrast color space, with the two coordinate axes corresponding to L-M and S cone contrast, respectively (Figure 1a). In this color space, the distance from the center corresponds to chroma, the azimuth angle corresponds to hue, and the orthogonal third axis corresponds to luminance contrast. Cone contrasts were defined with respect to a neutral gray (106.7 cd/m^2, CIE [x, y] = [0.307, 0.314]). S-cone contrasts were scaled by a factor of 2.6, yielding approximately equally salient stimuli for all hues (Teufel and Wehrhahn, 2000). Individual perceptual isoluminance with respect to the reference gray was determined for 16 stimuli of different hues using heterochromatic flicker photometry (Kaiser and Boynton, 1996). From these data, an isoluminant plane in cone-opponent color space was calculated for each subject (Teufel and Wehrhahn, 2000).

Stimuli were generated using the software Psychopy 2020.1.2 (RRID:SCR_006571, Peirce et al., 2019) based on Python 3.6, consisting of a target stimulus, a reference stimulus, and a gradient color bar as a reference hue sequence along the color space azimuth. The target stimulus consisted of arrays of 16 circular patches with diameters of $0.75°$ of visual angle, evenly spaced on a 4×4 grid extending $3° \times 3°$ of visual angle (Figure 1b). Within each stimulus, the circular patches were randomly positioned on the grid of the array. The reference stimulus was a $0.8° \times 4.0°$ rectangular patch. The gradient color bar had an extent of$30° \times 2°$ of visual angle.

On a neutral gray background ($46.01° \times 29.68°$), the stimulus was presented at the screen center. The reference stimulus was presented on the upper part of the screen ($6°$ above the center). The gradient color bar was placed at the same height as the reference and split horizontally into two parts by the inserted reference stimulus (Figure 1c).

All stimulus chromaticities were moderately saturated, with a cone contrast $c = 0.12$ with respect to a neutral gray background. All stimuli and the gray background were isoluminant. The hues of the reference stimulus θ_r, were regularly spaced along the azimuth of color space at $0°$, $45°$, $90°$, $135°$, $180°$, $225°$, $270°$, and $315°$. For each θ_r, the corresponding gradient color bar was filled by 60 evenly spaced hue angles from a uniform distribution with the boundaries [θ_r -

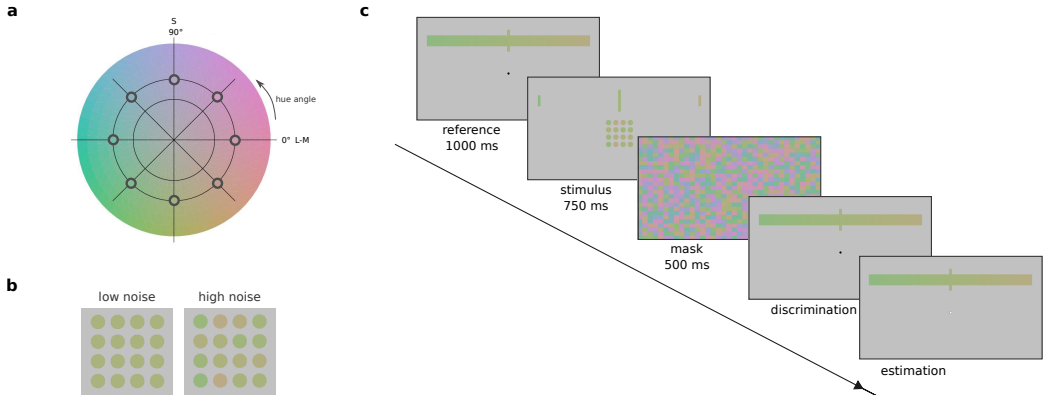

Figure 1: Experiment stimuli and paradigm. (a) Eight reference hues were defined by azimuth angle θ_r in opponent cone-contrast color space (unfilled circles). (b) Examples of stimuli with two noise levels. Both ensemble stimuli had an average hue of 270°. (c) Experiment paradigm. A 1000-ms presentation of the reference along with the gradient color bar was followed by a 750-ms presentation of the ensemble stimulus. After a 500-ms chromatic mask, subjects were instructed on a discrimination task and an estimation task in sequence. In the discrimination task, subjects had to indicate whether the stimulus was on the left or right side relative to the reference. In the estimation task, subjects had to report the memorized hue average of the stimulus by clicking on the gradient color bar.

30° and θ_r + 30°]. The average hues of the corresponding target stimulus θ_s were $\theta_r + \lambda$, where λ was evenly chosen from the range of $[-18°, 18°]$ with steps of 3°. The hues of the circular patches were generated according to two noise levels (Figure 1b). All hues were identical within a low-noise target stimulus. For a high-noise target stimulus, the hues were drawn from a mixture of two uniform distributions centered at $\theta_r + \lambda$, in which the hue angles of 10 patches were evenly drawn from a uniform distribution over a range of 32° and the hue angles of the remaining 6 patches were evenly drawn from a uniform distribution over a range of 16°.

2.3 Procedures

During the experiment, the subject sat in a dimly lit room and viewed the display binocularly from a distance of 57 cm. A central fixation dot (radius 0.2°) was displayed before the target stimulus presentation and during the response delay. Subjects were instructed to maintain their eyes to the fixation throughout the entire trial.

Each trial started with the presentation of the reference stimulus and the gradient color bar for 1000 ms, followed by a 750-ms presentation of the target stimulus. During the stimulus presentation, only the two ends (both $0.5° \times 2°$) of the color bar remained presented to indicate the sequence of hues along the color space azimuth. To prevent afterimages, a full-screen checkerboard pattern of chromatic squares was presented after the target stimulus. After 500 ms, the reference stimulus and the gradient color were presented again during the response delay until the trial was completed. Subjects were instructed to memorize the hue average of the target stimulus to complete a dual task. First, subjects were cued by a black fixation dot to indicate that, compared with the reference hue, whether the hue average of the target stimulus was closer to the left or the right end of the gradient color bar. The judgment response was given by pressing

the left or right arrow key with the right hand. The fixation dot turned white after the judgment response, cueing subjects to indicate the hue average of the target stimulus by clicking on the gradient color bar with a computer mouse. If the response time was longer than 5 seconds for judgment or 10 seconds for estimation, the corresponding trial was discarded and repeated in the same block. Average response times were 1.90 seconds.

Each block consisted of 52 trials, in which a pair of reference stimuli, with 180° as the difference in their mean hue angles, were randomly interleaved. All corresponding target hues and the two noise levels were randomized within a block. Before the main experiment, subjects completed a few practice blocks with feedback as texts ("correct" or "incorrect") about the correctness of their judgment responses. Each subject performed at least 40 blocks, resulting in 2080 trials divided into 16 conditions (8 reference stimulus hues x 2 noise levels).

2.4 Data Analysis

Data analysis was performed for each individual's dataset as well as for the pooled data. For the discrimination task, we fitted a cumulative Gaussian function to the binary responses using the Psignifit package (Schütt et al., 2016) and estimated the mean and standard deviation of the function. The former represented the 50% threshold of the psychometric function (the point of subjective equality, PSE), and the latter corresponded to the discrimination thresholds.

For analyzing the bias of the estimates, we selected the trials only with correct discrimination judgment (90.84% of the total trials). We computed the repulsive bias by combining the biases of the stimuli that had the same hue angular distance to the reference. The absolute value of repulsive bias was equal to the absolute bias of the estimate, with a positive sign if the bias was repulsive from the reference.

A significant aim of the study was to examine whether reference repulsion effects show different characteristics between hues. Therefore, for the following analysis, we separated data by reference hues. We first analyzed the course of bias over all stimuli for each reference hue, to make our results comparable to the previous findings about contextual modulation (Klauke and Wachtler, 2015). Moreover, we fitted an ellipse model to normalized repulsive biases to investigate the systematic pattern of the biases and determine the reference hue angle that induced the largest overall repulsion effects. We selected all repulsive biases (i.e., repulsive bias larger than zero) and normalized them within each subject so that the relative weight of each reference hue summed to unity. The parameters of the ellipse model were optimized using non-linear least squares.

2.5 Modeling Analysis

To explain the repulsive bias and its non-uniformity over hues, we adopted an encoding-decoding model (Jazayeri and Movshon, 2007) that posited the bias arose from combining the encoding and decoding stages of visual information. The model hypothesized that the noisy encoding of the stimulus led to fluctuated measurements at the encoding stage, which formed a measurement distribution centered on the hue average of the stimulus. At the decoding stage, it assumed discrimination choices re-weighted the sensory presentations by combining the measurement distribution with a re-weighting function. The model consisted of a Gaussian-like measurement

distribution and a re-weighting function that had maxima moderately shifted to the sides of the boundary.

Given the periodicity and symmetry of perceptual measurements shown in the present color space, we further assumed the parameters of the model components as functions of the reference hue angles. We modeled the measurement distribution of a target stimulus hue μ as a Gaussian probability density function $N(\mu, \sigma(\theta))$, where $\sigma(\theta)$ was a sine function of the reference hue angle θ with a fixed period of $180°$. For modeling convenience, we assumed $\sigma(\theta)$ was approximately equal to the width of the measurement distribution of stimulus hues around θ. Given that the measurement variability was likely to depend on the stimulus noise, $\sigma_l(\theta)$ and $\sigma_h(\theta)$ were modeled for the low-noise and high-noise conditions, respectively. We modeled the re-weighting function as a symmetric Gamma mixture of two identical Gamma density functions. Each function $\Gamma(\alpha(\theta), \beta(\theta), \delta)$ consisted of a shape parameter $\alpha(\theta)$, a scale parameter $\beta(\theta)$, and a shift parameter δ. Both $\alpha(\theta)$ and $\beta(\theta)$ were sine functions of the reference hue angle θ with a fixed period of $180°$. In addition, the model included a constant representing the individual's motor bias that was independent of the stimulus settings. In summary, our model contained a set of parameters for each sine function of the reference hue angle ($\sigma_l(\theta)$, $\sigma_h(\theta)$, $\alpha(\theta)$, $\beta(\theta)$), two subject-specific parameters δ and ϵ. We obtained the optimal parameters by maximizing the likelihood of measured estimates given the model using the Nelder-Mead algorithm. The optimization included all trials and was applied individually to each subject's data.

Predicted estimates of the optimized model were drawn from the product of the measurement distribution and the re-weighting function. For each particular stimulus presented in the experiment, we randomly sampled 500 estimates from the corresponding product distribution. The model's predicted estimates were selected and analyzed following the same procedure of analyzing experimental measurements.

3 Results

3.1 Behavioral Results

The primary aim of the study was to examine the reference repulsion effects in hue perception. Thus, we adopted a classic dual-task paradigm to hue perception and analyzed subjects' discrimination data and the reported estimates.

Figure 2 shows that, in general, subjects were able to discriminate between the target and reference hues. The slopes of the psychometric function were steeper for the target stimulus with higher noise, which were also shown in the discrimination measurements around every one of the reference hues (Supplementary Figure S1). Such results indicate stimulus noise elevated discrimination thresholds for all subjects (sign test, $p < 0.001$). The psychometric functions showed shifts in the point of subjective equality (0.93 ± 0.30 (SE) on average), suggesting small discrimination biases with inter-subject differences (Supplementary Figure S2).

A typical characteristic of the reference repulsion effects is a bimodal-shaped distribution of subjects' estimates that are biased away from the reference. Figure 3(a-b) shows that the reported hues followed a bimodal distribution under both noise conditions (dip test $p < 0.001$ for both noise conditions). In line with previous studies, the estimates were repulsive away from

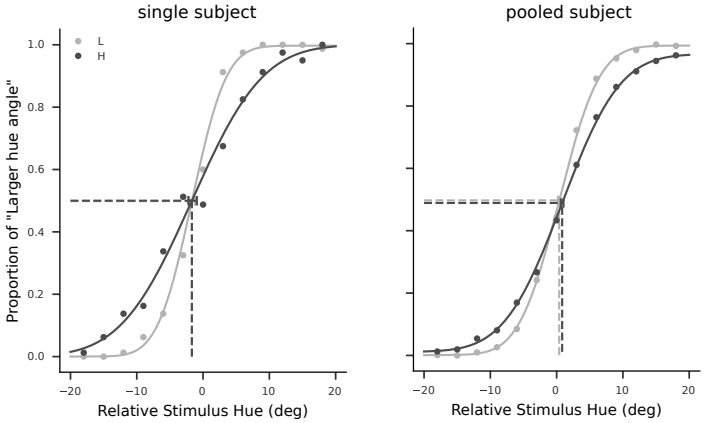

Figure 2: Psychometric functions of discrimination judgment for a representative subject ("single subject", s5) and the pooled data ("pooled subject"). Data are shown for the low noise condition ("L") and the high noise condition ("H"), respectively. The y-axis represents the proportion of subjects' judgment as "the target stimulus hue is closer to the right end than the reference hue" (i.e., the target stimulus hue angle is perceived as larger than the reference hue angle). The x-axis represents the stimulus hue angle relative to the reference hue angle. Data are from all subjects' pooled discrimination responses. Solid lines denote the cumulative Gaussian function fitted to the data. Dashed lines denote the 50% threshold of discrimination. The error bar denotes the 68% confidence interval of the estimated 50% threshold.

the reference. Figure 3(c-d) shows that, for both noise conditions, repulsive biases were larger for the stimulus hue closer to the reference hue. The magnitudes of the repulsion effects were up to a maximum of about $4.59^\circ \pm 0.14^\circ$ (SE) for low noise stimulus and $7.02^\circ \pm 0.17^\circ$ (SE) for high noise stimulus. As the target stimulus hue was less similar to the reference hue, the biases became less repulsive and even attractive. When the hue angle difference between the target stimulus and reference was smaller than 9°, subjects showed larger repulsive bias was larger for the target stimulus with higher noise (repeated measures ANOVA, $F(1, 8) = 85.15$, $p < 0.001$). On the contrary, when the target stimulus was quite different from the reference in hues (hue difference larger than 12°), the repulsive bias decreased with increasing the stimulus noise (repeated measures ANOVA, $F(1, 8) = 22.03$, $p = 0.002$).

To further test the uniformity of the effects across different hues, we separated the biases of reported estimates by the reference hues. Figure 4 shows the biases as functions of the target stimulus hues relative to each reference hue. At the hue distance of approximately 3°, the biases under both low and high noise conditions reached maximums of about $3.30^\circ \pm 0.52^\circ$ (SE) and $5.31^\circ \pm 0.41^\circ$ (SE), respectively. Beyond the maximum, biases decreased with increasing the difference between the target stimulus and reference hues. Notably, although such systematic changes of biases were qualitatively the same, it varies in shape for different reference hues. The shape shows similarities between the reference pairs with a hue distance of 180°, suggesting the symmetry in the reference-induced biases along the azimuth of the color space.

Thus, we fitted an ellipse to normalized biases so that the overall bias was computed as a weighted sum of the biases around each reference hue. If the biases were uniform across hues, the fitted ellipse would have an eccentricity of 1. Figure 5a shows the fitted ellipse for all subjects'

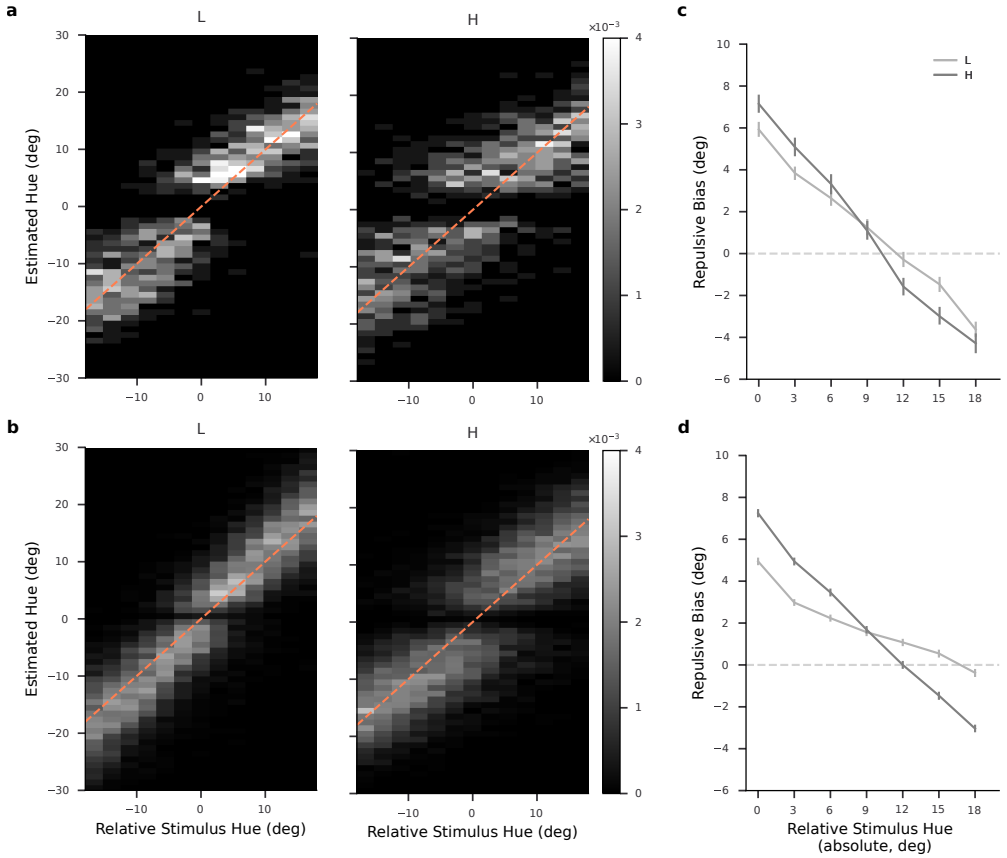

Figure 3: Estimate Distribution and repulsive bias. (a-b) Distributions of the subject's estimates for each particular stimulus hue angle. Data are shown for the low noise condition ("L") and the high noise condition ("H"), respectively, from the representative subject (a) and all subjects' pooled data (b). The density was presented with a lightness scale. All the values on the x-axis and y-axis are hue angles relative to the reference hue angle. The dashed lines indicate where estimated hue angles are equal to stimulus hue angles. (c-d) Repulsive bias of the representative subject (c) and all subjects' pooled data (d). Data are shown for the low noise condition ("L") and the high noise condition ("H"), respectively. Data are from trials where the subject's discrimination judgment was correct. The x-axis represents the absolute difference between the stimulus hue angle and the reference hue angle. Error bars denote one standard error of the mean.

pooled normalized biases. All fitted ellipses (see Supplementary Figure S6 for individual's fitted ellipses) had an eccentricity between zero and one (0.71 ± 0.20 on average, Figure 5b). On average, the longest axes of the ellipses were along the hue angle of $87.93° \pm 15.14°$ for the low noise condition and $112.53° \pm 9.02°$ for the high noise condition (Figure 5c).

Taken together, the estimates of target hues showed repulsion biases away from the reference hue. The repulsion effects were stronger for the target stimulus closer to the reference and with higher stimulus noise. Such repulsive bias showed non-uniformity across hues, with the largest overall biases around blue and yellow.

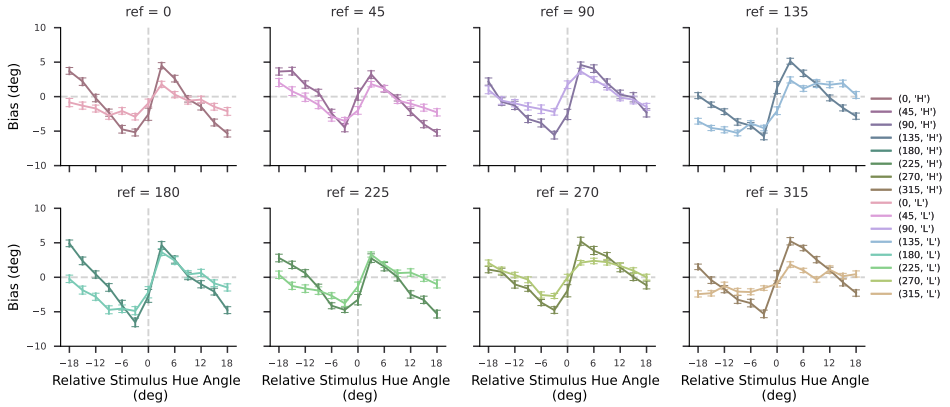

Figure 4: Bias of all subjects' pooled data for different hues. Data are from trials where the subject's discrimination judgment was correct. The x-axis represents the hue angle difference between the stimulus and the reference. Error bars denote one standard error of the mean.

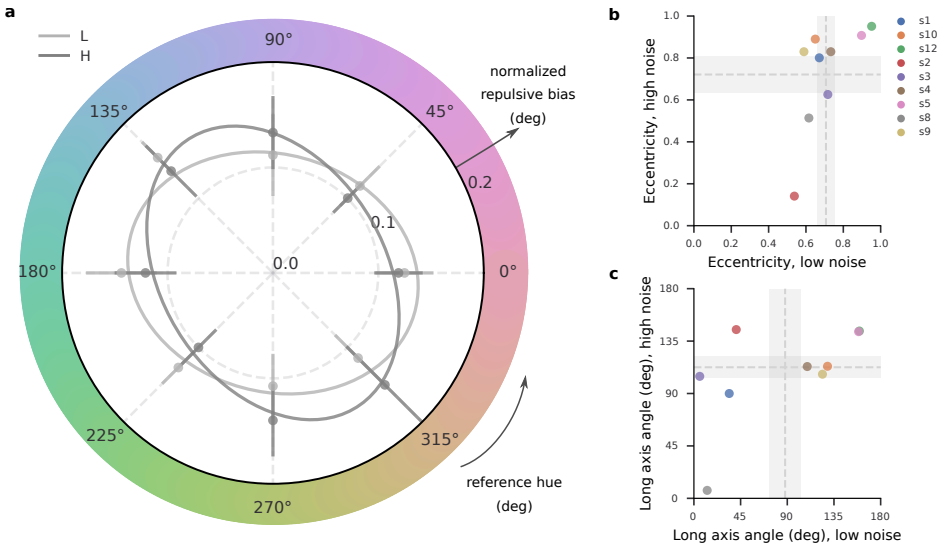

Figure 5: Fitted ellipses of the within-subject normalized repulsive bias. (a) Fitted ellipses of all subjects' pooled normalized repulsive bias. Data are shown for the low noise condition ("L") and the high noise condition ("H"), respectively. Data points are the averages of repulsive biases that were normalized within each subject from trials where the subject's discrimination judgment was correct. Error bars denote standard deviation. (b-c) Characteristics of the fitted ellipses on individual's data (Supplementary Figure S6): eccentricities of the fitted ellipses (b), and the hue angles correspond to the longest axes of the individual's fitted ellipses within the range of $[0°, 180°]$ (c). In (b) and (c), the gray dashed lines represent the mean values across subjects and the light gray shades represent the standard errors of the mean values.

3.2 Modeling Results

An encoding-decoding model has been posited to explain the reference repulsion effects as a consequence of re-weighting sensory representations by discrimination choices (Jazayeri and Movshon, 2007). The model consists of two components: a measurement distribution and a re-weighting function. The measurement distribution results from fluctuated measurements of a

particular stimulus during the noisy sensory encoding. At the decoding stage, the measurement distribution multiplies a re-weighting function that results from the discrimination judgment and has maxima moderately shifted to the sides of the categorical boundary (such as in the shape of a Gamma density function). The measurement corresponding to the peak of this product is thus regarded as the estimate of the particular stimulus.

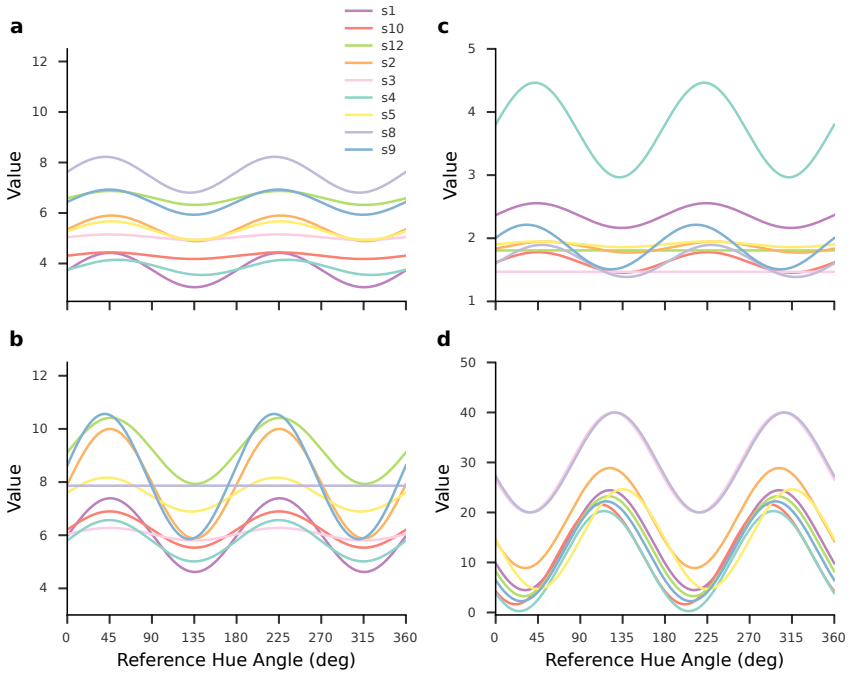

Figure 6: Estimated model parameters as sine functions of reference hue angles. (a-b) The widths of the measurement distributions, for low-noise and high-noise stimuli, respectively. (c-d) The shape and scale parameters of the re-weighting profile as a gamma density function, respectively. Different colors denote estimates for individuals.

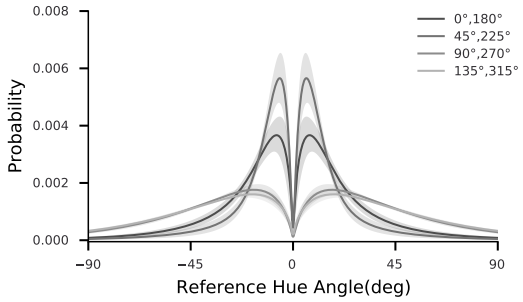

Figure 7: Estimated re-weighting functions. The re-weighting profiles were averaged across subjects. Note that each model represents two identical profiles of a pair of reference hues that are 180° apart. The shade denotes ±1 standard error.

In the present study, we adopted this model on the subject's estimates of hues. Moreover, given the observed non-uniformity of the repulsive biases across hues, we assumed the parameters of the encoding-decoding model varied systematically with hues, likely in a sine-like fashion.

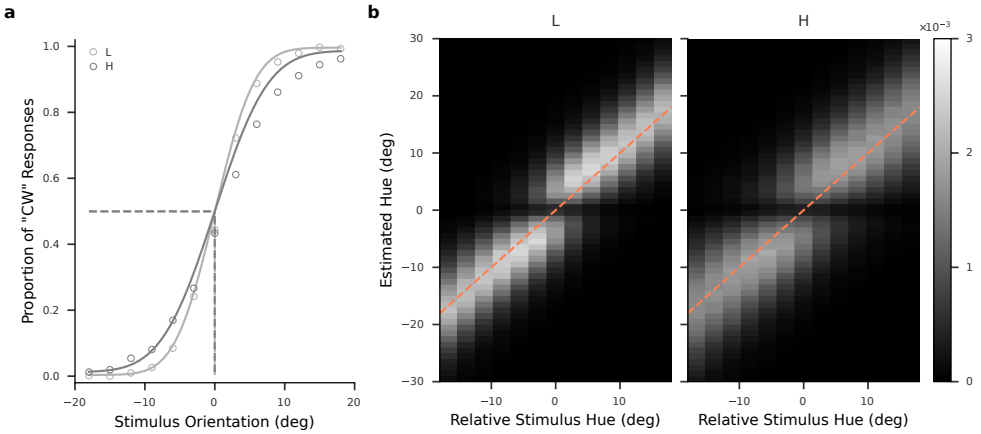

Figure 8: Model-predicted responses. Predictions are shown for the low noise condition ("L") and the high noise condition ("H"), respectively. (a) Psychometric functions of model-predicted discrimination judgment. The y-axis represents the proportion of predicted subjects' judgment as "the target stimulus hue is closer to the right end than the reference hue" (i.e., the target stimulus hue angle is perceived as larger than the reference hue angle). The x-axis represents the target stimulus hue angle relative to the reference hue angle. Open circles denote all subjects' pooled discrimination responses measured in the experiment (same data as in Figure 2). Solid lines denote the cumulative Gaussian function fitted to the predicted data. Dashed lines denote the 50% threshold of discrimination. (b) Distributions of predicted all subjects' pooled estimates for each particular stimulus hue angle. The density was presented with a lightness scale. All the values on the x-axis and y-axis are hue angles relative to the reference hue angle. The dashed lines indicate where estimated hue angles are equal to stimulus hue angles.

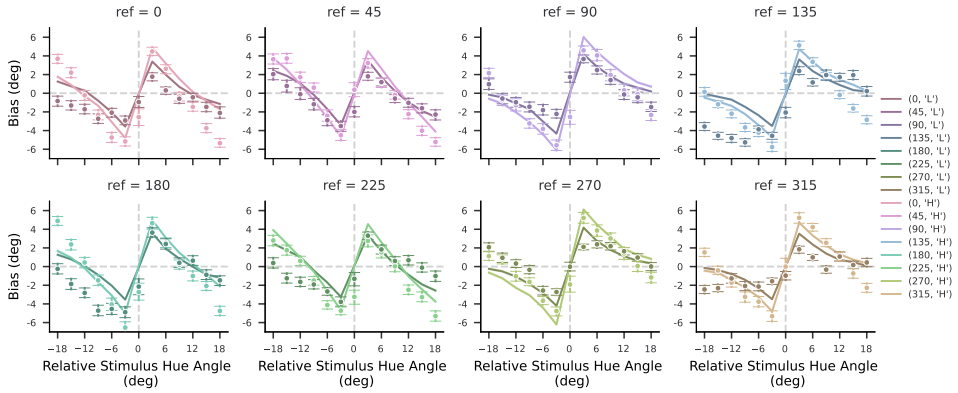

Figure 9: Model-predicted bias of all subjects' pooled data for different hues. Lines denote model-predicted biases. Dots are biases measured in the experiments (same data as in Figure 4). Error bars denote one standard error of the mean. The x-axis represents the hue angle difference between the stimulus and the reference.

Specifically, we assumed the widths of measurement distributions, and the shape and the scale of the re-weighting functions were sine functions of reference hues with a fixed period of $180°$. We hypothesized the relationship based on the observed symmetries in the bias patterns between every pair of reference hues that were $180°$ apart. The assumed symmetry and periodicity were

also in line with findings on color discrimination and hue contextual modulation (Boynton et al., 1986; Krauskopf and Gegenfurtner, 1992; Danilova and Mollon, 2010; Witzel and Gegenfurtner, 2013; Klauke and Wachtler, 2015). Figure 6 shows the relationships between these model parameters and reference hue angles. On average, the estimated widths of measurement distributions showed the lowest values at $135.91° \pm 3.43°$ and $315.91° \pm 3.43°$ for the low-noise stimulus. The lowest estimated widths for the high-noise stimulus were at $134.35° \pm 1.93°$ and $314.35° \pm 1.93°$, indicating the highest precision around blue and yellow, which was consistent between noise conditions. The shape parameter of the re-weighting profile, determining the function's skewness and kurtosis, showed the lowest values at $134.90° \pm 5.49°$ and $314.90° \pm 5.49°$. The scale parameter of the re-weighting function peaked at $121.67° \pm 7.09°$ and $301.67° \pm 7.09°$. The shape and scale parameters together led to the distinct profiles of the estimated re-weighting functions for different hues (Figure 7). The closer the hue was to an oblique space axis connecting unique blue and unique yellow (approximately around $112°$ and $292°$, see Mollon (2006) and Klauke and Wachtler (2015)), the wider was the spread of the re-weighting functions. The estimated model was able to predict the data in both discrimination and estimation tasks (Figure 8). As Figure 9 shows, the model's prediction also captured the different profiles of bias for different colors. Taken together, the two-component model was able to predict the repulsion effects in hue perception. The model also explained the non-uniformity with different profiles of the model components for different hues, suggesting that colors showed differences in both sensory encoding precision and sensory representation re-weighting.

4 Discussion

As one of the significant contextual biases, reference repulsion has been found in the subject's estimates of different visual features such as motion direction and orientation, whereas the phenomenon remained unveiled for color perception. To examine the reference repulsion effects in color perception, we measured the subject's estimates of a hue stimulus after an explicit comparison between the stimulus and a color reference. The subject's hue estimates were repulsive away from the reference, showing the largest repulsive biases for the stimulus closer to the reference and with larger chromatic noise. While the patterns of biases were qualitatively similar among different hues, the largest overall repulsive biases occurred around blue and yellow. In line with the findings in other visual domains, an encoding-decoding model predicted the overall repulsion effects and explained the non-uniformity of biases among colors with model components differing between distinct hues. Our results thus suggest a common mechanism of processing contextual information for various visual features.

4.1 Reference repulsion as a common mechanism

One of the research interests in visual perception is a general mechanism underlying contextual information processing. Studies on color perception have revealed that, similar to orientations, color estimates are susceptible to temporal and spatial contexts (Barbosa and Compte, 2020; Olkkonen et al., 2014; Klauke and Wachtler, 2015). In the temporal domain, the biases of color estimates could arise from the history and distribution of stimuli (Barbosa and Compte, 2020; Olkkonen et al., 2014), similar to the well known serial dependence (Fischer and Whitney, 2014) and central tendency effects (Urban, 1911), respectively. The hue induction effect resembles the orientation tilt affects, strongly supporting a common mechanism of contextual modulation between orientation and color perception (Klauke and Wachtler, 2015). In line with these findings, our study shows that reference repulsion is possibly a common contextual bias across different visual features, indicating a general mechanism of utilizing categorical context for perceptual inference.

4.2 The nature of reference repulsion

Nevertheless, there remain debates about the perceptual nature of reference repulsion. Several studies have posited that the repulsive effects occurred in the early sensory encoding stage, even though with different mechanism accounts (Jazayeri and Movshon, 2007; Ye and Liu, 2020). On the contrary, recent studies have found that repulsive biases could be modified by manipulating the tasks and presentations after stimulus encoding, suggesting reference repulsion is a late decision-related bias (Zamboni et al., 2016; Luu and Stocker, 2021). For example, Zamboni et al. (2016) showed that the presence of reference during stimulus reproduction was necessary to induce the repulsive effects. When the reference was jittered during the reproduction, the repulsive bias was shifted and yoked to the jittered reference. Moreover, Luu and Stocker (2021) showed that, given feedback on the discrimination choices, subjects could recombine the probabilistic information and generate an estimate following the corrected choice, especially when the feedback indicated an incorrect choice.

Our study followed the classic paradigm to examine the reference repulsion effects and, therefore, could not directly disentangle the processes underlying the effects. Nevertheless, our findings suggested a consistency between perceptual biases and reference-induced biases. Although the discrimination biases were negligible when the data were pooled across hues, the biases for particular hues appeared non-negligible for some subjects (for example, see s12 in Supplementary Figure S2). In these cases, subjects tended to follow their discrimination choices, even when the choices were biased (95.45% of trials with incorrect discrimination choices). For all subjects and all colors, the proportion of estimates falling into a particular category correlated with the proportion of the corresponding choices (Supplementary Figure S3, Pearson correlation $r(70) = 0.99, p < 0.001$ for low noise stimuli, $r(70) = 0.98, p < 0.001$ for high noise stimuli). In other words, when the reference mismatched the point of subjective equality (PSE) of discrimination, the estimates still followed the categorical choices but showed repulsion exclusively around the reference. In line with other studies (Zamboni et al., 2016; Luu and Stocker, 2018, 2021), our findings imply that subjects tend to maintain self-consistency in consecutive tasks, while the repulsion effect is related to the fine estimation with memory recall and depends on the reference presented during the estimation.

To further examine the nature of reference repulsion, future studies could include an additional discrimination task in the experiment scenario, similar to the orientation study by Fritsche and de Lange (2019). For instance, after subjects reported the memorized target stimulus, subjects would need to compare the hue of the target stimulus with a presented comparison hue ensemble. If reference repulsion affects the perception of the target stimulus, we would expect non-negligible perceptual biases that are repulsive away from the reference in the second discrimination task.

4.3 Reference repulsion vs. color-tilt

The pattern of the bias revealed in this study appears similar to that of the bias induced by chromatic surrounds (Klauke and Wachtler, 2015). In addition to showing similar profiles, the biases we observed and the ones reported by Klauke and Wachtler (2015) both show non-uniformity across hues, however, exhibiting opposite characteristics. While Klauke and Wachtler (2015) have reported the strongest induction effect along a blue-yellow axis, we found the largest overall repulsion effects around blue and yellow hues. It is likely that different mechanisms underlie the two phenomena, given that these two types of biases were measured with different stimulus configurations and task settings. Underlying these biases, the significant distinctions between the contextual processes were whether a memory recall and a categorical decision were involved. Contextual modulation embedded in stimulus encoding has been proposed to explain the tilt effect including the color-tilt (Klauke and Wachtler (2015), see Schwartz et al. (2007) for a review). For example, Clifford et al. (2000) have proposed to explain the orientation tilt effects by the shift of preferred tuning values of neurons in the primary visual cortex. On the contrary, as mentioned above, it remains debated whether reference repulsion arises from early sensory encoding or late visual processing. Even though the surround might implicitly resemble a reference, the perceptual task did not involve an explicit discrimination choice, which could not reject the possibility of the difference between implicit and explicit processes.

4.4 Non-uniformity in the color space

Our results showed pronounced non-uniformity of the repulsive biases across hues. We found the largest repulsion effects were around blue and yellow hues, in line with the non-uniformity of contextual effect along a blue-yellow axis (Klauke and Wachtler, 2015). Such non-uniformity was explained by the systematic changes of model parameters as hue varied. The estimated measurement distributions revealed the highest precision of sensory information encoding around blue and yellow hues, which is consistent with the behavioral measurements of color perceptual variability (Boynton et al., 1986; Krauskopf and Gegenfurtner, 1992; Danilova and Mollon, 2010; Witzel and Gegenfurtner, 2013). Moreover, the re-weighting functions that showed the widest spread around blue and yellow matched the observations that the blue and yellow contexts show wider ranges of modulation than other colors (Klauke and Wachtler, 2015). The modeling results thus imply that the perceptual non-uniformity may arise from the non-uniform encoding and re-weighting of sensory presentations among different hues. One explanation may lie in the adaptation of the visual system to natural environments. Given that the oblique blue-yellow axis coincides with the highest variation in the natural spectra (Webster and Mollon, 1997; Mollon, 2006), it is likely that the visual system has developed lower variability and wider re-weighting for the daylight colors dominating in natural environments than other colors.

However, such non-uniformity remains not considered when measuring reference repulsion in other visual features. Previous studies usually pooled data corresponding to different references. We re-analyzed the subjects' estimates of orientations in the study by Luu and Stocker (2018) and did not find systematic relation between the repulsive bias and reference orientation (data not shown). This is likely due to that rich contexts of orientations in the experimental environment might play the role of references (such as the orientations of a monitor's edges). Moreover, one could not exclude the possibility that the pronounced non-uniformity of reference repulsion is exclusive to color vision.

4.5 Color categorical effects

The categorical effect has been one of the central debates in color vision. For color working memory, Bae et al. (2015) have reported the biases of memorized colors that were away from the color category boundary and towards the color category center. We examined the color categorical effects by plotting the distribution of estimates on a continuous scale (Supplementary Figure S5). Due to the focus on the induction of color references, we sampled the stimulus hues locally around each reference, instead of sampling the hues covering a continuous range over the color space. Nevertheless, the systematic repulsion effects could be found around the reference hue and absent at the color category boundary. We consider our results do not contradict the findings by Bae et al. (2015), but reconcile with the framework that color working memory relies on stimulus categories – the key is, which categories do subjects use? Such categories should facilitate maintaining memory representations and provide task-relevant information. Thus, in our study, the categories originating from discrimination choices might mask or replace the subjective color categories and dominate in biasing the memorized colors.

4.6 Limitations

Finally, we consider several limitations of the present study. First, previous experiments on motion and orientation perception usually sampled the values of stimuli stochastically. However, given the difficulty of performing the color perception tasks for naive subjects, the stimulus hues were relatively fixed across trials. The range of tested colors was thus limited. Second, the encoding variability of each stimulus was approximated to that of its closest reference, while the perceptual variability could be non-uniform within such a hue angle range of $36°$. Moreover, we modeled the re-weighting function as a mixture of two symmetrical gamma density functions, possibly ignoring the asymmetry between the choice-generated categories. One could model different profiles of the re-weighting functions for the two categories around the same reference, which might give a better explanation for the estimates distributed in an unbalanced fashion around some reference hues.

Acknowledgments

Supported by DFG (RTG 2175 "Perception in Context and its Neural Basis") and Bernstein Center for Computational Neuroscience Munich. We thank Jule Kaserer for her help with data collection. We thank all participants for participating in the experiments.

References

Bae, G.-Y., Olkkonen, M., Allred, S. R., and Flombaum, J. I. (2015). Why some colors appear more memorable than others: A model combining categories and particulars in color working memory. *Journal of Experimental Psychology. General*, 144(4):744–763.

Bae, G.-Y., Olkkonen, M., Allred, S. R., Wilson, C., and Flombaum, J. I. (2014). Stimulus-specific variability in color working memory with delayed estimation. *Journal of Vision*, 14(4).

Barbosa, J. and Compte, A. (2020). Build-up of serial dependence in color working memory. *Scientific Reports*, 10(1):10959.

Boynton, R. M., Nagy, A. L., and Eskew, Jr, R. T. (1986). Similarity of normalized discrimination ellipses in the constant-luminance chromaticity plane. *Perception*, 15(6):755–763.

Clifford, C. W., Wenderoth, P., and Spehar, B. (2000). A functional angle on some after-effects in cortical vision. *Proceedings Biological sciences*, 267(1454):1705–1710.

Danilova, M. V. and Mollon, J. D. (2010). Parafoveal color discrimination: a chromaticity locus of enhanced discrimination. *Journal of Vision*, 10(1):4.1–9.

Fischer, J. and Whitney, D. (2014). Serial dependence in visual perception. *Nature Neuroscience*, 17(5):738–743.

Fritsche, M. and de Lange, F. P. (2019). Reference repulsion is not a perceptual illusion. *Cognition*, 184:107–118.

Fritsche, M., Spaak, E., and de Lange, F. P. (2020). A Bayesian and efficient observer model explains concurrent attractive and repulsive history biases in visual perception. *Elife*, 9:e55389.

Gibson, J. J. and Radner, M. (1937). Adaptation, after-effect and contrast in the perception of tilted lines. I. Quantitative studies. *Journal of Experimental Psychology*, 20(5):453.

Jazayeri, M. and Movshon, J. A. (2007). A new perceptual illusion reveals mechanisms of sensory decoding. *Nature*, 446(7138):912–915.

Kaiser, P. K. and Boynton, R. M. (1996). *Human Color Vision*. Washington: Optical Society of America.

Klauke, S. and Wachtler, T. (2015). "Tilt" in color space: Hue changes induced by chromatic surrounds. *Journal of Vision*, 15(13):17–17.

Krauskopf, J. and Gegenfurtner, K. (1992). Color discrimination and adaptation. *Vision Research*, 32(11):2165–2175.

Luu, L. and Stocker, A. A. (2018). Post-decision biases reveal a self-consistency principle in perceptual inference. *Elife*, 7.

Luu, L. and Stocker, A. A. (2021). Categorical judgments do not modify sensory representations in working memory. *PLoS Computational Biology*, 17(6):e1008968.

Mollon, J. (2006). Monge: The Verriest lecture, Lyon, July 2005. *Visual Neuroscience*, 23(3-4):297–309.

Olkkonen, M., McCarthy, P. F., and Allred, S. R. (2014). The central tendency bias in color perception: effects of internal and external noise. *Journal of Vision*, 14(11).

O'Toole, B. and Wenderoth, P. (1977). The tilt illusion: repulsion and attraction effects in the oblique meridian. *Vision Research*, 17(3):367–374.

Peirce, J., Gray, J. R., Simpson, S., MacAskill, M., Höchenberger, R., Sogo, H., Kastman, E., and Lindeløv, J. K. (2019). PsychoPy2: Experiments in behavior made easy. *Behavior Research Methods*, 51(1):195–203.

Rauber, H. J. and Treue, S. (1998). Reference repulsion when judging the direction of visual motion. *Perception*, 27(4):393–402.

Schütt, H. H., Harmeling, S., Macke, J. H., and Wichmann, F. A. (2016). Painfree and accurate Bayesian estimation of psychometric functions for (potentially) overdispersed data. *Vision Research*, 122:105–123.

Schwartz, O., Hsu, A., and Dayan, P. (2007). Space and time in visual context. *Nature Reviews Neuroscience*, 8(7):522–535.

Smith, S., Clifford, C. W. G., and Wenderoth, P. (2001). Interaction between first- and second-order orientation channels revealed by the tilt illusion: psychophysics and computational modelling. *Vision Research*, 41(8):1057–1071.

Spicer, J., Zhu, J.-Q., Chater, N., and Sanborn, A. N. (2022). Perceptual and cognitive judgments show both anchoring and repulsion. *Psychological Science*, 33(9):1395–1407.

Talluri, B. C., Urai, A. E., Bronfman, Z. Z., Brezis, N., Tsetsos, K., Usher, M., and Donner, T. H. (2021). Choices change the temporal weighting of decision evidence. *Journal of Neurophysiology.*, 125(4):1468–1481.

Talluri, B. C., Urai, A. E., Tsetsos, K., Usher, M., and Donner, T. H. (2018). Confirmation Bias through Selective Overweighting of Choice-Consistent Evidence. *Current Biology*, 28(19):3128–3135.e8.

Teufel, H. J. and Wehrhahn, C. (2000). Evidence for the contribution of S cones to the detection of flicker brightness and red-green. *Journal of the Optical Society of America. A, Optics, Image Science, and Vision*, 17(6):994–1006.

Urban, F. M. (1911). Review of the central tendency of judgment. *Psychological Bulletin*, 8(6):220–220.

Webster, M. A., Malkoc, G., Bilson, A. C., and Webster, S. M. (2002). Color contrast and contextual influences on color appearance. *Journal of Vision*, 2(6):505–519.

Webster, M. A. and Mollon, J. D. (1997). Adaptation and the color statistics of natural images. *Vision Research*, 37(23):3283–3298.

Witzel, C. and Gegenfurtner, K. R. (2013). Categorical sensitivity to color differences. *Journal of Vision*, 13(7):1.

Ye, R. and Liu, X. (2020). How the known reference weakens the visual oblique effect: a Bayesian account of cognitive improvement by cue influence. *Scientific Reports*, 10(1):20269.

Zamboni, E., Ledgeway, T., McGraw, P. V., and Schluppeck, D. (2016). Do perceptual biases emerge early or late in visual processing? Decision-biases in motion perception. *Proceedings. Biological Sciences*, 283(1833).

5 Supplementary Figures

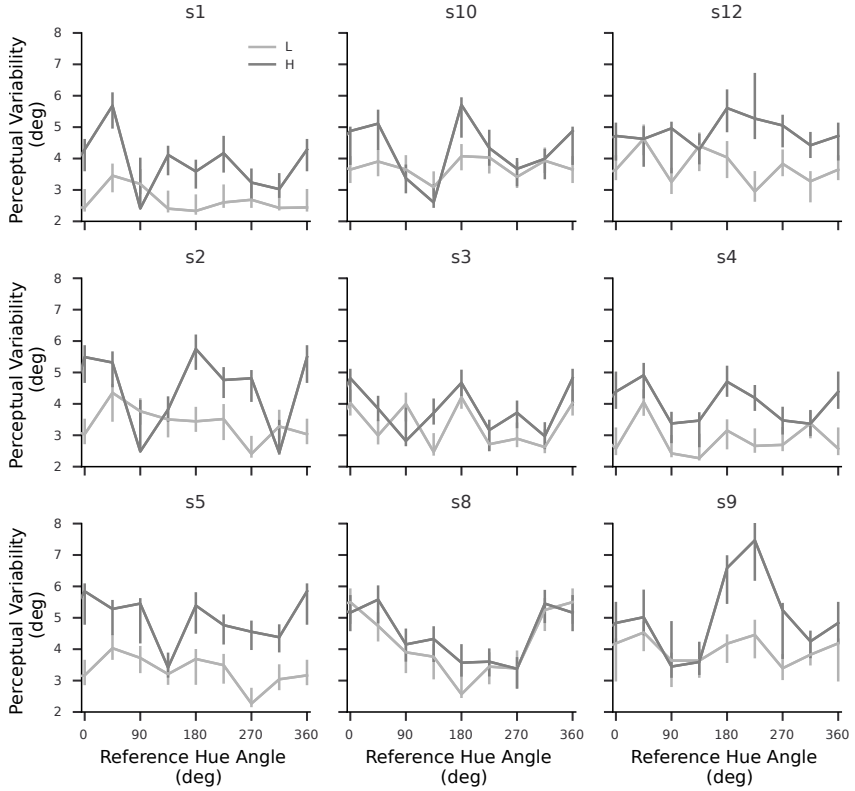

Figure S1: Individual's perceptual variability of discrimination responses. Error bars denote 68% confidence interval. Dash lines denote zero bias.

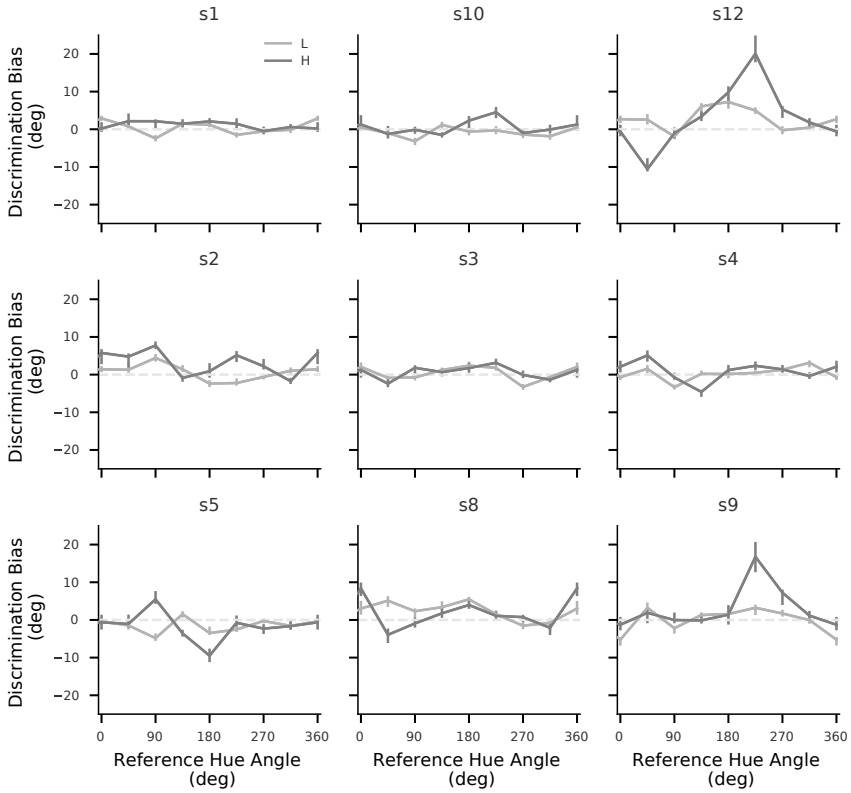

Figure S2: Individual's discrimination biases. Error bars denote 68% confidence interval.

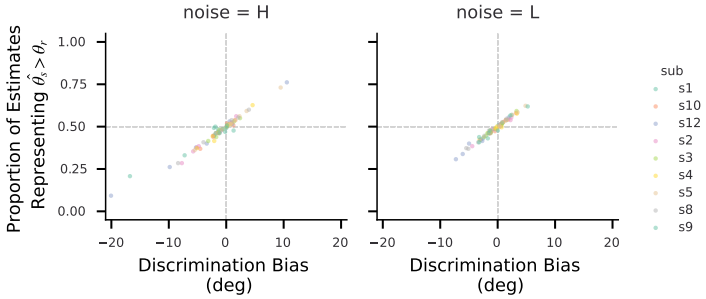

Figure S3: Correlation between the proportion of estimates representing the perceived stimulus hue $\hat{\theta}_s$ larger than reference hue θ_r and discrimination biases. The discrimination biases were computed as the shift of PSE. Each dot represent a pair of data for one subject and one reference color. Dash lines denote zero bias in discrimination choices and reported estimates.

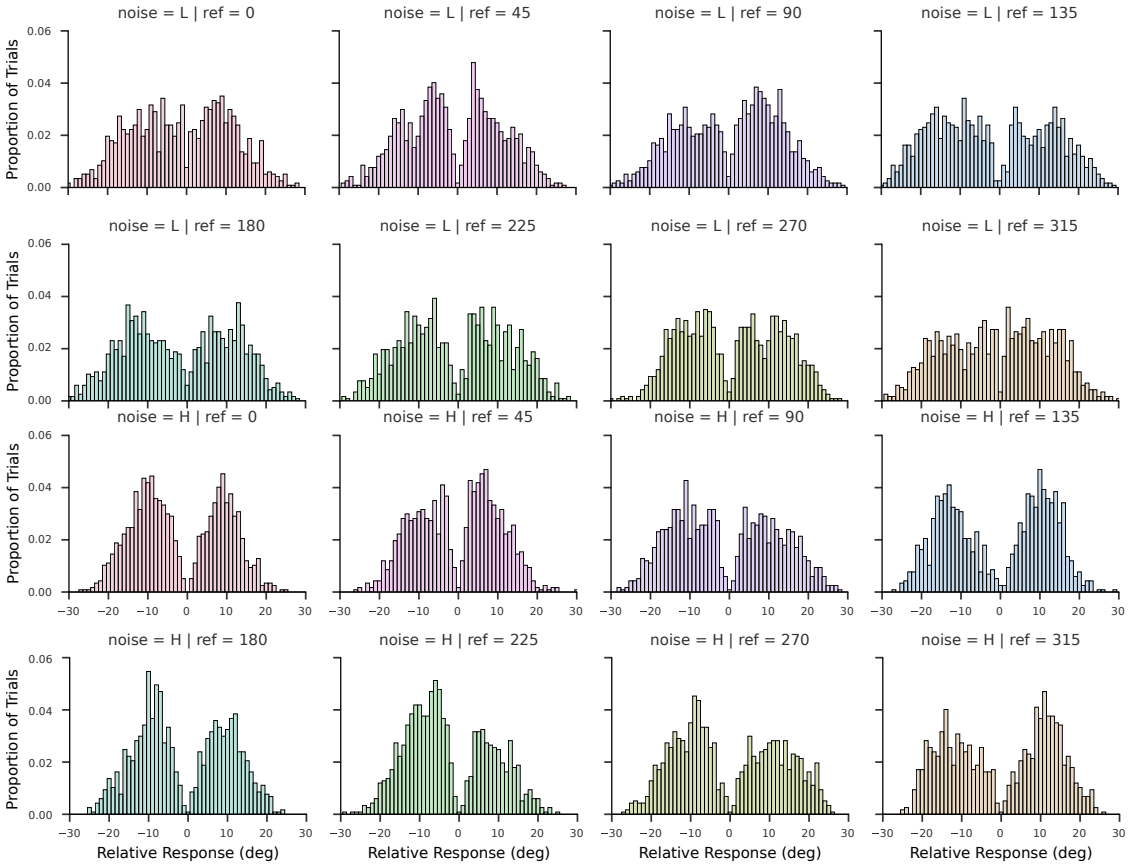

Figure S4: Distribution of pooled subjects' estimates of stimulus hue angles under low noise ("L") and high noise ("H") conditions.

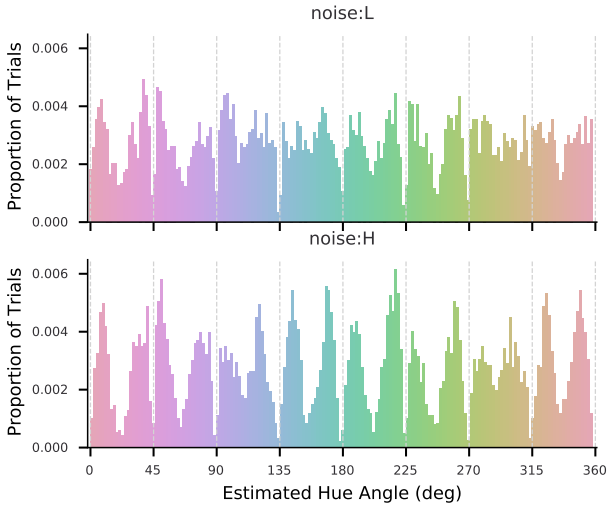

Figure S5: Distribution of subjects' estimates of stimulus hue angles on a continuous scale. Vertical dashed lines denote the hue angles of reference hues.

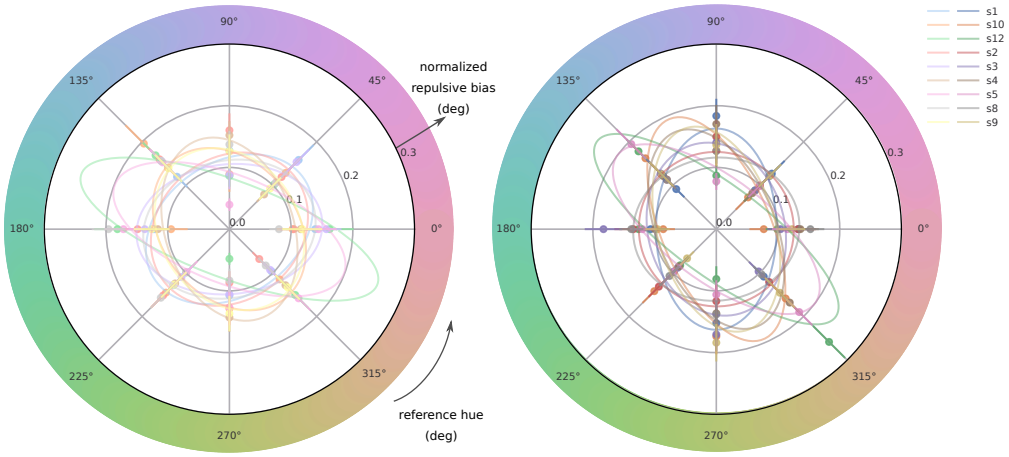

Figure S6: Fitted ellipse of within-subject normalized repulsive biases for each individual, under the low noise (left) and high noise (right) conditions. Data points are normalized repulsive biases from trials where the subject's discrimination judgment was correct. Error bars denote standard deviation.

5 Discussion

5.1 Summary of findings

Various types of contexts have been found to bias visual percepts, as evidenced by psychophysical measurements and explained by computational models. While contextual biases provide valuable insights into how the brain processes and infers visual information, there are still many unresolved questions regarding the general mechanisms involved in contextual information processing for various visual features. Even for specific biases induced by certain types of contexts, debates persist regarding the stages of visual processing at which these biases occur. This thesis aims to shed light on these issues by investigating the contextual biases in two specific visual features, color and orientation, within natural or task-specific contexts.

The first study in this thesis (Chapter 2) examined whether perceptual biases in color vision are related to natural contexts. Our hypothesis was that the visual system may adapt to natural scenes and incorporate environmental statistics into perceptual properties. To test this, we measured color perceptual variability and bias using two-alternative forced-choice discrimination experiments between hue ensembles. For the isoluminant ensemble with hue defined by azimuth angle in cone-opponent color space, perceptual variability showed a bimodal pattern with the lowest values near a non-cardinal blue-yellow axis. Near this axis, perceptual bias showed zero crossings, which was attractive towards blue and repulsive from yellow. We explained the perceptual bias using a Bayesian observer model and revealed a non-uniform prior that favored blue. This prior coincides with the variation of natural daylights, suggesting that observers exploit knowledge of colors in natural environments to process hue information.

In Study 2 and Study 3, we focused on how an explicit reference acts as a context that biases visual estimates and leads to repulsion effects. Study 2 (Chapter 3) addressed whether reference repulsion occurs in the early or late stages of visual information processing. We measured participants' estimates of an orientation ensemble and found the repulsion effect from a reference orientation presented after the disappearance of the ensemble. This revealed that a reference that oc-

curs in late visual processing can induce repulsive biases, suggesting reference repulsion as a late, decision-related bias. Moreover, whether the tasks involved explicit discrimination choices affected the direction and magnitude of the biases, which could be elucidated by an encoding-decoding model that suggests different reweightings of sensory representations between implicit and explicit processes.

Study 3 (Chapter 4) extended the investigation of reference repulsion from orientation perception to hue perception, aiming at a common mechanism for processing contextual information across different visual domains. We measured participants' estimates of a hue ensemble after they made an explicit comparison between the ensemble and a hue reference. We found the bias in hue estimates was repulsive away from the reference, showing quantitative differences among different hues. This was explained by an observer model similar to the one applied to orientation perception. The model also revealed non-uniformities in both encoding and reweighting of sensory presentations among different hues. Overall, these results support that reference repulsion is likely to be a common contextual effect for various visual features, including color.

5.2 Contextual processing across visual domains

One contribution of the present thesis is to demonstrate general mechanisms of contextual information processing across two visual domains: orientation and color. Study 1 (Chapter 2) expands the notion of a natural prior in the Bayesian observer model from orientation to color, and the other two studies (Chapter 3 and Chapter 4) together suggest a common effect from instructive contexts for both visual features. These findings are generally in line with previous findings that have hinted at similarities between the perceptual processes of orientation and color (Klauke and Wachtler, 2015, Olkkonen et al., 2014, Barbosa and Compte, 2020, Chunharas et al., 2022).

Orientation and color are naturally comparable in perception studies, as they are both fundamental features of natural scenes and both show the predominance of particular feature values in environmental distributions. As the visual system has evolved through adaptation to environments, visual perception should exhibit the best sensitivity and the least bias for these predominant

stimuli (Simoncelli, 2003), such as cardinals for orientation perception (Girshick et al., 2011) and daylight colors for hue perception (Mollon, 2006). This hypothesis has been supported by a variety of behavioral measurements (Girshick et al., 2011), which our study (Chapter 2) also contributes to. Perceptual variability has been shown to have the lowest values at cardinals regardless of whether it arises in orientation discrimination (Orban et al., 1984, Girshick et al., 2011) or orientation reproduction (de Gardelle et al., 2010, van Bergen et al., 2015), known as the oblique effect. Accordingly, participants' estimates of cardinals tend to be unbiased (Girshick et al., 2011, van Bergen et al., 2015). Similarly, for hue perception, our findings not only agree with previous findings that perceptual variability is lowest around daylight colors (Boynton et al., 1986, Krauskopf and Gegenfurtner, 1992, Danilova and Mollon, 2010, Witzel and Gegenfurtner, 2013), but also provide the first evidence of systematic biases that are about zero near these daylight colors. Our observer model further reveals that participants may internalize the environmental color statistics and form a perceptual prior, which is similar to the findings that the internal prior for orientation perception reflects natural contextual information (Girshick et al., 2011).

Color perception also shares similarities with orientation perception in how task-specific contextual information modulates sensory representations. Studies 2 and 3 (Chapter 3 and Chapter 4) indicate that a memorized stimulus could be biased away from category boundaries, showing a repulsion effect that has similar characteristic features between orientation and color perception. As this similar effect has also been reported in the perception of motion direction, reference repulsion likely reflects a higher-level mechanism of information processing shared by various visual features. Furthermore, given that working memory may be involved in the repulsion effect, our findings imply comparable processing of memory representations between color and orientation, which is consistent with previous findings on color working memory (Olkkonen et al., 2014, Bae and Luck, 2017, Barbosa and Compte, 2020, Chunharas et al., 2022). Similarities between color and orientation working memory have been reported in the dependence of the range and sequence of stimuli, known as central tendency effect (Urban, 1911, Olkkonen et al., 2014) and serial dependence (Fischer and Whitney, 2014, Barbosa and Compte, 2020). Moreover, when multiple stimuli are held in visual working memory, the interactions between working-memory representations of hues have been found comparable to those of orientations

(Bae and Luck, 2017, Chunharas et al., 2022). Taken together with our results, it is likely that contextual information affects working memory representations in similar ways for different visual features.

5.3 Obstacles for a unified framework

While a unified framework for contextual information processing holds promise, the processing of color information by the visual system is more complex than that of spatial visual features such as orientation. The results of studies 1 and 3 (Chapters 2 and 4) support the idea that hue perceptual non-uniformity is tuned to an oblique blue-yellow axis instead of the cardinal axes in color space. This highlights a misalignment between perceptual attributes and cone contrast coordinates. This mismatch is also evident in the neural responses between the LGN cells and visual cortex neurons. The color selectivity of V1 neurons seems more diverse than that of the LGN cells (Hanazawa et al., 2000, Wachtler et al., 2003, Kuriki et al., 2015), whose responses cluster around the two cone-opponent axes (Derrington et al., 1984). The transformation of color signals from the LGN to the visual cortex is likely responsible for color perception and underscores the intricate processing of color information.

Furthermore, our findings demonstrate one of the complexities of color vision – individual differences, which are rarely found in orientation perception and shown by only a few of the findings on the strength of anisotropy (Timney and Muir, 1976). Individual variations at different levels of color processing influence many aspects of color vision, from color discrimination to the appearance of the viral image #theDress (see Bosten (2022) for a review). Our results contribute to the evidence of color inter-subject variability in different environmental and task settings. In study 1 (Chapter 2) we observed between-subject differences in the pattern of perceptual biases, resulting in some participants' prior peak locations deviating from the majority. Similarly, in study 3 (Chapter 4), we reported individual differences in the reference repulsion effects of colors, where the hues of the reference which induced the largest overall repulsive biases differed between some participants.

One possible explanation for these inter-subject variabilities could be an individual's adaptation of color vision to environmental statistics. Color vision

is tuned to the chromatic and illumination statistics of environments, which may develop from infancy (Skelton et al., 2023) and continue to vary throughout the life span (see Maule et al. (2023) for a review). While blue and yellow dominate the variation of daylights in most natural scenes (Mollon, 2006), substantial variation may lie in color statistics among individuals' environments due to geographic or seasonal variations (Laeng et al., 2007, Juricevic and Webster, 2009, Welbourne et al., 2015), resulting in variability in color vision. For example, adults born below the Arctic Circle showed poorer discrimination of purple and better discrimination of green than adults born above the Arctic Circle who experienced the purplish twilight of polar night (Laeng et al., 2007). Furthermore, visual perception might be relatively robust to changes in colors, as suggested by Brainard et al. (2006) who derived an illuminant prior that is substantially broader than natural illuminants. This tuning account may also imply between-subject differences in the perceptual color space and the representation of chromatic information in the visual cortex, although many aspects of cortical processing of color vision remain unknown.

Moreover, when studying sensory processing in color vision, a critical challenge lies in determining whether there is an influence from color categorization. Unlike orientations, hues are often associated with subjective color categories. However, the role of color categories in visual information processing remains controversial. Categorical effects have been shown in the reaction times and error rates for discriminating suprathreshold colors, suggesting their involvement in high-level visual processing (Bornstein and Korda, 1984, Witzel and Gegenfurtner, 2015). Yet, it is still debated whether color categories affect how participants *perceptually* distinguish colors. If so, two distinguishable colors within the same category should appear more similar than two comparable colors that are on different side of a category boundary (Bornstein et al., 1976, Bornstein and Korda, 1984). This hypothesis has been challenged by several systematic measurements of color sensitivity, which found no evidence for categorical effects on category borders (Danilova and Mollon, 2010, Witzel and Gegenfurtner, 2013). Similarly, the perceptual variability reported in study 1 (Chapter 2) shows no categorical effects in distinguishing hue ensembles that consisted of cross-category colors, supporting the idea that color sensitivity is independent of discrete color categories. Correspondingly, we did not find contributions of color categorization to perceptual bias. These results contradict the

notion of categorical effects on ensemble perception hue (Maule et al., 2014).

Categorization effect has also been found to play a significant role in color working memory. It can influence how participants estimate memorized color, such as biasing their estimates away from category boundaries and towards category centers (Bae et al., 2014, 2015). In study 3 (Chapter 4), we found similar category-related biases, while the categorical representations of hues arose from a task-related instructive context (i.e., a hue reference) rather than subjective color categories. Although our measurements did not include every hue at the color category boundary, our results show no evidence for the effects of color categories in hue estimates. This may be due to the effect of choice-induced categories possibly substituting or masking the effect of color categories, indicating an interaction between categorical information and working memory maintenance at high-level processes.

5.4 Stages of processing contextual information

The question that arises at the end of the last section is: what does the *high-level process* mean in color perception? In the experiments of study 3 (Chapter 4), this process possibly involves top-down controls, as choice-induced categories may override color categories since they are relevant to particular tasks and can guide subsequent decisions and actions. We may conclude that there is a hierarchy of color perception that includes several stages. At the lower level, cone opponent signals convey color information, laying the foundation for seeing and distinguishing colors. This stage may correspond to certain perceptual characteristics, such as color sensitivity (Brown et al., 2011, Witzel and Gegenfurtner, 2013, 2018). More complex processes occur at a higher level, where, for example, color categorization takes place (Brouwer and Heeger, 2013, Bird et al., 2014, Persichetti et al., 2015, Kim et al., 2020). On top of these levels, there may be a level of decision-related processing that interacts with upstream processes (Koida and Komatsu, 2007). In this section, I will discuss the stages of contextual information processing applied in a broad sense.

Different types of contextual biases may correspond to distinct levels of visual processing and involve diverse neural mechanisms, depending on the specific context and associated behavioral demand. Many studies have suggested

that contextual bias can occur in early sensory processes. Electrophysiological measurements have shown that context modulates the population codes of orientation-selective neurons in the primary visual cortex (V1) in different ways (Sengpiel et al., 1997, Dragoi et al., 2000, Cavanaugh et al., 2002). Some studies have indicated that contextual stimuli suppress the responses of the neurons tuned to them (Sengpiel et al., 1997, Cavanaugh et al., 2002), while others have suggested repulsive shifts in the preferred orientations of neurons away from the contextual stimuli (Gilbert and Wiesel, 1990, Felsen et al., 2005). These modulations have been found in sensory processes, resulting from intrinsic horizontal connections within V1 and feedback connections between V1 and higher visual areas such as V2 and V3 (Stettler et al., 2002, Bair et al., 2003, Nassi et al., 2013). Another potential example of low-level sensory information processing is the perceptual biases that are associated with the orientation distributions in natural scenes. Some theories attribute these biases to non-uniformities in the neural population codes for orientations (Girshick et al., 2011, Wei and Stocker, 2015). This pertains to the incorporation of prior probabilities into optimal neural populations, in which visual neurons efficiently encode stimuli from environmental distributions (Barlow and Others, 1961, Ganguli and Simoncelli, 2010).

Reference repulsion, on the other hand, is demonstrated as a late, decision-related bias by our results (Chapter 3), which aligns with the hypothesis that it may arise from cognitive processes (Luu and Stocker, 2018, 2021). Multiple explanations may support that reference repulsion involves processing at a higher level. For example, as reference stimuli share some features with target stimuli, they may draw feature-oriented attention and gain more cognitive resources (Treue and Martínez Trujillo, 1999). Moreover, behavioral context and task demands may also elicit top-down controls over visual cortical pathways (see Gilbert and Li (2013) for a review). For example, as shown in study 2 (Chapter 3), reference repulsion effects may depend on the task being performed, even when participants receive the same reference stimulus. Such task-dependent modulations have also been reported in the selection of task-relevant components of stimuli, supported by both behavioral and neural evidence (Li et al., 2004). The top-down influences may involve feedback connections from multiple cortical areas including those in the dorsal and ventral visual pathways, such as middle temporal visual area (MT) (Rockland and Knutson, 2000), V4 (Rockland et al.,

1994) and inferior temporal cortex (IT) (Rockland and Van Hoesen, 1994), as well as prefrontal cortex (Morishima et al., 2009, Paneri and Gregoriou, 2017), to provide information about attentional allocation and perceptual tasks.

Although the levels of contextual information processing are complex, fortunately, we can develop computational models to gain deeper insights into visual processing. The encoding-decoding model in our studies 2 and 3 (Chapter 3 and 4) supports this notion: by showcasing distinct reweightings of neural responses between implicit and explicit processes, the modeling results suggest that reference-induced contextual biases can originate from late decision- and task-related processes. Likewise, previous studies have employed models that assist in targeting the level of visual processing. For instance, some studies predicted contextual biases using a model constrained to self-consistency principles, indicating a higher level of processing (Luu and Stocker, 2018, 2021). These models have proven valuable in predicting contextual biases and shedding light on the level of visual processing.

In summary, when investigating a specific contextual effect, it is crucial to consider the level of contextual information processing. It is necessary to apply appropriate task designs and utilize models that enable the differentiation of various processes. Furthermore, obtaining neural evidence that aids in comprehending the underlying mechanisms would be highly advantageous.

5.5 Outlook

Reliable and systematic psychophysical measurement data are crucial for investigating visual processing and building related theories. In our studies, we developed a series of paradigms that allowed for the systematic measurement of color discrimination. However, the extensive experiment duration limited the sample size of measured colors in some instances, such as study 1 (Chapter 2). Therefore, there is a need for efficient paradigms that can expedite measurements. One approach is to employ appropriate adaptive measurement methods to accelerate the process (Leek, 2001). Additionally, it is important to consider and utilize the non-uniformities observed among hues in order to adjust the stimulus design for different colors effectively. Similar to our study 1 (Chapter 2), it is imperative not to disregard the nonuniform perceptual variability

among hues, particularly when incorporating stimulus noises or predefining hue-associated measurement ranges. Consequently, there is a clear need to establish a colorspace wherein hue representations exhibit perceptual uniformity, enabling the transformation of measured hue into a uniform scale. Such transformation may in turn help us understand the underlying mechanisms of perceptual non-uniformities.

Moreover, given the prominent individual differences shown by our findings in color perception, it is necessary to address two potential directions for future research. Firstly, it is crucial to establish a link between color vision and the adaption to the color statistics of different environments. This objective can be achieved by measuring hue discrimination thresholds and biases of participants who have undergone short- or long-term exposures to specific scenes. A recent study has demonstrated that adapting to particular stimuli can alter discrimination variability and bias of orientations (Szpiro et al., 2022). Similar effects of adaptation might also occur in color perception, leading to changes in participants' priors. The second approach is to conduct cross-experiment analyses within the same group of participants to gain insights into individual differences in color vision. This could involve a series of systematic measurements, including perceptual variability and bias in hue discrimination, contextual modulation effects of chromatic reference, subjective color categories, color constancy, and so on. Future studies in this direction may help identify consistent individual characteristics across various measurements, potentially elucidating the individual differences observed in our studies. Altogether, this approach has the potential to enhance our comprehension of the intricate nature of inter-subject variations in color vision (Mollon et al., 2017).

Last but not least, there are improvements that can be made in the future to integrate computational models with neural evidence of visual perception. While our models successfully explained the observed perceptual data, similar to previous models, they are often oriented towards efficient information processing and optimal behavior. In other words, while these models are helpful in understanding the goals of neural processing, they are not comprehensive in their ability to fully determine the various stages of information processing or unveil the underlying neural mechanisms. From the standpoint of Marr's theory (Marr, 1982), these models may describe the information processing system at a computational level rather than an algorithmic level. The absence of the latter

has generally been shown in computational models of neural systems. Taking Bayesian models as an example: although recent studies have provided preliminary evidence for the corresponding neural basis (van Bergen and Jehee, 2019, Walker et al., 2020), Bayesian theories of perception have faced longstanding criticism for their lack of neuroscientific evidence (Bowers and Davis, 2012). Looking ahead, further research could address the aforementioned limitations by exploring alternative models that may better capture the underlying neural mechanisms. Additionally, future studies could focus on closely examining the neural correlates of contextual biases to gain a better understanding of the visual processing involved in perceptual phenomena.

5.6 Concluding remarks

In conclusion, this thesis has addressed research questions related to contextual information processing by examining contextual biases in color and orientation perception and explaining perceptual phenomena with computational models. Throughout the thesis, several key findings have demonstrated that contextual biases correspond to intricate information processing that occurs across various visual features and involves different stages. These findings imply a general rule of statistical inference in vision that, for optimal performance, visual systems combine sensory representations with regularities from natural environments and behavioral task contexts. This thesis also identified some limitations that suggest opportunities for further research. Among them, a deeper understanding of how the brain processes color information is essential for a unified view on the visual processing mechanisms in different visual domains. In addition, there is a need to consider underlying neural mechanisms and levels of processing when investigating biases in visual perception. Overall, I hope this thesis will contribute to our understanding of visual information processing and provide a foundation for future research to build upon.

Bibliography

Adams, W. J., Graf, E. W., and Ernst, M. O. (2004). Experience can change the 'light-from-above' prior. *Nature Neuroscience*, 7(10):1057–1058.

Bae, G.-Y. and Luck, S. J. (2017). Interactions between visual working memory representations. *Attention, Perception & Psychophysics*, 79(8):2376–2395.

Bae, G.-Y., Olkkonen, M., Allred, S. R., and Flombaum, J. I. (2015). Why some colors appear more memorable than others: A model combining categories and particulars in color working memory. *Journal of Experimental Psychology. General*, 144(4):744–763.

Bae, G.-Y., Olkkonen, M., Allred, S. R., Wilson, C., and Flombaum, J. I. (2014). Stimulus-specific variability in color working memory with delayed estimation. *Journal of Vision*, 14(4).

Bair, W., Cavanaugh, J. R., and Movshon, J. A. (2003). Time course and time-distance relationships for surround suppression in macaque V1 neurons. *The Journal of Neuroscience*, 23(20):7690–7701.

Barbosa, J. and Compte, A. (2020). Build-up of serial dependence in color working memory. *Scientific Reports*, 10(1):10959.

Barlow, H. B. and Others (1961). Possible principles underlying the transformation of sensory messages. *Sensory Communication*, 1(01):217–233.

Battaglia, P. W., Jacobs, R. A., and Aslin, R. N. (2003). Bayesian integration of visual and auditory signals for spatial localization. *Journal of the Optical Society of America. A, Optics, Image Science, and Vision*, 20(7):1391–1397.

Bird, C. M., Berens, S. C., Horner, A. J., and Franklin, A. (2014). Categorical encoding of color in the brain. *Proceedings of the National Academy of Sciences of the United States of America*, 111(12):4590–4595.

Bornstein, M. H., Kessen, W., and Weiskopf, S. (1976). The categories of hue in infancy. *Science*, 191(4223):201–202.

Bornstein, M. H. and Korda, N. O. (1984). Discrimination and matching within and between hues measured by reaction times: some implications for categorical perception and levels of information processing. *Psychological Research*, 46(3):207–222.

Bosten, J. M. (2022). Do You See What I See? Diversity in Human Color Perception. *Annual Review of Vision Science*, 8:101–133.

Bowers, J. S. and Davis, C. J. (2012). Bayesian just-so stories in psychology and neuroscience. *Psychological Bulletin*, 138(3):389–414.

Boynton, R. M., Nagy, A. L., and Eskew, Jr, R. T. (1986). Similarity of normalized discrimination ellipses in the constant-luminance chromaticity plane. *Perception*, 15(6):755–763.

Brainard, D. H., Longère, P., Delahunt, P. B., Freeman, W. T., Kraft, J. M., and Xiao, B. (2006). Bayesian model of human color constancy. *Journal of Vision*, 6(11):1267–1281.

Brouwer, G. J. and Heeger, D. J. (2013). Categorical clustering of the neural representation of color. *The Journal of Neuroscience*, 33(39):15454–15465.

Brown, A. M., Lindsey, D. T., and Guckes, K. M. (2011). Color names, color categories, and color-cued visual search: sometimes, color perception is not categorical. *Journal of Vision*, 11(12).

Cavanaugh, J. R., Bair, W., and Movshon, J. A. (2002). Selectivity and spatial distribution of signals from the receptive field surround in macaque V1 neurons. *Journal of Neurophysiology*, 88(5):2547–2556.

Chunharas, C., Rademaker, R. L., Brady, T. F., and Serences, J. T. (2022). An adaptive perspective on visual working memory distortions. *Journal of Experimental Psychology. General*.

Clifford, C. W. G. (2014). The tilt illusion: phenomenology and functional implications. *Vision Research*, 104:3–11.

Dacey, D. M. (2000). Parallel pathways for spectral coding in primate retina. *Annual Review of Neuroscience*, 23:743–775.

Danilova, M. V. and Mollon, J. D. (2010). Parafoveal color discrimination: a chromaticity locus of enhanced discrimination. *Journal of Vision*, 10(1):4.1–9.

de Gardelle, V., Kouider, S., and Sackur, J. (2010). An oblique illusion modulated by visibility: non-monotonic sensory integration in orientation processing. *Journal of Vision*, 10(10):6.

Derrington, A. M., Krauskopf, J., and Lennie, P. (1984). Chromatic mechanisms in lateral geniculate nucleus of macaque. *The Journal of Physiology*, 357:241–265.

Dragoi, V., Sharma, J., and Sur, M. (2000). Adaptation-induced plasticity of orientation tuning in adult visual cortex. *Neuron*, 28(1):287–298.

Eagleman, D. M., Jacobson, J. E., and Sejnowski, T. J. (2004). Perceived luminance depends on temporal context. *Nature*, 428(6985):854–856.

Ernst, M. O. and Banks, M. S. (2002). Humans integrate visual and haptic information in a statistically optimal fashion. *Nature*, 415(6870):429–433.

Faisal, A. A., Selen, L. P. J., and Wolpert, D. M. (2008). Noise in the nervous system. *Nature Reviews Neuroscience*, 9(4):292–303.

Felsen, G., Touryan, J., and Dan, Y. (2005). Contextual modulation of orientation tuning contributes to efficient processing of natural stimuli. *Network*, 16(2-3):139–149.

Fischer, J. and Whitney, D. (2014). Serial dependence in visual perception. *Nature Neuroscience*, 17(5):738–743.

Foster, D. H. (2011). Color constancy. *Vision Research*, 51(7):674–700.

Fritsche, M. and de Lange, F. P. (2019). Reference repulsion is not a perceptual illusion. *Cognition*, 184:107–118.

Fritsche, M., Spaak, E., and de Lange, F. P. (2020). A Bayesian and efficient observer model explains concurrent attractive and repulsive history biases in visual perception. *Elife*, 9:e55389.

Ganguli, D. and Simoncelli, E. P. (2010). Implicit encoding of prior probabilities in optimal neural populations. *Advances in Neural Information Processing Systems*, 2010:658–666.

Gibson, J. J. and Radner, M. (1937). Adaptation, after-effect and contrast in the perception of tilted lines. i. quantitative studies. *Journal of Experimental Psychology*, 20(5):453.

Gilbert, C. D. and Li, W. (2013). Top-down influences on visual processing. *Nature Reviews. Neuroscience*, 14(5):350–363.

Gilbert, C. D. and Wiesel, T. N. (1990). The influence of contextual stimuli on the orientation selectivity of cells in primary visual cortex of the cat. *Vision Research*, 30(11):1689–1701.

Girshick, A. R., Landy, M. S., and Simoncelli, E. P. (2011). Cardinal rules: visual orientation perception reflects knowledge of environmental statistics. *Nature Neuroscience*, 14(7):926–932.

Hanazawa, A., Komatsu, H., and Murakami, I. (2000). Neural selectivity for hue and saturation of colour in the primary visual cortex of the monkey. *The European Journal of Neuroscience*, 12(5):1753–1763.

Hansmann-Roth, S., Kristjánsson, Á., Whitney, D., and Chetverikov, A. (2021). Dissociating implicit and explicit ensemble representations reveals the limits of visual perception and the richness of behavior. *Scientific Reports*, 11(1):3899.

Hochberg, J. E. (1950). Figure-ground reversal as a function of visual satiation. *Journal of Experimental Psychology*, 40(5):682–686.

Jazayeri, M. and Movshon, J. A. (2006). Optimal representation of sensory information by neural populations. *Nature Neuroscience*, 9(5):690–696.

Jazayeri, M. and Movshon, J. A. (2007). A new perceptual illusion reveals mechanisms of sensory decoding. *Nature*, 446(7138):912–915.

Jazayeri, M. and Shadlen, M. N. (2010). Temporal context calibrates interval timing. *Nature Neuroscience*, 13(8):1020–1026.

Juricevic, I. and Webster, M. A. (2009). Variations in normal color vision. V. Simulations of adaptation to natural color environments. *Visual Neuroscience*, 26(1):133–145.

Kellner, C. J. and Wachtler, T. (2016). Stimulus size dependence of hue changes induced by chromatic surrounds. *Journal of the Optical Society of America. A, Optics, Image Science, and Vision*, 33(3):A267–72.

Kersten, D. and Mamassian, P. (2009). Ideal Observer Theory. In *Encyclopedia of Neuroscience*, pages 89–95. Elsevier.

Kersten, D., Mamassian, P., and Yuille, A. (2004). Object perception as bayesian inference. *Annual Review of Psychology*, 55:271–304.

Kim, I., Hong, S. W., Shevell, S. K., and Shim, W. M. (2020). Neural representations of perceptual color experience in the human ventral visual pathway. *Proceedings of the National Academy of Sciences of the United States of America*, 117(23):13145–13150.

Klauke, S. and Wachtler, T. (2015). "Tilt" in color space: Hue changes induced by chromatic surrounds. *Journal of Vision*, 15(13):17–17.

Knill, D. C. (2007). Learning Bayesian priors for depth perception. *Journal of Vision*, 7(8):13.

Koida, K. and Komatsu, H. (2007). Effects of task demands on the responses of color-selective neurons in the inferior temporal cortex. *Nature Neuroscience*, 10(1):108–116.

Körding, K. P. and Wolpert, D. M. (2004). Bayesian integration in sensorimotor learning. *Nature*, 427(6971):244–247.

Körding, K. P. and Wolpert, D. M. (2006). Bayesian decision theory in sensorimotor control. *Trends in Cognitive Sciences*, 10(7):319–326.

Krauskopf, J. and Gegenfurtner, K. (1992). Color discrimination and adaptation. *Vision Research*, 32(11):2165–2175.

Kuriki, I., Sun, P., Ueno, K., Tanaka, K., and Cheng, K. (2015). Hue selectivity in human visual cortex revealed by functional magnetic resonance imaging. *Cerebral Cortex*, 25(12):4869–4884.

Laeng, B., Brennen, T., Elden, A., Gaare Paulsen, H., Banerjee, A., and Lipton, R. (2007). Latitude-of-birth and season-of-birth effects on human color vision in the arctic. *Vision Research*, 47(12):1595–1607.

Lee, B. B. (2011). Visual pathways and psychophysical channels in the primate. *The Journal of Physiology*, 589(Pt 1):41–47.

Leek, M. R. (2001). Adaptive procedures in psychophysical research. *Perception & Psychophysics*, 63(8):1279–1292.

Li, W., Piëch, V., and Gilbert, C. D. (2004). Perceptual learning and top-down influences in primary visual cortex. *Nature Neuroscience*, 7(6):651–657.

Luu, L. and Stocker, A. A. (2018). Post-decision biases reveal a self-consistency principle in perceptual inference. *Elife*, 7.

Luu, L. and Stocker, A. A. (2021). Categorical judgments do not modify sensory representations in working memory. *PLoS Computational Biology*, 17(6):e1008968.

Marr, D. (1982). *Vision: A Computational Investigation into the Human Representation and Processing of Visual Information*. W.H. Freeman, San Francisco, USA.

Martin, P. R., White, A. J., Goodchild, A. K., Wilder, H. D., and Sefton, A. E. (1997). Evidence that blue-on cells are part of the third geniculocortical pathway in primates. *The European Journal of Neuroscience*, 9(7):1536–1541.

Maule, J., Skelton, A. E., and Franklin, A. (2023). The development of color perception and cognition. *Annual Review of Psychology*, 74:87–111.

Maule, J., Witzel, C., and Franklin, A. (2014). Getting the gist of multiple hues: metric and categorical effects on ensemble perception of hue. *Journal of the Optical Society of America. A, Optics, Image Science, and Vision*, 31(4):A93–102.

Mollon, J. (2006). Monge: The Verriest lecture, Lyon, July 2005. *Visual Neuroscience*, 23(3-4):297–309.

Mollon, J. D., Bosten, J. M., Peterzell, D. H., and Webster, M. A. (2017). Individual differences in visual science: What can be learned and what is good experimental practice? *Vision Research*, 141:4–15.

Morishima, Y., Akaishi, R., Yamada, Y., Okuda, J., Toma, K., and Sakai, K. (2009). Task-specific signal transmission from prefrontal cortex in visual selective attention. *Nature Neuroscience*, 12(1):85–91.

Nassi, J. J., Lomber, S. G., and Born, R. T. (2013). Corticocortical feedback contributes to surround suppression in V1 of the alert primate. *The Journal of Neuroscience*, 33(19):8504–8517.

Olkkonen, M., McCarthy, P. F., and Allred, S. R. (2014). The central tendency bias in color perception: effects of internal and external noise. *Journal of Vision*, 14(11).

Orban, G. A., Vandenbussche, E., and Vogels, R. (1984). Human orientation discrimination tested with long stimuli. *Vision Research*, 24(2):121–128.

O'Toole, B. and Wenderoth, P. (1977). The tilt illusion: repulsion and attraction effects in the oblique meridian. *Vision Research*, 17(3):367–374.

Paneri, S. and Gregoriou, G. G. (2017). Top-Down Control of Visual Attention by the Prefrontal Cortex. Functional Specialization and Long-Range Interactions. *Frontiers in Neuroscience*, 11:545.

Persichetti, A. S., Thompson-Schill, S. L., Butt, O. H., Brainard, D. H., and Aguirre, G. K. (2015). Functional magnetic resonance imaging adaptation reveals a noncategorical representation of hue in early visual cortex. *Journal of Vision*, 15(6):18.

Pouget, A., Dayan, P., and Zemel, R. (2000). Information processing with population codes. *Nature Reviews Neuroscience*, 1(2):125–132.

Rauber, H. J. and Treue, S. (1998). Reference repulsion when judging the direction of visual motion. *Perception*, 27(4):393–402.

Rockland, K. S. and Knutson, T. (2000). Feedback connections from area MT of the squirrel monkey to areas V1 and V2. *The Journal of Comparative Neurology*, 425(3):345–368.

Rockland, K. S., Saleem, K. S., and Tanaka, K. (1994). Divergent feedback connections from areas V4 and TEO in the macaque. *Visual Neuroscience*, 11(3):579–600.

Rockland, K. S. and Van Hoesen, G. W. (1994). Direct temporal-occipital feedback connections to striate cortex (v1) in the macaque monkey. *Cerebral Cortex*, 4(3):300–313.

Schwartz, O., Hsu, A., and Dayan, P. (2007). Space and time in visual context. *Nature Reviews Neuroscience*, 8(7):522–535.

Sengpiel, F., Sen, A., and Blakemore, C. (1997). Characteristics of surround inhibition in cat area 17. *Experimental Brain Research*, 116(2):216–228.

Shepard, R. N. (1992). The perceptual organization of colors: An adaptation to regularities of the terrestrial world? In Barkow, J. H., editor, *The adapted mind: Evolutionary psychology and the generation of culture*, volume 666, pages 495–532. Oxford University Press, New York.

Shi, Z., Church, R. M., and Meck, W. H. (2013). Bayesian optimization of time perception. *Trends in Cognitive Sciences*, 17(11):556–564.

Simoncelli, E. P. (2003). Vision and the statistics of the visual environment. *Current Opinion in Neurobiology*, 13(2):144–149.

Skelton, A. E., Franklin, A., and Bosten, J. M. (2023). Colour vision is aligned with natural scene statistics at 4 months of age. *Developmental Science*, page e13402.

Smith, S., Clifford, C. W. G., and Wenderoth, P. (2001). Interaction between first- and second-order orientation channels revealed by the tilt illusion: psychophysics and computational modelling. *Vision Research*, 41(8):1057–1071.

Sotiropoulos, G. and Seriès, P. (2015). Probabilistic inference and Bayesian priors in visual perception. *Biologically Inspired Computer Vision*.

Spicer, J., Zhu, J.-Q., Chater, N., and Sanborn, A. N. (2022). Perceptual and cognitive judgments show both anchoring and repulsion. *Psychological Science*, 33(9):1395–1407.

Stettler, D. D., Das, A., Bennett, J., and Gilbert, C. D. (2002). Lateral connectivity and contextual interactions in macaque primary visual cortex. *Neuron*, 36(4):739–750.

Stocker, A. A. and Simoncelli, E. P. (2006). Noise characteristics and prior expectations in human visual speed perception. *Nature Neuroscience*, 9(4):578–585.

Stocker, A. A. and Simoncelli, E. P. (2007). A Bayesian Model of Conditioned Perception. *Advances in Neural Information Processing Systems*, 2007:1409–1416.

Sun, J. and Perona, P. (1998). Where is the sun? *Nature Neuroscience*, 1(3):183–184.

Szpiro, S. F. A., Burlingham, C. S., Simoncelli, E. P., and Carrasco, M. (2022). Perceptual learning improves discrimination while distorting appearance. bioRxiv: 2022.09.08.507104.

Talluri, B. C., Urai, A. E., Bronfman, Z. Z., Brezis, N., Tsetsos, K., Usher, M., and Donner, T. H. (2021). Choices change the temporal weighting of decision evidence. *Journal of Neurophysiology.*, 125(4):1468–1481.

Talluri, B. C., Urai, A. E., Tsetsos, K., Usher, M., and Donner, T. H. (2018). Confirmation Bias through Selective Overweighting of Choice-Consistent Evidence. *Current Biology*, 28(19):3128–3135.e8.

Thomas, R., Nardini, M., and Mareschal, D. (2010). Interactions between "light-from-above" and convexity priors in visual development. *Journal of Vision*, 10(8):6.

Thompson, P. (1982). Perceived rate of movement depends on contrast. *Vision Research*, 22(3):377–380.

Timney, B. N. and Muir, D. W. (1976). Orientation anisotropy: incidence and magnitude in caucasian and chinese subjects. *Science*, 193(4254):699–701.

Treue, S. and Martínez Trujillo, J. C. (1999). Feature-based attention influences motion processing gain in macaque visual cortex. *Nature*, 399(6736):575–579.

Urban, F. M. (1911). Review of the central tendency of judgment. *Psychological Bulletin*, 8(6):220–220.

Valberg, A. (2001). Unique hues: an old problem for a new generation. *Vision Research*, 41(13):1645–1657.

van Bergen, R. S. and Jehee, J. F. M. (2019). Probabilistic representation in human visual cortex reflects uncertainty in serial decisions. *The Journal of Neuroscience*, 39(41):8164–8176.

van Bergen, R. S., Ma, W. J., Pratte, M. S., and Jehee, J. F. M. (2015). Sensory uncertainty decoded from visual cortex predicts behavior. *Nature Neuroscience*, 18(12):1728–1730.

von Helmholtz, H. (1867). *Handbuch der physiologischen Optik*. Voss.

Wachtler, T., Sejnowski, T. J., and Albright, T. D. (2003). Representation of color stimuli in awake macaque primary visual cortex. *Neuron*, 37(4):681–691.

Walker, E. Y., Cotton, R. J., Ma, W. J., and Tolias, A. S. (2020). A neural basis of probabilistic computation in visual cortex. *Nature Neuroscience*, 23(1):122–129.

Wallach, H. (1935). Über visuell wahrgenommene Bewegungsrichtung. *Psychological Research*, 20(1):325–380.

Webster, M. A. (2015). Visual adaptation. *Annual Review of Vision Science*, 1:547–567.

Webster, M. A., Kaping, D., Mizokami, Y., and Duhamel, P. (2004). Adaptation to natural facial categories. *Nature*, 428(6982):557–561.

Webster, M. A., Miyahara, E., Malkoc, G., and Raker, V. E. (2000). Variations in normal color vision. II. Unique hues. *Journal of the Optical Society of America. A, Optics, Image Science, and Vision*, 17(9):1545–1555.

Webster, M. A. and Mollon, J. D. (1997). Adaptation and the color statistics of natural images. *Vision Research*, 37(23):3283–3298.

Wei, X.-X. and Stocker, A. A. (2015). A Bayesian observer model constrained by efficient coding can explain 'anti-bayesian' percepts. *Nature Neuroscience*, 18(10):1509.

Weiss, Y., Simoncelli, E. P., and Adelson, E. H. (2002). Motion illusions as optimal percepts. *Nature Neuroscience*, 5(6):598–604.

Welbourne, L. E., Morland, A. B., and Wade, A. R. (2015). Human colour perception changes between seasons. *Current Biology*, 25(15):R646–7.

Witzel, C. and Gegenfurtner, K. R. (2013). Categorical sensitivity to color differences. *Journal of Vision*, 13(7):1.

Witzel, C. and Gegenfurtner, K. R. (2015). Categorical facilitation with equally discriminable colors. *Journal of Vision*, 15(8):22–22.

Witzel, C. and Gegenfurtner, K. R. (2018). Are red, yellow, green, and blue perceptual categories? *Vision Research*, 151:152–163.

Wuerger, S., Shapley, R., and Rubin, N. (1996). "On the Visually Perceived Direction of Motion" by Hans Wallach: 60 Years Later. *Perception*, 25(11):1317–1367.

Wuerger, S. M., Atkinson, P., and Cropper, S. (2005). The cone inputs to the unique-hue mechanisms. *Vision Research*, 45(25-26):3210–3223.

Ye, R. and Liu, X. (2020). How the known reference weakens the visual oblique effect: a Bayesian account of cognitive improvement by cue influence. *Scientific Reports*, 10(1):20269.

Zamboni, E., Ledgeway, T., McGraw, P. V., and Schluppeck, D. (2016). Do perceptual biases emerge early or late in visual processing? Decision-biases in motion perception. *Proceedings of the Royal Society B: Biological Sciences*, 283(1833).

Acknowledgment

The brain appears to possess a special area which we might call poetic memory and which records everything that charms or touches us, that makes our lives beautiful.

Milan Kundera

All in all, it is not only about the brain but also about the heart. The completion of this four-year journey would not have been possible without the brilliant minds and warm hearts that have supported me along the way.

First and foremost, I am immensely grateful to my supervisors, Prof. Thomas Wachtler and Prof. Zhuanghua Shi (Strongway), for their invaluable guidance and unconditional support throughout my Ph.D. journey. I would like to express my thanks to Thomas for his openness to new ideas and his guidance in overcoming obstacles. I would also like to thank Strongway for fostering our collaborations and providing constructive feedback. It is difficult to encapsulate all the ways in which I appreciate both of my supervisors, as their guidance has been instrumental in shaping my ability to conduct good research and be a proficient scientist.

I extend my sincere gratitude to my TAC member, Dr. Virginia Flanagin, for her insightful comments and suggestions on both my research and career development. She has been a role model as a female scientist, and I am grateful for the opportunity to learn from her. This dissertation would not be complete without her willingness to review it.

I would like to thank all the people who have made my days delightful in the Wachtler Lab: Reema Gupta, Giulia Manca, Michael Sonntag, Achilleas Koutsou, and all the bachelor and master students who have contributed to my research work. Particularly, I would like to express my gratitude to my colleague Felix Schrader for his support and accompany. Thanks to him for trying out my experiments, engaging in valuable discussions, and providing generous technical and mental support.

Many thanks to the members of the MSense lab for offering cross-faculty communications and fostering a friendly atmosphere. The academic exchanges and get-togethers have made this journey more meaningful and enjoyable.

I am indebted to the participants who generously shared their time and experiences. Their willingness to participate has significantly advanced scientific research.

My great thanks to the Research Training Group 2175 "Perception in Context and its Neural Basis", not only for the financial support that facilitated my studies but also for creating a warm and supportive community since the inception of my Ph.D. journey.

I would like to thank the Graduate School of Systemic Neurosciences for their kind support and the excellent opportunities they have provided. A special thank you to the incredible coordinator, Verena Winkler, for her patient and kind assistance with all administrative matters.

Of course, I am grateful for the friendships I have cultivated in Munich and around the world. I extend my thanks to my friends for always being there, whether physically or virtually, and for sharing valuable moments with me. Their friendship and unwavering belief in my abilities have been a constant source of motivation and inspiration.

Last, I would like to express my deepest appreciation to my family. To my parents, thank you for your unconditional love and constant encouragement. Your belief in me, your understanding during challenging times, and your support in pursuing my dreams have been invaluable. To my beloved grandparents, in all I know and what I have done, I take you along. The final appreciation goes to my dear best friend Peng, having you as my rock has been an incredible blessing.

List of Publications

JOURNAL PUBLICATIONS

Su, Y., Shi, Z., & Wachtler, T. (2024). A Bayesian observer model reveals a prior for natural daylights in hue perception. *Vision Research*, *220*, 108406. https://doi.org/10.1016/j.visres.2024.108406

Su, Y., Wachtler, T., & Shi, Z. (2023). Reference induces biases in late visual processing. Scientific Reports, 13(1), 18624. https://doi.org/10.1038/s41598-023-44827-8

Wang, H., Yu, K., Yang, Z., Zhang, G., Guo, S., Wang, T., Liu, D., Jia, R., Zheng, Y., **Su, Y.**, Lou, Y., Weiss, K.R., Zhou, H., Liu, F., Cropper, E.C., Yu, Q., & Jing, J. (2023). A Single Central Pattern Generator for the Control of a Locomotor Rolling Wave in Mollusc Aplysia. Research, 6.

Yang, C., Yu, K., Wang, Y., Chen, S., Liu, D., Wang, Z., **Su, Y.**, Yang, S., Chen, T., Livnat, I., Vilim, F.S., Cropper, E.C., Weiss, K.R., Sweedler, J.V., & Jing, J. (2016). Aplysia Locomotion: Network and Behavioral Actions of GdFFD, a D-Amino Acid-Containing Neuropeptide. PLoS ONE, 11.

CONFERENCE PAPER PRESENTATIONS

Su, Y., Wachtler, T. (2023). A Bayesian observer model reveals a prior for natural daylights underlying perceptual bias in color vision. 32nd Annual Computational Neuroscience Meeting.

Su, Y., Wachtler, T. (2022). A Bayesian observer model reveals a prior for natural daylights underlying perceptual bias in hue perception. Bernstein Conference 2022. doi: 10.12751/nncn.bc2022.302

Schrader, F., Eltaş, Z., **Su, Y.**, Wachtler, T. (2022). A population coding model explaining dynamics of contextual influences on color perception. Bernstein Conference 2022. doi: 10.12751/nncn.bc2022.296

Su, Y., Kaserer, J., Wachtler, T. (2022). Reference repulsion in hue perception. 44th European Conference on Visual Perception (ECVP).

Su, Y., Wachtler, T. (2021). Discrimination and bias of perceived hues with stimulus uncertainty. 43rd European Conference on Visual Perception (ECVP) Online. Perception, 50(1_suppl), 1–244.

DATA PUBLICATIONS

Su, Y., Shi, Z., & Wachtler, T. (2023). Perceptual variability, bias, and prior in hue perception. https://doi.gin.g-node.org/10.12751/g-node.rp2ft3

Su, Y., Wachtler, T., & Shi, Z. (2023). Reference induces biases in late visual processing. https://doi.gin.g-node.org/10.12751/g-node.46h2gl

Affidavit

Eidesstattliche Versicherung/Affidavit

Yannan Su

(Studierende / Student)

Hiermit versichere ich an Eides statt, dass ich die vorliegende Dissertation Contextual Biases and Information Processing in Visual Perception selbstständig angefertigt habe, mich außer der angegebenen keiner weiteren Hilfsmittel bedient und alle Erkenntnisse, die aus dem Schrifttum ganz oder annähernd übernommen sind, als solche kenntlich gemacht und nach ihrer Herkunft unter Bezeichnung der Fundstelle einzeln nachgewiesen habe.

I hereby confirm that the dissertation Contextual Biases and Information Processing in Visual Perception is the result of my own work and that I have only used sources or materials listed and specified in the dissertation.

München / Munich, 05.12.2023

Yannan Su

Author Contributions

Manuscript 1: A Bayesian observer model reveals a prior for natural daylights in hue perception

Su, Y., Shi, Z., Wachtler, T.

Y.S. designed and carried out the experiments, analyzed and interpreted the data, and wrote the manuscript. Z.S. revised and commented on the manuscript. T.W. conceived and supervised the study, designed the experiments, interpreted the data, and revised and commented on the manuscript.

My contribution to this manuscript in detail:

For this manuscript, I designed and programmed the psychophysical experiment to measure participants' discrimination of hue ensembles. I recruited participants, collected and analyzed the data, created figures, built computational models, interpreted the results, wrote the original draft of the manuscript, and revised the manuscript.

Manuscript 2: Reference induces biases in late visual processing

Su, Y., Wachtler, T., Shi, Z.

Y.S. designed and carried out the experiments, analyzed and interpreted the data, and wrote the manuscript. T.W. revised and commented on the manuscript. Z.S. conceived and supervised the study, interpreted the data, and revised and commented on the manuscript.

My contribution to this manuscript in detail:

For this manuscript, I designed and programmed the psychophysical experiment to measure participants' discrimination and reproduction of orientation stimuli. I recruited participants, collected and analyzed the data, created figures, built computational models, interpreted the results, wrote the original draft of the manuscript, and revised the manuscript.

Manuscript 3: Reference repulsion effects in hue perception

Su, Y., Wachtler, T.

Y.S. conceived, designed and carried out the experiments, analyzed and inter-

preted the data, and wrote the manuscript. T.W. conceived and supervised the study, interpreted the data, and revised and commented on the manuscript.

My contribution to this manuscript in detail:

For this manuscript, I designed and programmed the psychophysical experiment to measure participants' discrimination and reproduction of hue stimuli. I recruited participants, collected and analyzed the data, created figures, built computational models, interpreted the results, wrote the original draft of the manuscript, and revised the manuscript.

Yannan Su

Prof. Thomas Wachtler